ISSN 2518-7198 (Print)
ISSN 2663-5089 (Online)

# BULLETIN
## OF THE KARAGANDA UNIVERSITY

# PHYSICS
## Series

№ 1(101)/2021

**ISSN 2663-5089 (Online)**
**ISSN-L 2518-7198 (Print)**
Индексі 74616
Индекс 74616

# ҚАРАҒАНДЫ УНИВЕРСИТЕТІНІҢ ХАБАРШЫСЫ

# ВЕСТНИК КАРАГАНДИНСКОГО УНИВЕРСИТЕТА

# BULLETIN OF THE KARAGANDA UNIVERSITY

**ФИЗИКА сериясы**

**Серия ФИЗИКА**

**PHYSICS Series**

## № 1(101)/2021

Қаңтар–ақпан–наурыз
30 наурыз 2021 ж.
Январь–февраль–март
30 марта 2021 г.
January–February–March
March 30th, 2021

1996 жылдан бастап шығады
Издается с 1996 года
Founded in 1996

Жылына 4 рет шығады
Выходит 4 раза в год
Published 4 times a year

Қарағанды, 2021
Караганда, 2021
Karaganda, 2021

*Редакцияның мекенжайы:* 100024, Қазақстан, Қарағанды қ., Университет к-сі, 28
Тел.: +7 701 531 4758; факс: (7212) 35-63-98.
E-mail: vestnikku@gmail.com; karabekova71@mail.ru
Сайты: physics-vestnik.ksu.kz

*Редакторлары*

Ж.Т. Нурмуханова, С.С. Балкеева

*Компьютерде беттеген*

Г.Қ. Жанбосова

**Қарағанды университетінің хабаршысы. «Физика» сериясы.**

**ISSN-L 2518-7198 (Print). ISSN 2663-5089 (Online).**

Меншік иесі: «Академик Е.А. Бөкетов атындағы Қарағанды университеті» КЕАҚ.

Қазақстан Республикасы Ақпарат және қоғамдық даму министрлігімен тіркелген. 30.09.2020 ж. № KZ38VPY00027378 қайта есепке қою туралы куәлігі.

Басуға 29.03.2021 ж. қол қойылды. Пішімі 60×84 1/8. Қағазы офсеттік. Көлемі 9,0 б.т. Таралымы 200 дана. Бағасы келісім бойынша. Тапсырыс № 9.

«Акад. Е.А. Бөкетов ат. Қарағанды ун-ті» КЕАҚ-ның баспасының баспаханасында басылып шықты. 100024, Қазақстан, Қарағанды қ., Университет к-сі, 28. Тел. (7212) 35-63-16. E-mail: izd_kargu@mail.ru

*Адрес редакции:* 100024, Казахстан, г. Караганда, ул. Университетская, 28
Тел.: +7 701 531 4758; Факс: (7212) 35-63-98.
E-mail: vestnikku@gmail.com; karabekova71@mail.ru
Сайт: physics-vestnik.ksu.kz

*Редакторы*
Ж.Т. Нурмуханова, С.С. Балкеева

*Компьютерная верстка*
Г.К. Жанбосова

**Вестник Карагандинского университета. Серия «Физика».**
**ISSN-L 2518-7198 (Print). ISSN 2663-5089 (Online).**
Собственник: НАО «Карагандинский университет имени академика Е.А. Букетова».
Зарегистрирован Министерством информации и общественного развития Республики Казахстан. Свидетельство о постановке на переучет № KZ38VPY00027378 от 30.09.2020 г.

Подписано в печать 29.03.2021 г. Формат 60×84 1/8. Бумага офсетная. Объем 9,0 п.л. Тираж 200 экз. Цена договорная. Заказ № 9.
Отпечатано в типографии издательства НАО «Карагандинский университет им. акад. Е.А. Букетова». 100024, Казахстан, г. Караганда, ул. Университетская, 28. Тел. (7212) 35-63-16. E-mail: izd_kargu@mail.ru

*Postal address*: 28, University Str., 100024, Karaganda, Kazakhstan
Tel.: +7 701 531 4758; Fax: (7212) 35-63-98.
E-mail: vestnikku@gmail.com; karabekova71@mail.ru
Web-site: physics-vestnik.ksu.kz

*Editors*
Zh.T. Nurmukhanova, S.S. Balkeyeva

*Computer layout*
G.K. Zhanbossova

**Bulletin of the Karaganda University. «Physics» series.**
**ISSN-L 2518-7198 (Print). ISSN 2663-5089 (Online).**
Proprietary: NLC «Karagandy University of the name of academician E.A. Buketov».
Registered by the Ministry of Information and Social Development of the Republic of Kazakhstan. Rediscount certificate No. KZ38VPY00027378 dated 30.09.2020.

Signed in print 29.03.2021. Format 60×84 1/8. Offset paper. Volume 9,0 p.sh. Circulation 200 copies. Price upon request. Order № 9.
Printed in the Publishing house of NLC «Karagandy University of the name of acad. E.A. Buketov».
28, University Str., Karaganda, 100024, Kazakhstan. Tel. (7212) 35-63-16. E-mail: izd_kargu@mail.ru

# МАЗМҰНЫ — СОДЕРЖАНИЕ — CONTENTS

## ТЕХНИКАЛЫҚ ФИЗИКА
## ТЕХНИЧЕСКАЯ ФИЗИКА
## TECHNICAL PHYSICS



## ФИЗИКАНЫ ОҚЫТУ ӘДІСТЕМЕСІ
## МЕТОДИКА ПРЕПОДАВАНИЯ ФИЗИКИ
## METHODS OF TEACHING PHYSICS

DOI 10.31489/2021Ph1/6-11
UDC 536.5

A.P. Sarode[1,*], O.H. Mahajan[2]

[1]*Physics Department, Dr.A.G.D. Bendale Girls College, Jalgaon 425001, India;*
[2]*Physics Department, M.J. College, Jalgaon 425001, India*
*(*E-mail: abhijitsarode@yahoo.com)*

# Displacement fields of a Cuboid crystal in a Photoacoustic Cell: Mathematical aspects

Photo acoustic effect is popular due to a minimal sample preparation during execution, the ability to examine scattering and opaque sample along with the capability to access depth profile. These features enable Photoacoustic spectroscopy to be used in depth-resolved characterization of solids. Thermal interaction is a basic perspective in solid state physics research regarding industrial devices and components. It is a key factor of fabrication and performance of such devices and components. Today, crystalline solids are widely studied due to their wide scientific and industrial applications. Displacement field resulting in thermal stresses is one of the important aspects of premature failure of industrial components and devices. In this paper, displacement fields in photoacoustic effect with solid cuboid crystal are mathematically presented. According to our opinion, displacement fields in photoacoustic effect in three dimensional analysis are not reported earlier. Hence that will be a major contribution of this paper. For a simple cuboid homogeneous crystal kept in a photoacoustic cell, an airy stress function is determined based on laser interaction with surface of the crystal. By applying the finite Marchi-Fasulo integral transform method within the crystal size limitations, displacement field is exactly determined.

Keywords: airy stress function, cuboid crystal, displacement field, energy transfer, light – matter interaction, Marchi- Fasulo transform, non-radiative de-excitation, photoacoustic cell, photoacoustic effect.

## *Introduction*

A displacement field is a scalar function which enables us to determine different stresses in an elastic body by simple differentiation method. In this paper, an attempt has been made to calculate displacement fields of a homogeneous isotropic cubic crystal kept in a modified photoacoustic cell. Determination of displacement field will be helpful in the development of a methodology of application of displacement field to stress determination in photoacoustic problems.

When incident radiation is absorbed by molecules of the target material, photoacoustic effect is generated [1-2]. Photoacoustic effect can be used in depth-resolved thermal characterization of materials [3]. The interaction of incident radiation with the atoms of the material in the crystal results in the generation of heat [4]. This heat generation is applied to calculate displacement fields in the crystal. The Marchi-Fasulo integral transform method is used here to calculate displacement fields in an isotropic cuboid crystal in photoacoustic effect.

Initial theoretical explanation of temperature of solids during photoacoustic interaction was presented by Rosencwaig [5]. A one dimensional model regarding heat flow and temperature was formulated by Rosencwaig and Gersho [6]. McDonald and Wetsel published temperature calculations of photoacoustic interaction in three dimensional model with restrictions on thermal waves in transverse direction [7]. Quimby

and Yen primarily calculated the surface heat conductance in temperature estimation [8]. Chow developed a three dimensional model in a general way without any restrictions on sample size in photoacoustic cell [9]. In the recent years, Merzadinova et. al calculated ambient temperature of a solid in thermal diffusivity determination of structurally inhomogeneous, multilayer and composite solids in photoacoustic interaction [10].

*Situation of the crystal*

Consider a cuboid crystal placed in a photoacoustic cell. The crystal is isotropic and traction free in nature. This crystal is placed in a cylindrical cavity of a photoacoustic cell which produces a photoacoustic signal. The cell is air tight. Hence the cell has a constant volume of gas surrounding the crystal. The crystal is irradiated by a proper modulated laser source. The crystal absorbs heat and generates photoacoustic signal.

The Photoacoustic effect is directly related with on heating of the sample due to the phenomenon of optical absorption [11-12]. Periodic processes of heating and cooling of the solid sample are necessary because it will develop pressure fluctuations should be generated in the cell [13]. These fluctuations can be detected by a sensitive sensor.

In the process of modulated excitation, sources of radiation are used in which intensity fluctuates periodically [14-17]. These fluctuations in the intensity of radiation are in the form of a sine wave or a square wave. This is similar to mechanical chopping of a radiation source. To modulate the phase of the optical signal instead of its amplitude is the best way to overcome this method [18-20]. In Photoacostic analysis, the most common sources are the use of modulated continuous wave lasers.

*Mathematical formulation*

Assume that the cubic crystal placed in the cell is occupying the space. This space is defined mathematically, as

$$\mathrm{D}: -a \le x \le a,\ -b \le y \le b\ .\ 0 \le z \le -h$$

Consider a Cartesian co-ordinate system, in which the displacement components are $u_x$, $u_y$, $u_z$ in the *x, y, z* direction respectively. These displacement components can be expressed in the integral form as

$$u_x = \int \left[\frac{1}{Y}\left(\frac{\partial^2 U}{\partial y^2} + \frac{\partial^2 U}{\partial z^2} - \nu\frac{\partial^2 U}{\partial x^2}\right) + \lambda T\right] dx \tag{1}$$

$$u_y = \int \left[\frac{1}{Y}\left(\frac{\partial^2 U}{\partial z^2} + \frac{\partial^2 U}{\partial x^2} - \nu\frac{\partial^2 U}{\partial y^2}\right) + \lambda T\right] dy \tag{2}$$

$$u_z = \int \left[\frac{1}{Y}\left(\frac{\partial^2 U}{\partial x^2} + \frac{\partial^2 U}{\partial y^2} - \nu\frac{\partial^2 U}{\partial z^2}\right) + \lambda T\right] dz \tag{3}$$

where *Y*, $\nu$ and $\lambda$ are the Young modulus, the poisson ratio and the coefficient of linear thermal expansion of the material of the crystal respectively. Consider that *U(x, y ,z ,t)* is the airy stress function which satisfies the differential equation,

$$\left(\frac{\partial^2}{\partial x^2} + \frac{\partial^2}{\partial y^2} + \frac{\partial^2}{\partial z^2}\right)^2 U(x,y,z,t) = -\lambda Y \left(\frac{\partial^2}{\partial x^2} + \frac{\partial^2}{\partial y^2} + \frac{\partial^2}{\partial z^2}\right)^2 T(x,y,z,t) \tag{4}$$

Here $T(x,y,z,t)$ denotes the translational temperature of the crystal satisfying the following differential equation,

$$\frac{\partial^2 T}{\partial x^2} + \frac{\partial^2 T}{\partial y^2} + \frac{\partial^2 T}{\partial z^2} + \frac{\theta(x,y,z,t)}{k} = \frac{1}{\alpha}\frac{\partial T}{\partial t} \tag{5}$$

where $k$ is thermal conductivity and $\alpha$ is the thermal diffusivity of the material of the crystal.

Let $\theta(x,y,z,t)$ is heat generated within the crystal for $t > 0$ subject to initial conditions (5).

$$T(x,y,z,0) = F(x,y,z) \tag{6}$$

*Boundary Conditions*

Let us define boundary conditions on the crystal. These boundary conditions are

$$\left[\mathrm{T(x,y,z,t)} + \mathrm{k}_1\frac{\partial T(x,y,z,t)}{\partial x}\right]_{x=a} = F_1(y,z,t) \tag{7}$$

$$\left[\mathrm{T(x,y,z,t)} + \mathrm{k}_2\frac{\partial T(x,y,z,t)}{\partial x}\right]_{x=-a} = F_2(y,z,t) \tag{8}$$

$$\left[\mathrm{T(x,y,z,t)} + \mathrm{k_3}\frac{\partial T(x,y,z,t)}{\partial y}\right]_{y=b} = F_3\,(x,z,t) \tag{9}$$

$$\left[\mathrm{T(x,y,z,t)} + \mathrm{k_4}\frac{\partial T(x,y,z,t)}{\partial y}\right]_{y=-b} = F_4\,(x,z,t) \tag{10}$$

$$\left[\mathrm{T(x,y,z,t)} + \mathrm{k_5}\frac{\partial T(x,y,z,t)}{\partial z}\right]_{z=0} = \mathrm{f_1}\,(x,y,t) \tag{11}$$

$$\left[\mathrm{T(x,y,z,t)} + \mathrm{k_6}\frac{\partial T(x,y,z,t)}{\partial z}\right]_{z=-h} = \mathrm{f_2}\,(x,y,t) \tag{12}$$

The components in term *U (x, y, z, t)* are given by

$$\sigma_{xx} = \left(\frac{\partial^2 U}{\partial y^2} + \frac{\partial^2 U}{\partial z^2}\right) \tag{13}$$

$$\sigma_{yy} = \left(\frac{\partial^2 U}{\partial z^2} + \frac{\partial^2 U}{\partial x^2}\right) \tag{14}$$

$$\sigma_{zz} = \left(\frac{\partial^2 U}{\partial x^2} + \frac{\partial^2 U}{\partial y^2}\right) \tag{15}$$

The “Eq. (1)” to “(15)” constitute the mathematical formulation of the conditions of the crystal under consideration.

*Mathematical Solution*

The finite Marchi - Fasulo integral transform of *f (z)*, within limitations $-h < z < h$ is defined to be

$$\bar{F} = \int_{-h}^{h} f(z)\, P_n(z)\, dz \tag{16}$$

Then at each point of *(-h, h)* , the function *f (z)* is continuous. Again, the inverse finite Marchi - Fasulo transform for previous conditions is defined as

$$f(z) = \sum_{n=1}^{\infty} \frac{\bar{F}(n)}{\lambda_n} P_n(z) \tag{17}$$

Here,

$$P_n(z) = Q_n \cos(a_n z) - W_n \sin(a_n z)$$
$$Q_n = a_n(\alpha_1 + \alpha_2)\cos(a_n h) + (\beta_1 - \beta_2)\sin(a_n h)$$
$$W_n = (\beta_1 + \beta_2)\cos(a_n h) + (\alpha_1 - \alpha_2) a_n \sin(a_n h)$$
$$\lambda_n = \int_{-h}^{h} {P_n}^2\,(z)\,dz$$
$$\lambda_n = h\left[{Q_n}^2 + {W_n}^2\right] + \frac{\sin(2a_n h)}{2a_n}\left[{Q_n}^2 - {W_n}^2\right]$$

The Eigen values $a_n$ are the solutions of the equation

$$[\alpha_1 \operatorname{acos}(ah) + \beta_1 \sin(ah)] \times [\beta_2 \cos(ah) + \alpha_2 \operatorname{asin}(ah)] =$$
$$= [\alpha_2 \operatorname{acos}(ah) - \beta_2 \sin(ah)] \times [\beta_1 \cos(ah) - \alpha_1 \operatorname{asin}(ah)] \tag{18}$$

Here $\alpha_1, \alpha_2, \beta_1, \beta_2$ are constants.

By applying the finite Marchi - Fasulo transform three times to “Eq. (5)” and their inverses, we obtain

$$\frac{d\bar{\bar{T}}^M}{dt} + \propto q^2 \bar{\bar{T}}^{\nearrow} = \propto \left(\emptyset + \frac{\bar{\theta}^M}{k}\right) \tag{19}$$

where

$$\emptyset = P_m(a)F_2 - P_m(-a)F_1 + P_n(b)F_4 - P_n(-b)F_3 + P_l(h)f_2 - P_l(-h)f_1$$

and

$$q^2 = a_m^2 + a_n^2 + a_l^2 \tag{20}$$

is Eigen value.

"Eq. (10)" is first order differential equation and has solution

$$\bar{\bar{T}}^{\succ}(m,n,l,t) = e^{-\propto q^2 t}\left[\int_0^t \propto (\emptyset + \frac{\bar{\theta}^M}{k})\right] e^{-\propto q^2 t' dt'} + c, c = \bar{\bar{F}}^{\succ}(m,n,l) \tag{21}$$

$$\bar{\bar{T}}^{\succ}(m,n,l,t) = \int_0^t \propto (\emptyset + \frac{\bar{\theta}^M}{k}) e^{\propto (a_m^2 + a_n^2 + a_l^2)(t-t')dt'} + e^{-\propto (a_m^2 + a_n^2 + a_l^2)t} \bar{\bar{F}}^{\succ}(m,n,l) \tag{22}$$

If we apply inverse finite Marchi - Fasulo Transform three times with boundary conditions to this equation, we get

$$T(x,y,z,t) = \frac{k}{c^2}\sum_{m,n=1}^{\infty}\left[\frac{P_m(x)}{\lambda_m}\right]\left[\frac{P_n(y)}{\mu_n}\right][\varphi_1(z)\psi_1(t) - \varphi_2(z)\psi_2(t)] +$$

$$\frac{2k\pi}{h^2}\sum_{l,m,n=1}^{\infty}\left[\frac{P_m(x)}{\lambda_m}\right]\left[\frac{P_n(y)}{\mu_n}\right]\left[\frac{l}{\cos l\pi}\right]\left[\frac{1}{1+cl\pi^2}\right][n_1(z)\psi_3(t) - -n_2(z)\psi_4(t)] \tag{23}$$

Substituting the value of T( x, y, z ,t) from "Eq. (23)" in the "Eq. (4)", the airy stress function can be obtained as

$$U(x,y,z,t) = \lambda Y \frac{k}{c^2}\sum_{m,n=1}^{\infty}\left[\frac{P_m(x)}{\lambda_m}\right]\left[\frac{P_n(y)}{\mu_n}\right]\left[\frac{\varphi_1(z)\psi_1(t) - \varphi_2(z)\psi_2(t)}{a_m^2 + a_n^2 + \left\{\frac{1}{c}\right\}^2}\right] +$$

$$\frac{2\lambda Y k\pi}{h^2}\sum_{l,m,n=1}^{\infty}\left[\frac{P_m(x)}{\lambda_m}\right]\left[\frac{P_n(y)}{\mu_n}\right]\left[\frac{l}{\cos l\pi}\right]\left[\frac{\eta_1(x)\psi_3(t) - \eta_2(z)\psi_4(t)}{a_m^2 + a_n^2 + \left\{\frac{\pi}{h}\right\}^2}\right] \tag{24}$$

*Results*

The displacement field along x direction is calculated as

$$u_x = \alpha\frac{k}{c^2}\sum_{n,l=1}^{\infty}\left[\frac{(k_1+k_2)\sin 2a_m a}{\lambda_m}\right]\left[\frac{P_n(y)}{\mu_n}\right](1+\nu)a_m^2\left[\frac{\varphi_1(z)\psi_1(t) - \varphi_2(z)\psi_2(t)}{a_m^2 + a_n^2 + \left\{\frac{1}{c}\right\}^2}\right] +$$

$$\frac{2\propto k\pi}{h^2}\sum_{l,m,n=1}^{\infty}\left[\frac{(k_1+k_2)\sin 2a_m a}{\lambda_m}\right]\left[\frac{P_n(y)}{\mu_n}\right]\left[\frac{l}{\cos l\pi}\right]\left[\frac{\eta_1(z)\psi_3(t) - \eta_2(z)\psi_4(t)}{1 + \left\{\frac{l\pi}{h}\right\}^2}\right] \tag{24}$$

In the similar way, displacement fields in other directions could be determined.

*Conclusion*

The exact expression for displacement field of a cuboid crystal in a photoacoustic cell is determined. The expression allows the calculation of various parameters of cuboid crystals properties such as stress, strain, etc related with elasticity in photoacoustic cell. This mathematical approach constitutes an important step towards determination of various aspects of premature failure of industrial components and devices This work will be useful in research for scientific and industrial applications in future.

References

1 Bein, B.K. & Pelzl, J. (1983). Theory of signal generation in a photoacoustic cell. *Journal de Physique Colloques, 44 (C6),* 27–34.

2 Zheng, H., Dong, L., Sampaolo, A., Wu, H., Patimisco, P., & Yin, X., et al. (2016). *Optics Letters, 41(5),* 978–981.

3 Michaelian, K. (2010). *«Photoacoustic IR Spectroscopy: Instrumentation, Applications and Data Analysis», 3,* 8–14.

4 Yi, H. Chen, W., Sun, S., Liu, K., Tu, T, & Gao, X., (2012). T-shape microresonator-based high sensitivity quartz-enhanced photoacoustic spectroscopy sensor. *Optics Express, 20,* 9187–9196.

5 Rosencwaig, A. (1975). Photoacoustic spectroscopy of solids. *Physics Today, 28(9),* 23–30.

6 Rosencwaig, A., & Gersho, A. (1976). Theory of the photoacoustic effect with solids. *Journal of Applied Physics, 47,* 64–68.

7 McDonald, F., & Wetsel, G. (1978). Generalized theory of the photoacoustic effect. *Journal of Applied Physics, 49,* 2313–2322.

8 Quimby, R., & Yen, W. (1980). Photoacoustic theory including energy migration. *Journal of Applied Physics, 51,* 4985–4990.

9 Chow, H. (1980). Theory of three-dimensional photoacoustic effect with solids. *Journal of Applied Physics, 51,* 4053–4056.

10 Merzadinova, G., Sakipov, K., Sharifov, D., Mirzo, A., & Bekeshev, A. (2019). Laser photoacoustics method for determination of the coefficients of thermal conductivity and thermal diffusivity of materials. *Eurasian Physical Technical Journal, 16,* 1(31), 94–98.

11 Carslaw, H., & Jaeger, J. C. (1959). *Conduction of heat in solids*. Oxford: Oxford Clarendon Press.

12 Zheng, H., Dong, L., Sampaolo, A., Wu, H., Patimisco, P., Yin, X., et al. (2016). Single-tube on-beam quartz-enhanced photoacoustic spectroscopy. *Optics Letters, 41,* 978–981.

13 Nosaka, Y., Igarashi, R., & Miyama, H. (1985). Pulsed photoacoustic spectroscopy for powder suspension using a flash lamp. *Analytical Chemistry, 57(1),* 92–94.

14 Zhou, S., Slaman, M., & Iannuzzi, D. (2017). Demonstration of a highly sensitive photoacoustic spectrometer based on a miniaturized all-optical detecting sensor. *Opt. Express, 25,* 17541–17548.

15 Mikkonen, T., Amiot, C., Aalto, A., Patokoski, K., Genty, G., & Toivonen, J. (2018). Broadband cantilever-enhanced photoacoustic spectroscopy in the mid-IR using a supercontinuum. *Optics Letters, 43.* 5094–5097.

16 Salikhov, T., Melikkhudzha, N., Khodzhaev, Y., & Khodzhakhonov, I. (2017). To the theory of generation of photoacoustic signal by solid state samples. *Doklady Akademii auk Respubliki Tazhikistan, 60 (11–12),* 569–574.

17 Agilar, C., & Pachec, A. (2019). Photoacoustic Spectroscopy in the Optical Characterization of Foodstuff: A Review. *Hindawi Journal of Spectroscopy, Vol. 2019,* 1–34.

18 Zhou, M., Xia, H., & Zhong, H. (2019). A Noise Reduction Method for Photoacoustic Imaging *In Vivo* Based on EMD and Conditional Mutual Information. *IEEE Photonics Journal, 11(1),* 99–107.

19 Pan, Y., Dong, L., Wu, H., & Ma, W. (2019). Cavity-enhanced photoacoustic sensor based on a whispering-gallery-mode diode laser. *Atmospheric Measurements Techniques, 12,* 1905–1911.

20 Boley, B. A. & Weiner, J. H. (1960). «Theory of thermal stresses». Wiley, 12–47.

А.П. Сароде, О.Х. Махаджан

## Фотоакустикалық ұяшықтағы текше тәрізді кристалдың ығысу өрістері: математикалық аспектілер

Фотоакустикалық эффект үлгіні дайындаудың ең аз уақытына, шашыраңқы және мөлдір емес үлгіні зерттеуге және тереңдік профилінің қолжетімділігіне байланысты танымал. Бұл ерекшеліктер терең ажыратымдылықтағы қатты заттардың сипаттамаларын анықтау үшін фотоакустикалық спектроскопияны қолдануға мүмкіндік береді. Термиялық әсерлесу — өнеркәсіптік құрылғылар мен компоненттерге қатысты қатты дене физикасын зерттеудегі басты перспектива. Бұл осындай құрылғылар мен компоненттерді шығарудың және дайындаудың негізгі факторы. Бүгінгі таңда кристалды қатты заттар кең ғылыми және өнеркәсіптік қолданудың арқасында кеңінен зерттелуде. Жылу кернеуіне әкелетін ығысу өрісі өнеркәсіптік қондырғылар мен құрылғылардың мерзімінен бұрын істен шығуының маңызды аспектілерінің бірі болып табылады. Жұмыста қатты кубоидты кристалмен фотоакустикалық әсердегі ығысу өрістері математикалық түрде ұсынылған. Авторлардың ойынша үш өлшемді анализде фотоакустикалық әсер кезінде орын ауыстыру өрістері бұрын байқалмаған. Демек бұл нақты құжатқа негізгі үлес болады. Фотоакустикалық ұяшықта орналасқан қарапайым кубоидты біртекті кристалл үшін Эйри кернеу функциясы лазердің кристалл бетімен әрекеттесуі негізінде анықталады. Марчи-Фасулоның түпкілікті интегралдық түрлендіру әдісін кристалл өлшемінің шектеулері шегінде қолдана отырып, ығысу өрісі дәл айқындалған.

*Кілт сөздер:* Эйри кернеуінің функциясы, текше тәрізді кристалл, ығысу өрісі, энергияны беру, жарық пен заттың өзара әрекеттесуі, Марчи-Фасуло түрлендіруі, сәулеленбейтін қозу, фотоакустикалық ұяшық, фотоакустикалық әсер.

А.П. Сароде, О.Х. Махаджан

## Поля смещения кубовидного кристалла в фотоакустической ячейке: математические аспекты

Фотоакустический эффект популярен благодаря минимальной пробоподготовке во время выполнения возможности исследовать рассеивающийся и непрозрачный образец наряду с доступом к профилю глубины. Эти особенности позволяют применять фотоакустическую спектроскопию для определения

характеристик твердых тел с глубинным разрешением. Тепловое взаимодействие является основной перспективой в исследованиях физики твердого тела, касающихся промышленных устройств и компонентов. Это ключевой фактор изготовления и производительности таких устройств и компонентов. Сегодня кристаллические твердые тела широко изучены благодаря их широкому научному и промышленному применению. Поле смещений, приводящее к термическим напряжениям, является одним из важных аспектов преждевременного выхода из строя промышленных узлов и устройств. В работе математически представлены поля смещений в фотоакустическом эффекте с твердым кубовидным кристаллом. По мнению авторов, поля смещения при фотоакустическом эффекте в трехмерном анализе ранее не наблюдались. Следовательно, это будет главным вкладом в настоящий документ. Для простого кубовидного однородного кристалла, находящегося в фотоакустической ячейке, функция напряжения Эйри определена на основе взаимодействия лазера с поверхностью кристалла. Применение метода конечного интегрального преобразования Марчи–Фасуло в пределах ограничений размера кристалла позволило точно вычислить поле смещения.

*Ключевые слова:* функция напряжения Эйри, кубовидный кристалл, поле смещения, перенос энергии, взаимодействие света и вещества, преобразование Марчи–Фасуло, безызлучательное возбуждение, фотоакустическая ячейка, фотоакустический эффект.

DOI 10.31489/2021Ph1/12-17
UDC 620.192:534 – 16:53.887.45

D.D. Dann*, M.V. Petrov, P.I. Fedotov, E.A. Sheveleva

*National Research Tomsk Polytechnic University, Tomsk, Russia*
*(*E-mail: dddann@tpu.ru)*

# Changes in the Parameters of the Electromagnetic Response of Model Dielectric Samples with Air Cavity Defects under External Deterministic Acoustic Impact

The paper discusses the possibility of testing the air inclusions saturation in cement-sand samples using the acoustic-electrical transformations phenomenon in heterogeneous dielectric materials. An experiment technique is presented including contact external acoustic excitation and contactless registration of the electromagnetic response to such an impact. Methods of samples deterministic acoustic excitation by a ball impact and the experimental determination of the impact energy are described. The model samples size and composition are described, including air cavities in a polyethylene sheath. The experimental studies geometry is shown, indicating the direction of the samples acoustic excitation and the location of the electromagnetic receiving plates. It is shown that the defect-free samples and with air cavities, have different amplitude and frequency of the electromagnetic signals spectral components. The samples with air cavities have the average weight of the EMS spectrum changes towards lower frequencies. This frequency shift effectively reflects the concentration of air cavities defects in a cement-sand samples and this effect can be used when testing concrete products for the presence of air inclusions, and, accordingly, will allow determining the frost resistance of products.

*Keywords:* acoustic-elecrical transformations, acoustic excitation, electromagnetic signal, amplitude-frequency characteristics, dielectric structures, cement-sand mixture, defect, electrical double layer.

## *Introduction*

The reliability and durability of concrete products is always of great importance for the people safety, therefore, the determination of defects in such materials is an important task. Samples made from cement-sand mixture were used to simulate the impact of defects in the form of air cavities on the parameters of the electromagnetic response under external deterministic impact. It is known that preparation of such mixtures is followed by air entrainment, and air bubbles up to $10^{-3}$ meters have a beneficial effect on frost resistance and strength of concrete. However, this is not the most important characteristic for assessing its frost resistance. An important characteristic is the distance between air bubbles and their size. The larger the size of the air inclusions, the lower the strength of concrete or mortar under external loads. This is due to the fact that voids with the size exceeding $(5–7)\times10^{-3}$ meters serve as stress concentrators, which ultimately leads to concrete destruction [1]. The critical capillary length should not exceed $2\times10^{-4}$ meters. A reduced length ensures concrete with high impermeability up to $16\times10^{-4}$ m$^2$. This can be attained by entraining air into the concrete to form a system of numerous small bubbles where water can be squeezed out when frozen. Since the distance between the bubbles in the cement stone does not exceed the critical one, the destructive pressure will be higher, and the concrete will be frost-resistant.

However, non-destructive methods for testing air entrainment into concrete or cement stone are required. Non-destructive direct methods are used to measure the tensile strength of the glued steel disc separation, or partial separation of the product edges. The most interesting non-destructive indirect methods are ultrasound examination, impact excitation, and rebound and plastic deformation. In practice, these testing methods lack accuracy and mobility [2–5].

The phenomenon of mechanoelectric transformations in heterogeneous dielectric materials, including acoustic-electrical transformations, can be used to test the saturation of concrete or cement stone with air inclusions [6–14]. The principle of the proposed method lies in the fact that the research object is subjected to mechanical impact, and acoustic waves appear in the sample, which propagate along the sample. As a result of the deformation of the piezo-inclusions and double electrical layers in the concrete sample by acoustic waves, an electromagnetic response arises. Previous performed studies analyzed the main mechanisms of mechanoelectric transformations in heterogeneous dielectric structures. As a result, relationships were revealed between the parameters of the electromagnetic signal arising during quasi-elastic impact excitation of materials and their porosity, strength of the contact between components in composite materials, stress-strain

state, imperfection and strength, which indicates the potential of mechanoelectric transformations used to test the defectiveness and strength of engineering structures.

*Methods and materials*

The studies were conducted using a laboratory complex for recording the electromagnetic response of heterogeneous materials under acoustic deterministic impact. The block diagram of the complex is shown in Figure 1.

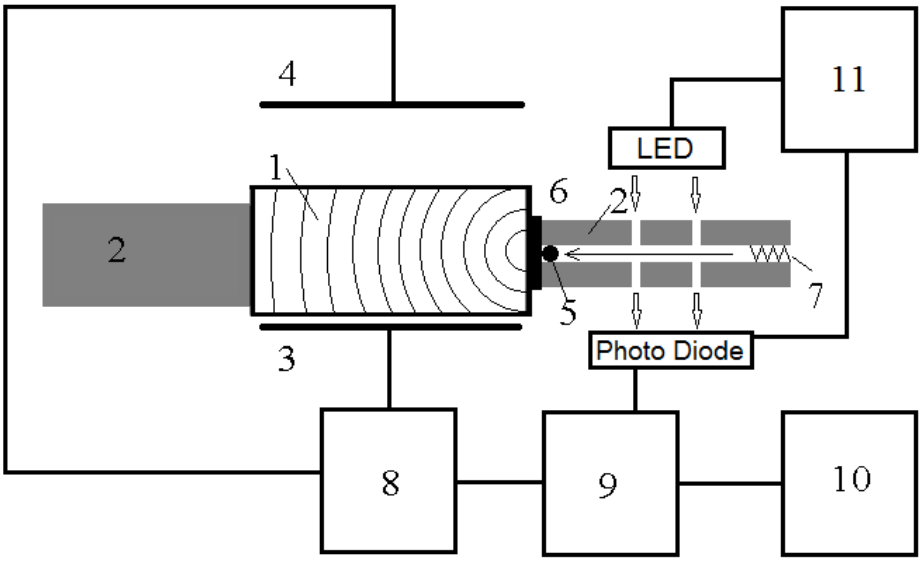


1 — sample, 2 — clamps, 3 — measuring electrode, 4 — compensation electrode,5 — ball, 6 — substrate, 7 — spring, 8 — differential amplifier,9 — data input-output board, 10- computer, 11 — power supply

Figure 1. Block diagram of the laboratory complex for recording the electromagnetic response of heterogeneous materials under deterministic acoustic impact

Sample1 was fixed between clamps 2; metal substrate 6 was placed on the sample surface at the impact point, which was in acoustic contact with the sample through a thin layer of mineral oil. Pulsed mechanical excitation of the samples was initiated with metal ball 5 using spring-loaded device 7. The impact energy was measured with respect to the speed of the ball's flight between two optical pairs of LEDs and PDs installed at a certain distance in clamp 2 with a flying hole. The substrate and the ball were made of steel of similar hardness. Battery 11 was used for power supply of the light and photodiodes. This excitation system enabled a point deterministic single impact. A differential transducer was used to record the EMC signal arising from pulsed acoustic excitation of the samples.

The input of electromagnetic sensor 8 consisted of two flat metal plates 3 and 4. Plate 3 (measuring) was placed at a distance of $10^{-3}$ meters from the sample surface, and plate4 (compensation) was installed at a distance of $2 \times 10^{-2}$ meters from the sample. The measuring plate received both a useful signal and the signal of remote electromagnetic interference. Since the compensation plate is placed at the distance from the source of the useful signal and received only distant electromagnetic interference, the level of distant interference at the differential sensor output significantly decreased, and the signal-to-noise ratio increased. The signals from the differential electromagnetic sensor were fed to the inputs of the preamplifiers and were recorded using multifunctional input-output board 9 to digitize the time realization of the electrical signal and perform fast Fourier transform. Computer 10 was used to record the results of EMC measurements and the spectrum.

The dimensions of the samples made from cement-sand mixture were $(50x50x100)\times10^{-9}$ $m^3$. An external deterministic acoustic pulse was excited by the ball impact towards the greater plane in the center. During the tests, smaller faces of the samples were placed in the clamps, and the impact device was fixed in the cell using special clamps. In this experimental geometry, attenuation of acoustic waves formed in the sample upon its impact excitation was determined by the characteristics of the sample only.

*Results and discussion*

In order to search for possible criteria to assess the dynamics of changes in imperfection, the nature of changes in patterns of mechanoelectric transformations was analyzed on physical models with artificial defects. Testing was performed on models with internal air cavities. To create internal air cavities, air-filled polyethylene balls with a diameter of $10^{-2}$ meters were used. The model samples were made from cement-sand mixture containing 1, 5, 20 and 50 air inclusions. Defects of this type simulate internal air cavities that can arise when preparing cement-sand mixture. In the experiment, they act as scattering centers for acoustic waves formed in the sample upon excitation by the ball impact. However, in contrast to real cavities, these models exhibit a polyethylene layer at the interface of the cement-sand matrix, which should form double electric layers during cement structure formation [9]. These samples were used to measure electromagnetic signals and their amplitude-frequency parameters at equal pulsed acoustic excitation. Figure 2 shows previously measured and re-obtained spectral characteristics of electromagnetic signals for model samples with a different number of air cavities. As can be seen, a slight increase in the number of air cavities leads to an insignificantly increased value of the main spectral maximum at a frequency of about 11 kHz, followed by its decreased amplitude and increased number of air inclusions.

In addition, the EMC spectrum is found to change as well. Due to the fact that air inclusions are located at different distances from the acoustic excitation source during model sample fabrication, additional spectral bands appear in the exciting acoustic pulse as a result of reflection from the surfaces of air inclusions in accordance with the laws of linear acoustics [15]. Acoustic-electrical transformations cause additional EMC spectrum ranges at the interface of inclusions. The initial increase in the amplitude of maximum is due increased non-overlapped electrical double layers, which does not compensate for their charge state. Further increase in the number of air inclusions causes strong attenuation of the acoustic pulse, compensation of charges on the walls of neighboring inclusions and, consequently, decrease in the EMS amplitude due to acoustic-electrical transformations. In addition, there is a steady shift of the EMS spectrum to the low-frequency region.

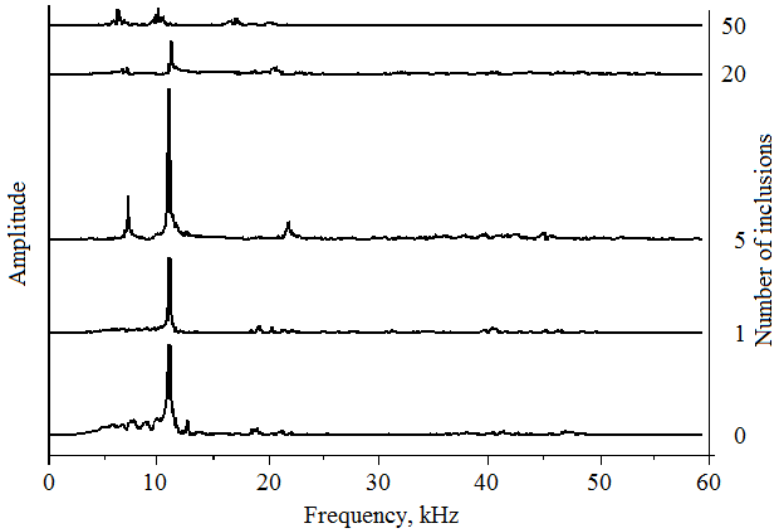


Figure 2. Changes in spectral characteristics of the electromagnetic signal caused by the concentration of internal air cavities

*Conclusion*

The purpose of the research presented in this paper is to study the possibility of testing the air inclusions saturation in cement-sand products using the phenomenon of acoustic-electrical transformations in heterogeneous dielectric materials. Acoustic-electric transformation is a consequence of the interaction of an acoustic wave caused by mechanical impact on the test object with piezoelectric inclusions and double electric layers in the heterogeneous dielectric material. For the purpose of the research, cement-sand samples with different concentrations of air inclusions were made and electro-magnetic responses were measured.

The study of the parameters of electromagnetic signals during deterministic acoustic excitation of model samples made from cement-sand mixture with a varying number of air inclusions showed that an increased number of air inclusions change both the amplitude of the spectral components and the EMS spectrum compared with defect-free samples. In this case, the average weight of the EMS spectrum changes towards lower frequencies. This frequency shift indicates the concentration of defects in the form of air inclusions in samples made from cement-sand mixture and can be used to test concrete products for air inclusions and determine the frost resistance of products.

*Acknowledgments*

This work was supported by the Russian Science Foundation, project No. 20–79–10156

References

1 Ахвердов И. Н. Основы физики бетона / И.Н. Ахвердов. — М.: Стройиздат, 1981. — 464 с.

2 Лужин О.В. Неразрушающие методы испытания бетона / О.В. Лужин. — М.: Стройиздат, 1985. — 236 с.

3 Chitnalah A. Pulse echo method for nonlinear ultrasound parameter measurement / A. Chitnalah, D. Kourtiche, H. Jakjoud & M.Nadi // Electron. J. Tech. Acoust. — 2007. — Vol. 13. — P. 138–145. http://www.ejta.org/en/node/326

4 Bray D.E. Nondestructive evaluation / D.E. Bray, R.K. Stanley. — New York: CRC Press, 1997. — 103 p.

5 Krautkramer J. Ultrasonic Testing of Materials / J. Krautkramer, H. Krautkramer. — Berlin: Springer-Verlag, 1990. — 677 p.

6 Khatiashvili N.G. Generation of the electromagnetic radiation during the passage of acoustic waves through crystalline dielectrics and some rocks / N.G.Khatiashvili, M.E. Perel'man // Dokl. Akad. Nauk SSSR. — 1982. — Vol.263(4). — P. 839–842.

7 Bespalko A.A. Influence Exerted by Siltstone Lamination on the Electromagnetic Signal Parameters during Acoustic Excitation of Samples / A.A.Bespal'ko, R.M. Gol'd, L.V.Yavorovich, D.I.Datsko // Journal of Mining Science. –2002. –Vol.38(2). — P. 124 — 128.

8 Surzhikov A.P. Mechanoelectrical transformations upon the elastic impact excitation of composite dielectric materials / A.P. Surzhikov, T.V. Fursa // Technical Physics. — 2008. — Vol. 53(4). — P. 462–465.

9 Bespalko A.A. Diagnostics of destruction zone development in rock specimens during uniaxial compression based on the spectral characteristics of electromagnetic signals / A.A. Bespalko, L.V. Yavorovich, P.I.Fedotov // Russian Journal of Nondestructive Testing. — 2011. — Vol. 47(10). — P. 680–686.

10 Fursa T.V. Mechanoelectrical transformations in heterogeneous materials with piezoelectric inclusions / T.V. Fursa, D.D. Dann // Technical Physics. — 2011. — Vol. 56(8). — P. 1112–1117.

11 Frid V. Fracture induced electromagnetic radiation / V. Frid, A. Rabinovitch, D. Bahat // J. Phys. D. — 2003. — Vol. 36. — P. 1620–1628.

12 Bespalko A.A. Transformation of acoustic pulses into electromagnetic response in stratified and damaged structures / A.A. Bespalko, Y.N. Isaev, L.V.Yavorovich // Journal of Mining Science. — 2016. — Vol. 52(2). — P. 279–285.

13 Laas R.A. Two-Dimensional Ray Mathematical Model of Mechanoelectric Transformations Method for Location of Macrodefects Identification in Solid Dielectric Structures / R.A. Laas, P.N. Khorsov, A.P. Surzhikov, A.A. Bespalko, A.S. Gyngazov, D.Zh. Karabekova, A.K.Khassenov // Bulletin of the University of Karaganda-Physics. — 2020. — Vol. 10(2). — P. 32–42.

14 Lacidogna G. Acoustic and electromagnetic emissions as precursor phenomena in failure processes / G. Lacidogna, A. Carpinteri, A. Manuello, G. Durin, A. Schiavi, G. Niccolini & A. Agosto // Strain. — 2010. — Vol. 47. — P. 144–152.

15 Голямина И.П. Ультразвук. Маленькая энциклопедия / И.П. Голямина. — М.: Сов. энцикл., 1979. — 400 с.

Д.Д. Данн, М. В. Петров, П.И. Федотов, Е.А. Шевелева

## Сыртқы детерминирленген акустикалық әсер ету кезінде ауа қуыстарынан ақаулары бар модельдік диэлектрлік үлгілердің электромагниттік реакция параметрлерінің өзгеруі

Мақалада гетерогенді диэлектрлік материалдардағы акустикалық-электрлік қайта құру құбылысын қолдана отырып, цемент-құм қоспасынан жасалған үлгілердің ауа қосылыстарымен қанықтылығын сынау мүмкіндігі қарастырылды. Эксперимент әдісі, оның ішінде сыртқы акустикалық қозу және осындай әсерге электромагниттік реакцияны контактісіз тіркеу ұсынылған. Шариктің соққысымен үлгілердің детерминирленген акустикалық қозуы және энергияны эксперименттік анықтау әдістері және полиэтилен қабығындағы ауа қуыстарының әр түрлі санын қамтитын модельдік үлгілердің

өлшемдері мен құрамы сипатталған. Үлгілердің акустикалық қозу бағытын және дабыл мен сыртқы электромагниттік шудың арақатынасының максималды мәнін қамтамасыз ететін электромагниттік дабылдардың қабылдау тақталарының орналасуын көрсете отырып, эксперименттік зерттеулердің жүргізу геометриясы көрсетілген. Ақаусыз үлгімен салыстырғанда, олардағы ауа қуыстарының саны артқан кезде спектрлік компоненттердің амплитудасы да, электромагниттік дабылдар спектрі де өзгеретіні көрсетілген. Осы жағдайда ЭМД спектрінің орташа салмағы төменгі жиілік аймағына өзгереді. Бұл жиіліктің жылжуы цемент-құм қоспасының үлгілеріндегі ауа қуыстары түріндегі ақаулардың концентрациясын тиімді көрсетеді және бетон өнімдерін ауа қосылыстарының болуына сынау кезінде қолдануға болады және сәйкесінше өнімдердің аязға төзімділігін анықтауға мүмкіндік береді. Мақалада келтірілген зерттеу нәтижелері ауа қуыстары түріндегі ақаулардың концентрациясының өзгеруі электромагниттік реакцияның сынақ спектрлік компоненттерінің ығысуымен жақсы бақыланатынын көрсетті.

*Кілт сөздер:* акустикалық-электрлік түрлендірулер, акустикалық қозу, электромагниттік реакция, амплитудалық-жиіліктік сипаттама, диэлектрлік құрылымдар, цемент-құм ерітіндісі, ақау, қос электр қабаты.

Д.Д. Данн, М.В. Петров, П.И. Федотов, Е.А. Шевелева

## Изменения параметров электромагнитного отклика модельных диэлектрических образцов с дефектами из воздушных полостей при внешнем детерминированном акустическом воздействии

В статье обсуждена возможность тестирования насыщенности воздушными включениями образцов из цементно-песчаной смеси, используя явление акустико-электрических преобразований в гетерогенных диэлектрических материалах. Представлена методика проведения эксперимента, включающая контактное внешнее акустическое возбуждение и бесконтактную регистрацию электромагнитного отклика на такое воздействие. Описаны способы детерминированного акустического возбуждения образцов ударом шарика и экспериментального определения энергии, а также размеры и состав модельных образцов, включающих различное количество воздушных полостей в полиэтиленовой оболочке. Показана геометрия проведения экспериментальных исследований с указанием направления акустического возбуждения образцов и расположения принимающих пластин электромагнитных сигналов, обеспечивающих максимальное значение соотношения сигнала и внешнего электромагнитного шума. Показано, что, по сравнению с бездефектным образцом, при увеличении количества воздушных полостей в них изменяется как амплитуда спектральных составляющих, так и спектр электромагнитных сигналов. При этом средний вес спектра ЭМС смещается в область более низких частот, которая эффективно отображает концентрацию дефектов в виде воздушных полостей в образцах цементно-песчаной смеси и может быть применена при тестировании бетонных изделий на присутствие воздушных включений, и, соответственно, позволит определить морозостойкость изделий. Результаты проведенных исследований показали, что изменение концентрации дефектов в виде воздушных полостей наилучшим образом отслеживается смещением тестовых спектральных составляющих электромагнитного отклика.

*Ключевые слова:* акустико-электрические преобразования, акустическое возбуждение, электромагнитный отклик, амплитудно-частотная характеристика, диэлектрические структуры, цементно-песчанный раствор, дефект, двойной электрический слой.

## References

1 Akhverdov, I.N. (1981). *Osnovy fiziki betona [Fundamentals of Concrete Physics]*. Moscow: Stroiizdat [in Russian].

2 Luzhin, O.V., Volokhov, V.A., Shmakov, G.B., & Pochtovik, G.Ya. (1985). *Nerazrushaiushchie metody ispytaniia betona [Nondestructive methods of testing concrete]*. Moscow: Stroiizdat [in Russian].

3 Chitnalah, A., Kourtiche, D., Jakjoud, H., & Nadi, M. (2007). Pulse echo method for nonlinear ultrasound parameter measurement. *Electron. J. Tech. Acoust,* 13, 138–145.

4 Bray, D.E., & Stanley, R.K. (1997). *Nondestructive evaluation.* New York: CRC Press.

5 Krautkramer, J., & Krautkramer, H. (1990). *Ultrasonic Testing of Materials*. Berlin: Springer-Verlag.

6 Khatiashvili, N.G. & Perel'man, M.E. (1982). Generation of the electromagnetic radiation during the passage of acoustic waves through crystalline dielectrics and some rocks. *Dokl. Akad. Nauk SSSR*, 263(4), 839–842.

7 Bespalko, A.A., Gold, R.M., Yavorovich, L.V. & Datsko D.I. (2002). Influence Exerted by Siltstone Lamination on the Electromagnetic Signal Parameters during Acoustic Excitation of Samples. *Journal of Mining Science,* 38(2), 124–128.

8 Surzhikov, A.P. & Fursa, T.V. (2008). Mechanoelectrical transformations upon the elastic impact excitation of composite dielectric materials. *Technical Physics*, 53(4), 462–465.

9 Bespalko, A.A., Yavorovich, L.V. & Fedotov, P.I. (2011), Diagnostics of destruction zone development in rock specimens during uniaxial compression based on the spectral characteristics of electromagnetic signals. *Russian Journal of Nondestructive Testing*, 47(10), 680–686.

10 Fursa, T.V., & Dann, D.D. (2011). Mechanoelectrical transformations in heterogeneous materials with piezoelectric inclusions. *Technical Physics*, 56(8), 1112–1117.

11 Frid, V, Rabinovitch, A. & Bahat, D. (2003). Fracture induced electromagnetic radiation. *J. Phys. D*, 36,1620–1628.

12 Bespalko, A.A., Isaev, Y.N. & Yavorovich, L.V. (2016). Transformation of acoustic pulses into electromagnetic response in stratified and damaged structures. *Journal of Mining Science*. 52(2), 279–285.

13 Laas, R.A., Khorsov, P.N., Surzhikov, A.P., Bespalko, A.A., Gyngazov, A.S., & Karabekova D.Zh. et al. (2020). Two-Dimensional Ray Mathematical Model of Mechanoelectric Transformations Method for Location of Macrodefects Identification in Solid Dielectric Structures. *Bulletin of the University of Karaganda-Physics*, 10(2), 32–42.

14 Lacidogna, G., Carpinteri, A., Manuello, A., Durin, G., Schiavi, A., & Niccolini, G. et al. (2010). Acoustic and electromagnetic emissions as precursor phenomena in failure processes. *Strain*. 47. 144–152.

15 Galyamina, I.P. (1979). *Ultrazvuk. Malenkaia entsiklopediia [Ultrasound. Little Encyclopedia]*. Moscow: Sovetskaia entsiklopediia [in Russian].

DOI 10.31489/2021Ph1/18-25
UDC 622.333

S.B. Imanbaeva[1], A.D. Mausymbaeva[2], V.M. Yurov[3], V.S. Portnov[1*], N.V. Reva[4], A.D. Sultan[1]

*[1*]Karaganda Technical University, Republic of Kazakhstan;*
*[2]Nazarbayev University, Republic of Kazakhstan;*
*[3]Karaganda University named after E.A. Buketov, Republic of Kazakhstan;*
*[4]Taras Shevchenko National University of Kyiv, Ukraine*
*(E-mail: svetakaz77@mail.ru,aliya_maussym@mail.ru, exciton@list.ru, [*]vs_portnov@mail.ru, mvreva@univ.kiev.ua)*

# Gas content of the $D_6$ coal seam

The article deals with the issues of gas content of the most thick and stable $D_6$ coal seam in the Tentek region. This complex structure seam is dangerous in underground mining for gas and dust outbursts, it consists of coal packs separated by interlayers of mudstones, while the lower layer 0.5-1.5 m thick is very soft, has a strong shear disturbance and is most saturated with methane. Extraction of coalbed methane is a necessary process to ensure the safety of mining operations, to reduce its emissions into the atmosphere, and to utilize it as a fuel and a product for obtaining synthetic materials. The regularity of changes in the particle size distribution of the upper thick pack and the lower thin pack indicates the difference in small coal particles in them, while there are much more of them in the lower layer therefore, the specific surface is larger, which is an important factor of the adsorption processes intensity in the accumulation of methane, and during the gas drainage from the seam. The activation energy of methane from carbohydrate has been determined. A quadratic relationship between methane gas evolution and its initial concentration has been shown. In carbohydrate, it depends on the energy of external forces. A complex relationship has been established between the gas pressure in the coal seam and its concentration and characteristics of the «coal-methane-natural moisture» system. Regularities of changing the methane content of the coal seam depending on its fracturing formed due to the effect of the energy of destruction and the energy appearing with increasing the area of a crack in the coal, have been obtained. The effect of the coal mineral composition on the gas content has been shown.

*Keywords:* methane, particle size distribution, fracturing, drainage, well, energy of destruction.

## *Introduction*

In the mixture of greenhouse gases, methane can remain in the atmosphere within 9 to 15 years. It retains 20 times more heat than carbon dioxide. Understanding the problem of the presence and interaction of methane with the environment increases the need to develop projects for its extraction from coal seams. Methane processing and utilization has advantages over direct emission into the atmosphere. Possible options of utilizing coalbed methane include power generation, production of compressed or liquefied gas, use in blast furnaces and for calcining lime at the metallurgical plant of the ArcelorMittal Temirtau JSC.

Extraction of methane from coal seams will provide the following benefits: improving the safety in coal mines and the health of miners, selling natural gas and its products, using carbon GNG credits for sale, and increasing coal production [1].

The gas concentration and pressure, the permeability coefficient, particle size distribution of coals are the main factors, which studying makes it possible to estimate the drainage parameters, as well as to calculate the gas balance during coal mining.

The $D_6$ seam consists of two seams. The upper layer 4.82 - 6.48 m thick is represented by brilliant coal with strong cleavage. The lower one varies in thickness from 0.5 to 1.5 m, has a strong strike-slip fault, and is very soft. The gas pressure in coal is at least 4.5 MPa with its content from 18 to 19 $m^3$/t. Based on this, the lower layer is highly hazardous in terms of emissions without the use of drainage. Its initial permeability is less than 0.1 md, and it can increase depending on the natural variability or the man-made impact.

## *Results and discussion*

Studying the particle size distribution of coals shows that in samples from the upper and lower layers of the seam, 66% of particles are smaller than 0.6 mm, the sample from the lower layer consists of 48% of particles that are smaller than 0.1 mm, while coal from the upper layer consists of only 14% of particles smaller than 0.1 mm (Figure 1) [1].

The larger particles of the upper layer of the $D_6$ seam are mainly disk-shaped, while the smaller particles are like cubes. The ratio of the shortest to the longest side is on average 3:1 for all sieve hole diameters. The breeze is approximately disk-shaped and 43% of the sample mass consists of "small" particles [1].

The particles of the lower layer of the $D_6$ seam are mainly rounded. The ratio between the shortest and the longest sides is in the range from 2:1 to 3:1. The particles are similar in shape to cubes and 66% of the sample mass consists of «small» particles.

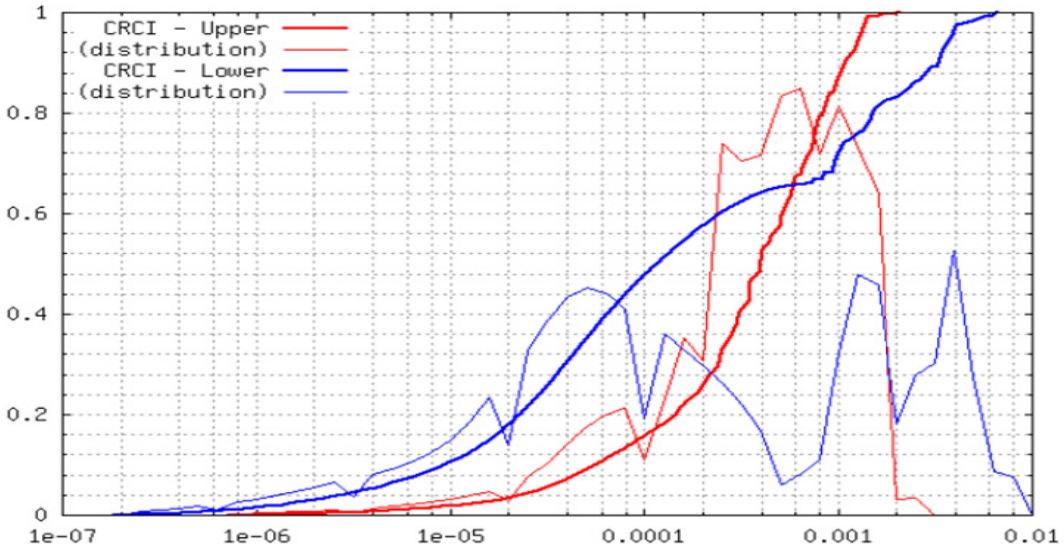


Figure 1. Particle size distribution: the upper and the lower layers of the $D_6$ seam [1]

To estimate the effect of permeability on drainage, a number of model studies have been carried out for a homogeneous coal seam with the thickness of 6 m and the initial pressure of 4.5 MPa, draining to a gauge pressure of 0.5 MPa. The results are shown in Figure 2, where the abscissa represents the distance between the wells, and the ordinate represents the time required to drain the gas to the pressure of 0.5 MPa [1].

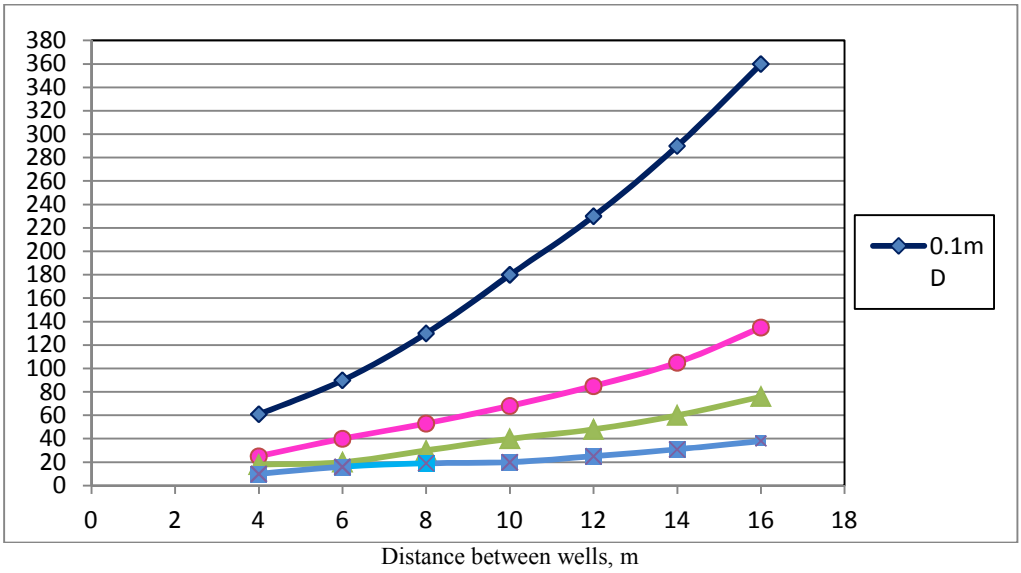


Figure 2. Methane drainage time in the coal seam before reaching pressure of 0.5 MPa depending on the seam permeability and the distance between the wells [1]

Gas permeability of coals is mainly determined by the permeability of endogenous and exogenous cracks, porosity. It inversely depends on the value of the external load and the degree of coal metamorphism, as well as on its gas content and on the degree of filling the filtering volume of pores and microcracks with natural moisture (phase permeability of coal). The amount of methane per unit of dry ash-free coal mass is

determined by the sorption isotherm, and regularly changes with the degree of metamorphism reaching maximum values for natural coals at the semi-anthrocyte stage of 43-45 $m^3$/t. Metamorphism processes lead to the transformation of coals, they affect inter-atomic interactions, the essence of which is to simplify their chemical composition and structure carbon in the organic mass of coal [2].

*Methane in coal*. Changing the geomechanical state of coal seams and coal-bearing rocks leads to deformation of interatomic bonds, initiation of chains of relaxation processes in the form of mechanochemical transformation of the organic mass of coal with the formation of gaseous products, mainly methane. The natural methane content of the $D_6$ coal seam ($m^3$/t) at various depths varies too. In the interval of the depth of the upper boundary of methane gases from 180-250 m to the depth of 300 m, the methane content varies within 3-18 $m^3$/t; in the depth intervals 301-600 m within 18-28 $m^3$/t, and 601-900 m within 30-32 $m^3$/t. The forecasted values of natural methane content at the depths from 900 to 1500 m range from 23 to 36 $m^3$/t. In works [3, 4] one of the options of the methane state in coals (as a percentage of the total amount) is considered as:

– free: inside macropores, microcracks and other defects of continuity in coals in natural conditions — 2-12%;

– adsorbed: on the carbon surfaces of natural pores and defects of continuity, interblock spaces (including the volumetric filling of transition pores and macroscopic defects-cracks) — 8-16%;

– solid coal-methane solution in the intermolecular space of the substance — 70-80%;

– chemical sorbed methane — 1-2% in defects in aromatic layers of crystallites;

– solid interstitial solution inside gas hydrates solid crystalline substances with the size of 0.38-0.92 nm, that form all hydrophobic gases including methane.

Methane adsorbed by coal is distributed between the solid solution (absorption) and the surface of cracks and pores (adsorption), and since coal has a large specific surface, about 20 $m^2/cm^3$, the amount of adsorbed methane can be comparable to the amount absorbed [2]. This is possible if the binding energy of the methane molecule with the coal surface $E_B$ is much lower than the energy of the methane molecule entering the solid solution ($E_B \geq 200$ kJ/mol) [4]. If the energy supplied is greater than the energy of the entry of the methane molecule into the solid solution, then the methane molecules begin to leave the coal particle. In this case, the mass of the coal methane particle begins to decrease, similar to the dissolution (melting) of the particle, and this process proceeds according to the law of phase transitions of the first kind. The bond of the methane molecule with the coal substance is mainly provided by the van der Waals forces.

Let's suppose that near the surface of a coal particle, the concentration of methane is $C_0$; by supplying external energy (changing the stress state of the coal mass), methane begins to be released from it, the concentration of which near the boundary is C1, and at a considerable distance from it is $C_\infty$.

Using these characteristics, we have obtained the parameter λ equal to [3]:

The dependence of the pairwise decomposition of a coal-methane particle (τ0) is determined by the expression $\tau_0=|\lambda|^{-1}$. It should be noted that the «apparent» changing of the radius of the coal-methane particle corresponds to changing its mass similar to the dissolution or melting of the coal-methane particle, in proportion to the methane emission from the solid solution. Since the parameter (λ) is proportional to the pressure $\Delta p$ at the phase interface, the comparison of the obtained regularities of the coal methane decomposition with the isobar of methane sorption at 1 atm. given for the coals of the Donetsk, Karaganda and Kuznetsk basins [4, 5], indicates their coincidence, since the process sorption and desorption are reversible.

When considering the changing of the coal-methane particle radius, it should be borne in mind that small-sized particles are characterized by the decreased surface tension, which leads to decreasing the «melting» temperature of coal-methane particles $T_{mp}$ , i.e. to reducing its decay energy [6]:

$$T_{mp}(r) = T_0\left(1 - \frac{d}{r}\right) \text{ for } d=\frac{2\delta V_0}{RT}, \quad (2)$$

where d is the critical radius starting from which the size effect takes place; $T_0$ is the melting point of the bulk sample; R is the universal constant, $V_0$ is the molar volume of methane, r is the particle radius, δ is the specific gravity of methane.

Expression (2) determines the decomposition rate of a coal-methane particle, i.e. methane release, which is caused by decreasing the surface tension, which is most typical for small particles of coal in the lower layer of the $D_6$ seam.

The process of the methane coal decomposition occurs under the effect of some external energy (thermal, mechanical, etc.) that occurs during the development of the seam and is an irreversible process.

The probability of dissipative processes is determined by the expression [7]:

$$P = \frac{2\Delta S}{k\tau} \exp\left\{-\frac{E_m - \frac{G^0}{N}}{kT}\right\}, \quad (3)$$

where $\Delta S$ is entropy changing in the dissipative process; $E_m$ is the mean value of the molecule basic state energy; $\tau$ is the relaxation time; $G^0$ is the Gibbs energy, k is the Boltzmann constant ($1.380649*10^{-23}$ J/k), N is the Avogadro number.

The energy of decomposition (destruction) activation of the coal matter for the i-th gas is determined by the expression:

$$E_{ai} = \frac{E_{mi} - G_i^0/C_i}{kT}, \quad (4)$$

where $E_{mi}$ is the energy of the gas molecule activation, $G^0$ is the Gibbs energy, T is the absolute temperature, $C_i$ is the i-th gas molecules concentration.

Taking into account the Gibbs energy additivity for non-mutually acting particles:

$$G^\circ = \sum_{i=1}^{n} C_i G_i^0;\ C = \sum_{i=1}^{n} C_i;\ E_m = \sum_{i=1}^{n} E_i, \quad (5)$$

From (5) it is obvious that the pure destruction of the coal matter is selective, an d the function of gas emission is stepwise depending on $E_{mi}$,; the more gas or volatile molecules, the lower the activation energy.

Let's consider the part of gas emission that is associated with methane. In this case the activation energy of coal methane will have the form:

$$E_a = \frac{200 - G_y^0/C}{kT}. \quad (6)$$

Here, $E_m$ = 200 kJ/mol is taken as the average binding energy of methane in coal matter. The activation energy for the decomposition of methane coal depends on the temperature, while the graph of gas evolution is also stepwise in accordance with $E_{mi}$.

Expression (6) based on the smallness of the ratio $G^0/C$ for methane equal to $536*10^{-23}$, where $G_y^0 0$ is the Gibbs energy of the hydrocarbon, can be written by denoting the binding energy (or decay energy) of methane in the form $G_y^0/C = E_m$. From the ratio it follows that the lower the Gibbs energy of the hydrocarbon ($G_y^0$), the lower the activation energy of coal-methane, so the temperature of the beginning of gas evolution, fusenite is 390°C, vitronite 335°C, enertite 250°C.

The average activation value for coals of varying degrees of metamorphism is determined - about 0.65 kJ/mol [7].

In work [4], a relationship was established between the gas evolution of methane (C) and its initial concentration ($C_0$) in the hydrocarbon (methane content) of the coal seam.

$$C = \frac{kT}{K_1} \frac{A}{G^0} M_0^2, \quad (7)$$

where A is the work (energy of external forces), $K_l$ is a constant. The last equation characterizes the quadratic dependence of gas emission on the seam methane content ($M_0$).

***Gas pressure in the seam.*** In the natural state, in the coal matter there is a dynamic equilibrium between the adsorbed, absorbed and free phase methane, which is characterized by the fact that at any moment in the absence of extreme external impacts, the number of methane molecules passing from the free phase to the sorbed state is practically equal to the number of molecules of the desorbed methane. Free methane in the coal bed under natural conditions occupies a volume within which its and the molecules interaction with the coal surface is relatively low therefore, the volume of methane in the free phase in voids and cracks of coal is usually insignificant. Under such conditions, it plays the role of a "back-up" for sorbed methane preventing its desorption. Disruption of the dynamic equilibrium between methane in the free and sorbed phases in the natural system "coal – methane – natural moisture" during redistribution of rock pressure (under the impact of tectonic processes or mining operations) is manifested in increasing the number of desorbed methane molecules over the number os molecules that are sorbed by coal.

It has been established [8] that the volume of methane in the free phase at the depth of 700-1200 m in coals of medium metamorphism ((Vdaf = 18-19%) is from 5 to 10% of the total methane contained in coal, in coals of a high degree of metamorphism ((Vdaf = 18-14%) it is from 4 to 6%, and in slightly metamorphosed coals ((Vdaf = 30-38%) it is up to 10-12%. When the established dynamic equilibrium in the natural system «coal-methane-natural moisture» is violated, the movement of methane molecules from natural coal pores occurs both by moving along their walls, and by passing from an absorbed state to an adsorbed one and then to a free state, that is , the decomposition of methane coal occurs, accompanied by a decrease in the pressure of methane in coal [9, 10]. Since G0=H-TS+PV1 then at C-C0,, where C0 is the initial concentration of methane in the hydrocarbon (coal seam), and C is the current value of the methane concentration, we obtain the methane pressure in the seam equal to:

$$\mathrm{P} = [\mathrm{C}_0 - \mathrm{K}_2(\mathrm{H} - \mathrm{TS})]/(\mathrm{K}_2\mathrm{V}), \tag{8}$$

where H is enthalpy, S is entropy, K2 is a constant, V is the volume, T is the environment absolute temperature. The equation shows a complex dependence of gas pressure in the coal seam on its concentration and properties of the coal matter. It is seen that increasing the pressure increases the methane content of coal [10].

***Formation of cracks in coals.*** Since characteristics of the methane content of the coal seam are associated with the surfaces and cracks of the massif, let us consider formation of cracks in coals as one of the reasons for its destruction including the instantaneous one, and formation of surfaces.

One of the important results of A. Griffiths [11] is the criterion he formulated for the destruction of a body with a crack, according to which the growth of a crack should be an energetically favorable process with energy conversion [12]. Let us express the condition of crack growth in the form of the energy balance:

$$\frac{\partial}{\partial \mathrm{l}}(\mathrm{W} - \Gamma) = 0, \tag{9}$$

where W is the potential energy of the plate deformation; Γ is the crack surface energy for a plate of a unit thickness, Γ=4$l\gamma$; $l$ is the half length of the crack, $\gamma$ is specific surface energy of destruction [3].

The condition of destruction can be written down as follows:

$$\frac{\partial \mathrm{W}}{\partial \mathrm{l}} \geq \frac{\partial \Gamma}{\partial \mathrm{l}}. \tag{10}$$

From condition (10) it follows that a crack in a solid (coal mass) will develop during its deformation, that is, the action of rock pressure exerted on the coal seam, provided that the rate of the potential deformation energy release is greater than increasing the surface energy of the body, which is formed as a result of the formation of new surfaces.

Let's suppose that the crack element is determined by the product of a linear surface element by some function $\Phi(u, v)$, which depends on the stress state in the vicinity of this linear element [4]. For brittle fracture, this function should be proportional to the normal, highest stress (F) or the highest linear deformation determined by Young modulus (E) and the Gibbs potential (G).

Thus, the trajectory of a crack is a geodesic line in the non-Euclidean space, the metric of which depends on the stress-strain state of the rock massif [4].

Then the Euler–Lagrange equation that can be used to obtain the equation of crack growth, takes the form:

$$\frac{\partial \mathrm{M}}{\partial \mathrm{u}} - \frac{\mathrm{d}}{\partial \mathrm{v}}\frac{\partial \mathrm{M}}{\partial \mathrm{v}'} = 0\,, \tag{11}$$

where $\mathrm{M}=\Phi(u, v)\sqrt{\mathrm{E} + 2Fv' + G(v')^2}$.

The behavior of stationary cracks can be described using the variation condition dE=0, and non—stationary using the equation Φ (u,$v$)

$$\int_{\mathrm{t}_0}^{\mathrm{t}} \mathrm{dEdt} = 0, \tag{12}$$

where $E=\int_{l_0}^{l(t)} lds$ is the functional reflecting the difference between the energy of absorption $\int_0^{l(e)} \gamma ds$ consumed for the destruction and supply process $\int_0^{l(t)} \varphi ds$ that is emitted with the crack growth, $L=\gamma - \varphi$. This functional can be considered as free energy or as the value proportional to the inner entropy increment.

The intensity of energy consumption for fracture ($\gamma$) represents the energy required to form a unit area of the emerging new crack surface. The value of $\gamma$ depends on the local resistance to separation of particles (petrographic composition of coals), plasticity, viscosity of the material and their change with the growth of the crack.

The intensity of the release of the supply energy arising in connection with increasing a unit area of the crack $\varphi$ is spent on its formation, and only after the crack element formation the excess supply energy can be dissipated or transformed into kinetic energy.

The majority of natural mechanical systems in free motion dissipate the ordered kinetic energy of their motion and convert it into the chaotic thermal motion of molecules. Generally speaking, the total mechanical (potential+kinetic) energy in them decreases, passing into other forms (seismo-acoustic and electromagnetic, arising during the crack formation), they, ultimately, are converted into into thermal energy. Such systems are called dissipative, and the process is called dissipation.

In case when the intensity of the supplied energy flow is such that the existing dissipation mechanism cannot cope with it, then such a system is destroyed due to the formation inside its elements, for a more intense energy dissipation. Such internal rearrangement leads to the internal dissipated structures formation with the aim of more intense dissipation of the energy supplied to the system. Their existence is possible only with a constant flow of energy from outside (rock pressure).

These processes form the conditions for the instant destruction of the coal massif.

***The coal mineral part effect on coal methane decomposition.*** Coal seams contain heterogeneous minerals, such as: kaolin, albite, orthoclase, calcite, quartz, siderite, aragonite, magnesite and other various mineral inclusions.

For ideal solid solutions, the Gibbs energy is additive, then the activation energy of methane ($E_a$) with the concentration of this gas (G) molecules will have the form:

$$E_a = \frac{1}{C}\sum_{i=1}^{n} X_i G_i^0, \quad (13)$$

where $X_i$ is the mole concentration of the coal mineral part component; C is the methane molecules concentration in coal; $G_i^0$ is the Gibbs energy of the i-th component.

From formula (13) it follows that increasing the proportion of the mineral part of coal, especially oxides, leads to increasing the activation energy and, consequently, to inhibiting the decomposition of coal methane.

*Conclusion*

The initial gas content of the $D_6$ seamr at the Kazakhstanskaya and Lenin mines is 18 $m^3$/ton, and the $D_6$ seam is gas-bearing, despite the high ash content. Natural seam pressure at the depth of 683 m is about 4.5 MPa. This is the reason for the high associated gas content, which is 67% of the hydrostatic pressure for the depth of 683 m.

The lower layer of the seam consists of highly outburst-prone coal. In general, the $D_6$ seam is considered to be sufficiently connected to the lower layer so that the initial gas pressure remains the same throughout the entire seam thickness. Variations in the petrophysical characteristics of the seam and the seam gas are associated with geological conditions, such as tectonic faults, folding, the presence of a crushing zone, etc. Possible increasing the in discharge during drainage of the seam is a sign of the effect of drainage or increasing permeability caused by coal shrinkage.

Drilling in the $D_6$ seam can be complicated by the soft coal of the lower layer, which has shear disturbances, and it is possible that the wells that cross this soft coal will be complicated during drilling with flushing, since sticking is possible in this interval, and there is also a high probability of the drilling tools loss, inclinometers for directional drilling.

A hyperbolic dependence of the complete disintegration of a coal particle on the ratio of the difference in the concentration of methane in the particle at its boundary and in the distribution has been established.

The energy of decomposition of the coal substance has been determined depending on the activation energy and the concentration of methane, the temperature and the Gibbs energy of the carbohydrate.

The regularity of changing the gas pressure in coal depending on the initial concentration of methane and the thermodynamic parameters of the system has been obtained.

The regularities of the crack formation in coals have been, which are determined by the destruction energy spent on the formation of a unit surface area of a new crack and the supply energy arising from increasing a unit area of the crack, while excess energy can dissipate or transform into kinetic energy.

The total mechanical energy, when exposed to loads decreases when passing into seismo-acoustic and electromagnetic energy, and ultimately into thermal energy.

It has been found that the ash content of coals leads to increasing the activation energy for methane emission from them, i.e., to inhibiting the decomposition of coal methane.

## References

1 Gray I. Mining gassy coals. Proceedings of the 12th Coal Operators' Conference [Electronic resource] / I. Gray // Mining Engineering, University of Wollongong. — 2012. — P. 249–259. — Access mode: https://ro.uow.edu.au/coal/414

2 Алексеев А.Д. Распад твердых углегазовых растворов / А.Д. Алексеев, А.Т. Айруни, И.В. Зверев, А.И. Балабин // Физико-технические горные проблемы разработки полезных ископаемых. — Новосибирск, 1994. — № 3. — С. 65–75.

3 Swapan K.H. Elements of Mining. Mineral Exploration [Electronic resource] / K.H. Swapan. — Kolkata: Presidency Universiti, 2018. — 378 p. — Access mode: https://doi.org/10.1016/C2017–0-00902–3

4 Газалиев А.М. Прогрессивные технологические решения добычи и транспортировки метана: моногр. / А.М. Газалиев, В.С. Портнов, Г.Г. Таткеева. — Караганда: Изд.-полиграф. центр Казах.-Рос. ун-та, 2010. — 204 с.

5 Ножкин Н.В. Заблаговременная дегазация угольных месторождений: учеб. пос. / Н.В. Ножкин. — М.: Недра, 1979. — 271 с.

6 Portnov V. New approaches to the problem of sudden outburst of gas and coal dust. Progressive Technologies of Coal, Coalbed Methane and Ores Mining: monography / V. Portnov, R. Kamarov, I. Shmidt, V. Yurov. — London: CRC Press, 2014. — 394 p.

7 Портнов В.С. Энергия диспергирования упорных руд и минералов: моногр. / В.С. Портнов, В.М. Юров, М.С. Ахметов. — Караганда: Изд-во Караганд. гос. техн. ун-та, 2014. — 160 с.

8 Portnov V. Link of specific electric resistance with qualitative and strength characteristic of ores. Progressive Technologies of Coal, Coalbed Methane and Ores Mining: Monography / V. Portnov, R. Kamarov, A. Mausymbayeva, V. Yurov. — London: CRC Press, 2014. — 534 p.

9 Айруни А.Т. Равновесное распределение газов в угольных пластах / А.Т. Айруни, Э.П. Фельдман // Письма в ЖТФ. — 2008. — Т. 34. — Вып. 14. — С. 48–53.

10 Шевкопляс В.Н. Взаимосвязь эффективной энергии активации процесса термического разложения твёрдых топлив с динамикой потери массы / В.Н. Шевкопляс, Л.Ф. Бутузова, С.Н Лящук // Вопросы химии и химической технологии. — 2008. — № 2. — С. 116–120.

11 Griffith A.A. The theory of rupture / A.A. Griffith. Proc. First Int. Congr. Appe. Mecu. Delft., 1924. — № 221. — P. 55–63.

12 Каркашадзе Г.Г. Разработка методики экспериментального определения удельной поверхностной энергии разрушения твердых тел / Г.Г. Каркашадзе, С.М Никитин, Д.С. Буянова // Горн. инф.-аналит. бюл. — 2014. — № 6. — С. 263-272.

С.Б. Иманбаева, А.Д. Маусымбаева, В.М. Юров, В.С. Портнов, Н.В. Рева, А.Д. Сұлтан

## $Д_6$ көмір қабатының газдылығы

Мақалада Тентек ауданындағы ең қуатты және тұрақты $Д_6$ көмір қабатының газдылығы мәселелері қарастырылған. Бұл күрделі құрылым қабаты жерасты қазбаларында газ бен шаң үшін қауіпті, ол сазтас қабаттарымен бөлінген көмір қабаттарынан тұрады, ал төменгі қабаты 0,5-1,5 м өте жұмсақ, ығысудың қатты бұзылысына ие және метанмен қаныққан. Көмір қабаттарынан метанды өндіру — шахталардағы тау-кен жұмыстарының қауіпсіздігін қамтамасыз ету, оның атмосфераға шығарылуын төмендету және синтетикалық материалдарды алу үшін оны отын және өнім ретінде пайдалану үшін қажетті процесс. Жоғарғы, қуатты қабаттың және төменгі жұқа қабаттың гранулометриялық құрамының өзгеру заңдылығы ондағы көмірдің кішкене бөлшектерінің айырмашылығын көрсетеді, ал олардың төменгі қабатында олардың көп мөлшері бар, демек, меншікті беті үлкен, бұл метанның жиналуындағы және газды құрғату кезінде адсорбциялық процестердің қарқындылығының маңызды факторы. Көмір заттарынан метанды белсендіру энергиясы анықталды. Метан газының бөлінуі мен оның бастапқы концентрациясы арасындағы квадраттық байланыс көрсетілген. Көмір затында бұл сыртқы күштердің энергиясына байланысты. Көмір қабатындағы газ қысымы оның концентрациясымен және «көмір-метан-табиғи ылғалдылық» жүйесінің сипаттамалары арасындағы күрделі байланыс анықталған. Көмір қабатының метандылығының жарықшақ бұрышында байқалатын аудан өсімімен пайда болатын энергия

мен энергияның ыдырауы әсерінен қалыптасатын, оның жарықшақтылығынан өзгеру заңдылықтары алынды. Көмірдің минералды құрамының газ құрамына әсері көрсетілген.

*Кілт сөздер:* метан, гранулометриялық құрам, жарықшақтық, дренаж, ұңғыма, энергияның ыдырауы.

С.Б. Иманбаева, А.Д. Маусымбаева, В.М. Юров, В.С. Портнов, Н.В. Рева, А.Д. Сұлтан

## Газоносность угольного пласта $Д_6$

В статье рассмотрены вопросы газоносности самого мощного и устойчивого угольного пласта $Д_6$ в Тентекском районе. Данный пласт по типу сложного строения, опасен при подземной добыче по газу и пыли. Состоит из угольных пачек, разделенных прослоями аргиллитов, при этом нижний слой мощностью 0,5–1,5 м очень мягкий, имеет сильное сдвиговое нарушение и наиболее насыщен метаном. Извлечение метана угольных пластов является необходимым процессом для обеспечения безопасности ведения горных работ в шахтах, снижения его выброса в атмосферу, утилизации в качестве топлива и продукта для получения синтетических материалов. Закономерность изменения гранулометрического состава верхней мощной пачки и нижней тонкой свидетельствует о различии в них мелких частиц угля, при этом в нижнем слое их значительно больше, и, следовательно, удельная поверхность больше, что является важным фактором интенсивности адсорбционных процессов накопления метана и при дренировании газа из пласта. Определена энергия активации метана из углевещества. Показана квадратичная связь между газовыделением метана и его начальной концентрацией. В углевеществе она зависит от энергии внешних сил. Установлена сложная связь между давлением газа в пласте угля от его концентрации и характеристик системы «уголь–метан–природная влага». Получены закономерности изменения метаноносности угольного пласта от его трещиноватости, формируемой за счет влияния энергии разрушения, и энергии, появляющейся с приростом площади трещины, возникающей в угле. Показано влияние минерального состава угля на его газоносность.

*Ключевые слова:* метан, гранулометрический состав, трещиноватость, дренаж, скважина, энергия разрушения.

## References

1 Gray, I. (2012). Mining gassy coals. Proceedings of the 12th *Coal Operators' Conference.* (pp. 249-259). Mining Engineering, University of Wollongong. Retrieved from: https://ro.uow.edu.au/coal/414

2 Alekseev, A.D., Airuni, A.T., Zverev, I.V., & Balabin, A.I. (1994). Raspad tverdykh uhlehazovykh rastvorov [Decomposition of solid coal-gas solutions]. *Fiziko-tekhnicheskie hornye problemy razrabotki poleznykh iskopaemykh — Physical and technical mining problems in the development of mineral deposits, 3,* 65-75 [in Russian].

3 Swapan, K.H. (2018). *Elements of Mining. Mineral Exploration*. Kolkata: Presidency Universiti. *doi.org.* Retrieved from https://doi.org/10.1016/C2017-0-00902-3

4 Gazaliev, A.M., Portnov, V.S., & Tatkeeva, G.G. (2010). *Prohressivnye tekhnolohicheskie resheniia dobychi i transportirovki metana* [*Progressive technological solutions for methane production and transportation*]. Karaganda: Izdatelsko-polihraficheskii tsentr Kazakhstansko-Rossiiskoho universiteta [in Russian].

5 Nozhkin, N.V. (1979). *Zablahovremennaia dehazatsiia uholnykh mestorozhdenii [Zablogovernaya degassing of coal deposits]*. Moscow: Nedra [in Russian].

6 Portnov, V., Kamarov, R., Shmidt, I., & Yurov, V. (2014). *New approaches to the problem of sudden outburst of gas and coal dust.Progressive Technologies of Coal. Coalbed Methane and Ores Mining*. London: CRC Press.

7 Portnov, V.S., Yurov, V.M., & Akhmetov, M.S. (2014). *Enerhiia disperhirovaniia upornykh rud i mineralov* [*Energy of dispersion of refractory ores and minerals*]. Karaganda: Izdatelstvo Karahandinskoho hosudarstvennoho tekhnicheskoho universiteta [in Russian].

8 Portnov, V., Kamarov, R., Mausymbayeva, A., & Yurov, V. (2014). *Link of specific electric resistance with qualitative and strength characteristic of ores. Progressive Technologies of Coal. Coalbed Methane and Ores Mining*. London: CRC Press.

9 Airuni, A.T., & Feldian, E.P. (2008). Ravnovesnoe raspredelenie hazov v uholnykh plastakh [Equilibrium distribution of gases in coal seams]. *Pisma v ZhTF — Technical Physics Letters, 34, 14,* 48-53 [in Russian].

10 Shevkoplias, V.N., Butuzova, L.F., & Leshchukh, S.N. (2008). Vzaimosviaz effektivnoi enerhii aktivatsii protsessa termicheskoho razlozheniia tverdykh topliv s dinamikoi poteri massy [The relationship of the effective activation energy of the process of thermal decomposition of solid fuels with the dynamics of weight loss]. *Voprosy khimii i khimicheskoi tekhnolohii — Chemistry & Chemical Technology, 2,*116-120 [in Russian].

11 Griffith, A.A. (1924). *The theory of rupture*. Proc. First Int. Congr. Appe. Mecu. Delft, 221, 55-63.

12 Karkashadze, G.G., Nikitin, S.M., & Buianova, D.S. (2014). Razrabotka metodiki eksperimentalnoho opredeleniia udelnoi poverkhnostnoi enerhii razrusheniia tverdykh tel [Development of a technique for the experimental determination of the specific surface energy of destruction of solids]. *Hornyi informatsionno-analiticheskii biulleten — Mining information and analytical bulletin (Scientific and technical journal), 6,* 263-272 [in Russian].

DOI 10.31489/2021Ph1/26-34
UDC: 621.9.047.7

B.K. Rakhadilov[1], R.S. Kozhanova[2,3,*], Yu.N. Tyurin[4], L.G. Zhurerova[1], Zh.B. Sagdoldina[1]

[1]*Sarsen Amanzholov East Kazakhstan University, Ust-Kamenogorsk, Kazakhstan;*
[2]*Shakarim University, Semey, Kazakhstan;*
[3]*PlasmaScience LLP, Ust-Kamenogorsk, Kazakhstan;*
[4]*E.O. Paton Electric Welding Institute, Kyiv, Ukraine*
(*E-mail: kozhanovars@yandex.ru)

# The technology of thermal cyclic electrolytic plasma hardening of steels

This work describes the technology of thermal cyclic electrolytic plasma hardening, as well as describes the design features of the electrolytic plasma heater. There are presented the results of the research of medium-carbon steel hardness treated by thermal cyclic electrolytic plasma hardening under different conditions. An industrial installation for thermal cyclic electrolytic plasma hardening of materials was developed to carry out thermal cyclic electrolytic plasma hardening of steels in an automated mode. Tempered layers were obtained on the surface of the samples with average thickness values from 0.5 to 10 mm and hardness up to 750 HV. Experimentally that the alternation of switching on the electric potential at a voltage of U1 = 320 V and U2 = 200 V provides heating of the product surface to a depth of 10 mm. In this case, the maximum hardness of the surface layer (750 HV) practically does not depend on the thickness of the hardened layer. The hardness of the hardened layer of the product gradually decreases from the maximum (750 HV) to the hardness of the base (280-300 HV). The developed installation allows to vary the electrophysical parameters within a wide range: to set the voltage, the duration of processing, the time of switching on and off the voltage.

*Keywords:* plasma, electrolyte, technology, structure, hardening, thermocyclic quenching.

## *Introduction*

One of the most important problems of modern mechanical engineering is to ensure maximum wear resistance of machine parts and tools. Machine parts and tools during operation are exposed to large contact loads, abrasive wear, and various types of friction. Therefore, an effective increase in the service characteristics of parts and tools is largely associated with the need to increase their wear resistance. In addition, the durability of parts depends not only on the properties of the material determined by the manufacturing technology and volumetric hardening, but largely, on the surface properties. Its role in ensuring the operational properties of products is constantly increasing, which has contributed to the emergence and development of a new direction - surface engineering by methods of energy and physicochemical effects along with the widespread use of traditional methods of chemical and thermal treatment. The implementation of this concept under choosing a material will improve the performance properties of parts, and in some cases reduce the consumption of expensive materials. Therefore, recently, low-alloy structural and tool steels are increasingly used and produced due to the use of protective coatings and surface hardening, which made it possible to reduce the cost of expensive high-alloy steels and alloys. At the same time, an important role in the use of protective coatings and surface hardening is played using resource-saving technologies that help to reduce the cost of resources and energy, increase labor productivity [1].

Surface treatment of steel parts with the use of heating by concentrated energy flows (electron beam, laser radiation, plasma arc) is a significant reserve for saving material, labor and energy costs [2]. Experience shows that a plasma source of surface heating in many cases can be used along with sources such as laser and electron beam, providing high technical and economic indicators of the process [3]. There are two directions of using plasma heating. The first area should include the technology of ion-plasma [4] and electrolyte-plasma processing [5]. Moreover, the second direction of plasma heating application is based on the use of a compressed arc of direct or indirect action generated by a special plasmatron [6]. The first direction has particular interest among them, specifically the technology of electrolytic plasma treatment, due to which it is possible to achieve sufficiently high operational properties. Electrolytic plasma treatment is one of the methods of high-speed heating, in which the workpiece is the cathode or anode relative to the aqueous electrolyte [5, 7]. The electrical circuit between the electrodes is closed through an electro-

lyte (aqueous salt solution). Conversion of electrical energy into heat occurs mainly in the layer adjacent to the product. As a result of heating, this layer turns into a vapor-gas state, in which micro-arcs are excited under the influence of the applied voltage. The power density reaches up to $3 \cdot 10^3$ W/cm$^2$ [1]. The technology allows varying the rate of heating and cooling and the thickness of the hardened layer within a wide range. By regulating the temperature and speed modes of plasma surface heating and cooling, as well as the use of various electrolytes, it is possible to carry out the processes of nitriding, carburizing, nitrocarburizing, boriding, sulfating and surface hardening [8-10].

In connection with the above, the purpose of this work is to develop a technology for thermal cyclic electrolytic plasma hardening of machine parts and tools, which will increase the wear resistance and hardness of their surface layer, as well as to establish the main regularities of structural-phase transformations in structural and tool steels during electrolytic plasma hardening by the way of surface hardening.

*Material and methods of research*

0.34CrNi1Mn medium-carbon steel was chosen as the object of research in accordance with the tasks set. The choice of research material is justified by the fact that 0.34CrNi1Mn structural alloy steel is used for the manufacture of highly loaded critical parts with high requirements for mechanical properties operating at temperatures not exceeding 500 °C - shafts, disks, rotors of compressor machines and turbines, excavator shafts, gear wheels, couplings, gear shafts, half couplings, power pins, bolts, other products. The chemical composition of 0.34CrNi1Mn steel is presented in Table 1.

Table 1

**The chemical composition of 0.34CrNi1Mn steel**

| Steel | C | Si | Mn | Ni | S | P | Cr | Mo |
|---|---|---|---|---|---|---|---|---|
| 0.34CrNi1Mn | 0.3 - 0.4 | 0.17 - 0.37 | 0.5 - 0.8 | 1.3 - 1.7 | up to 0.035 | up to 0.03 | 1.3 - 1.7 | 0.2 - 0.3 |

Electrolytic plasma hardening of steel samples was carried out in a laboratory setup at the Scientific Research Center «Surface Engineering and Tribology». General view and diagram of the installation for electrolytic plasma treatment is shown in Figure 1. The installation structurally consists of a power source, a chamber for electrolytic plasma processing of materials.

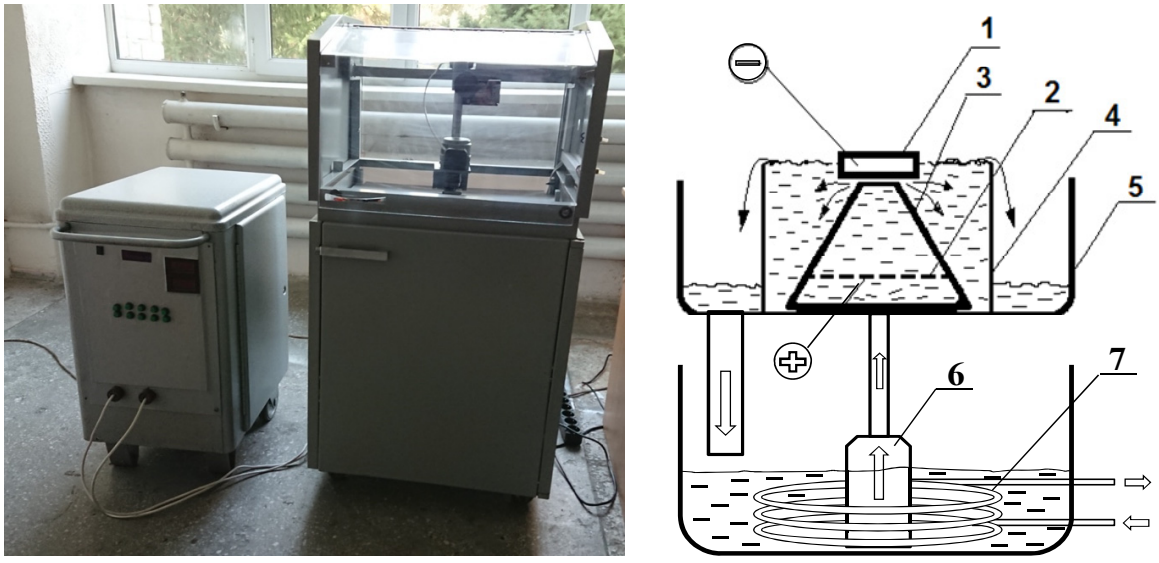


1- treated sample (cathode), 2- stainless steel anode with holes, 3- cone-shaped partition, 4- working chamber of bath with electrolyte, 5- pallet, 6- pump, 7- heat exchanger

Figure 1. General view and scheme of the electrolyte-plasma treatment

Electrolytic plasma hardening of steel samples is carried out as follows. The working bath is filled with electrolyte before starting work. Then the electrolyte is supplied to the electrolytic cell by means of a pump installed at the bottom of the working bath. In this case, the electrolyte flows out through the opening of the cone-shaped partition in the form of a jet and fills the electrolytic cell. Then the electrolyte is drained over the edge of the electrolytic cell into the sump and then back into the working bath. Thus, the electrolyte is in circulation mode. The feed rate of electrolyte 2 (flow rate) is 4-7 l/min. The flow rate of cooling running water into the heat exchanger is 3-6 l/min. The adopted parameters of electrolyte cooling make it possible to maintain the temperature within 40-70 °C when heating the samples to 800-900 °C. With the help of a device for fixing the workpieces, the workpiece is immersed in the electrolyte so that the workpiece area to be treated is at a distance of 2-3 mm from the opening of the tapered partition. In this case, through the opening of the cone-shaped partition, which is 10-15 mm lower than the height of the electrolytic cell, an electrolyte stream is fed to the treated area. Then the anode is connected to the positive pole of the power supply, and the work piece is connected to the cathode to its negative pole. For heating to the hardening temperature, a voltage of 320 V is applied between the electrodes and the current density is 25-30 A/cm$^2$. At such voltages, an intensely glowing plasma layer is formed in the near-cathode region, and the product is heated at a rate of 300-400 ° C/sec. In this case, an abnormal arc discharge is formed between the electrodes, due to which the workpiece is rapidly heated [11].

An optical microscope NEOPHOT-21 of the National Scientific Laboratory for Collective Use of Sarsen Amanzholov EKU to study the general nature of the structure. The preparation of metallographic sections of steel samples was carried out according to the methods described in [12]. It should be noted that for metallographic microanalysis, thin sections after polishing, using a paste of chromium dioxide, were etched with a 4 % alcohol solution of nitric acid. The microhardness of steel samples was measured at the National Scientific Laboratory for Collective Use of Sarsen Amanzholov EKU on the device PMT-3 in accordance with GOST 9450–76, with loads on the indenter P=1 N and holding time at this load 10 sec [13, 14].

*Results and discussions*

Currently, heating by radiation from a technological laser, electron guns or high-frequency currents is used for hardening heat treatment of the surface of tools and machine parts. The electrolytic plasma technology of product surface heating and quenching has been known for 50 years [15]. This technology is unique in its ability to change the surface properties of products. In electrolytic plasma technology, the transfer of electrical energy to the product-cathode is carried out from the metal anode through the electrolyte and plasma layer. The plasma layer is formed from the electrolyte material in the gap between the liquid electrode and the electrically conductive surface of the products [15-20].

A water-based electrolyte is used as a liquid electrode. An appropriate choice of the electrolyte composition and electrical modes provides a wide variety of processing technologies [19]. The main reason for the limitation when used in technology is the low reliability and stability of the heating technology. This is primarily due to the instability of the formation of an electrically conductive (plasma) layer between the liquid electrode and the surface of the product. The development of special heaters made it possible to stabilize the technology and increase the conductivity of the electrolyte jet, which, in turn, ensured the efficiency of heating and obtaining an energy density on the heated surface comparable in power density with the energy of a laser plasma.

Special heaters for electrolytic plasma treatment provided control of the power density on the heated surface in the range of $10^2 \ldots 10^4$ W/cm$^2$, which expands the scope of the technology. The electrical discharges in the plasma layer create local zones of high pressure and temperature on the metal surface underperforming electrolyte-plasma treatment, in which the processes of brittle destruction of non-metallic and organic films and exfoliation of loose contaminants take place. This makes it possible to combine the processes of cleaning the surface of the product and heating it to the required temperature. Experimental work shows that up to 80 % of the consumed electrical energy is introduced into the product in the form of heat when the electrolyte-plasma treatment is heated, and the cost of equipment for the electrolyte-plasma treatment is lower than, for example, at the same processing capacity for HFC in 5 ... 10. In addition, electrolyte-plasma treatment provides a wide range of control

over the heating rate, which allows heating and hardening thick layers of the product surface (up to 10 mm). The principal features of the heater for electrolyte-plasma treatment are presented in the diagram, Figure 2. The heater contains a metal anode with a characteristic size $D_a$ and through holes for electrolyte flow. The electrolyte in the heater is compressed by dielectric walls at a distance H to the diameter of the outlet nozzle $D_k$. The electrolyte speed increases in proportion to the ratio of the area of the holes in the anode and the area of the nozzle. In the volume of the electrolyte, between the electrodes, cross effects take place. On the one hand, an electric field acts on the medium. On the other hand, the hydrodynamic flows of a medium charged with electricity with a density j carry electric currents of convection.

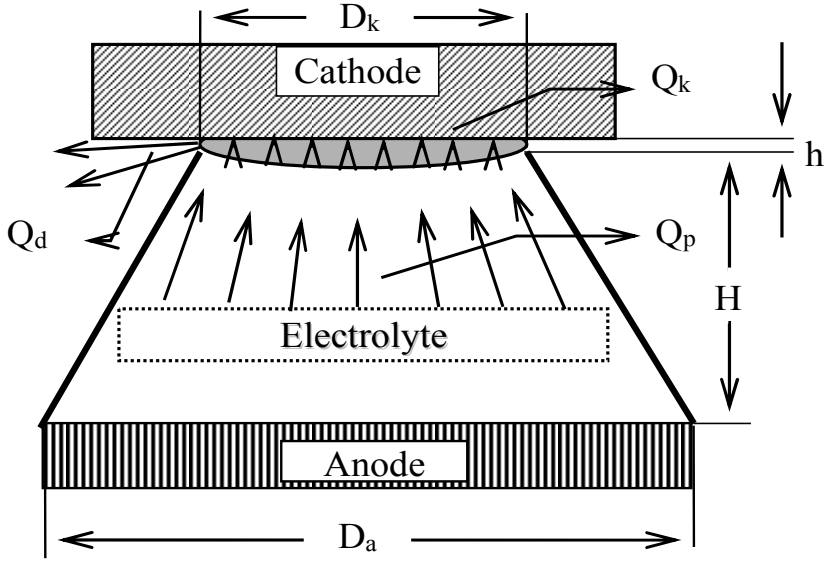


Figure 2. Electrolyte-plasma heater scheme

Heating of the electrolyte is a consequence of the action of the current, as well as radiation. The main energy costs are spent on the evaporation and heating of the electrolyte (formation of a plasma layer) and heating the surface of the product with electric discharges. The discharges are in the form of micro-arc discharges evenly distributed over the processing area.

A periodic increase and decrease in the heating rate is observed with periodic switching on of high voltage electric potential (320V) and low (180V), which makes it possible to increase the time and obtain a thicker heated layer. Connecting an electric potential at the time of cooling the surface of the product allows to reduce the cooling rate and creates the ability to harden products that are made of an alloy with a high carbon content.

Hardened layers can be obtained with a thickness of 0.5 mm, 2 mm, 4 mm, 7 mm, 8 mm and 10 mm by periodically changing the heating power density. As can be seen from Figure 3, heating at a high voltage of 320V without switching the low voltage makes it possible to obtain a hardened layer with a thickness of 0.5-0.6 μm. In order to obtain a hardened layer with a thickness of 4 mm, it is necessary to heat for 25 seconds with periodic switching on of high voltage U1 = 320V for 1 second and low voltage U2 = 180V for 4 seconds. Total heating for 50 seconds provides a hardened layer thickness of 10 mm. The experiment was carried out on a flat sample of 0.34CrNi1Mn steel, which had a thickness of 50 mm. Heating and cooling was carried out with a heater having an outlet nozzle diameter of 20 mm. The electrolyte used was an electrolyte from an aqueous solution containing 20 % sodium carbonate and 10 % carbamide. The microhardness of the hardened layer was measured with a PMT-3 microhardness tester.

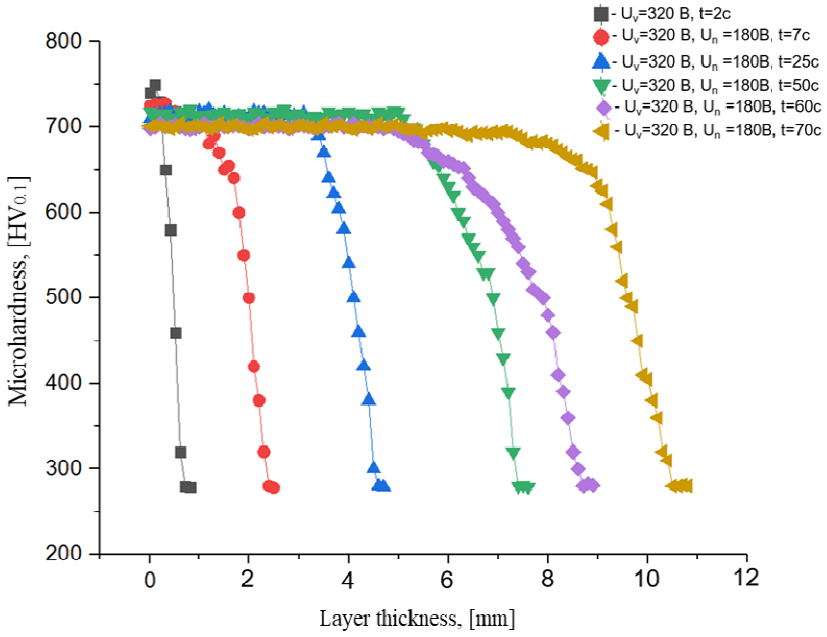


Figure 3. Microhardness of the tempered layer on the surface of steel 0.34CrNi1Mn depending on the heating time t and the voltage of the electric potential

Analysis of the experiment results (Figure 3) shows that the alternation of switching on the electric potential at a voltage of $U_1$ = 320 V and $U_2$ = 200 V provides heating of the product surface to a depth of 10 mm. In this case, the maximum hardness of the surface layer (750 HV) practically does not depend on the thickness of the hardened layer. The hardness of the hardened layer of the product gradually decreases from the maximum (750 HV) to the hardness of the base (280-300 HV) and, as a rule, does not depend on the heating time. A periodic change in the electric field strength between the surfaces of the liquid electrode and the product changes the power density of the surface heating, which ensures the control of the electrolyte-plasma heating and the creation of the necessary thermal conditions for the formation of quenching structures.

The heating power density was calculated from the experimentally measured values of current, voltage, and heating area. The heater had an outlet nozzle diameter of 30 mm. The current value varied in the range of 30 - 45A when the voltage of the electric current was changed from 200 to 300V. Accordingly, the heating power density varied from $1x10^3$ to $3x10^3$ W/cm$^2$. In addition, the ability to control the power density of electrical discharges will ensure the use of electrolytic plasma treatment in cleaning, melting and soldering technologies.

Experimental work has shown that it is possible to obtain hardened layers on the surface of the product depending on the technological conditions, which have a thickness of 0.5 to 10 mm and a hardness of up to 750 HV. The placement of thermally treated layers on the surface of the product depends on the speed, the trajectory of movement of the electrolyte heaters relative to the surface to be hardened and the design features of the heaters themselves.

The research results carried out show the wide possibilities of using the electrolytic plasma hardening technology to improve the service characteristics of alloy steels. In addition, this technology makes it possible to bend the product in the hardened state, weld the product and save energy by hardening only the wearable areas of the surface.

The regulation of the structural-phase state and thickness of the modified layer by varying the heating time and temperature makes it possible to implement optimal technological modes for obtaining various options for the physical-mechanical properties of steel.

The task was set to develop an installation for thermal cyclic electrolytic plasma hardening to carry out the thermal cyclic electrolytic plasma hardening of steels in an automated mode. For this, there were developed an electrolytic plasma treatment chamber and a direct current of power supply. An installation for thermal cyclic electrolytic plasma hardening of materials was created, which allows the processing of samples and steel products in an automated mode. The general view of the installation is shown in Figure 4.

Figure 4. The general view of the installation thermal cyclic electrolytic plasma hardening

The developed direct current of power supply allows varying electric-physical parameters within a wide range: setting voltages, processing duration, voltage on and off times. The power supply provides periodic high and low voltage switching. The power supply is equipped with software to control the operation of the power supply using a personal computer. The power supply specifications are shown in Table 2.

Table 2

**The main power supply specifications**

| | Name | Signification |
|---|---|---|
| | Input voltage | 380 V |
| | Regulation limit of the constant voltage output | 0 to 320 V |
| | Discreet output voltage, not more than | 10 V |
| | Maximum output current, not less than | 100 A |
| | maximum power supply capacity, not less than | 32 kW |

*Conclusions*

Analyzing the experimental results obtained in this work, the following conclusions can be done:

1. Experimental work has shown that, it is possible to obtain hardened layers on the surface of the product depending on the technological conditions, which have a thickness of 0.5 to 10 mm and a hardness of up to 750 HV. The placement of thermally treated layers on the surface of the product depends on the speed, the trajectory of movement of the electrolyte heaters relative to the surface to be hardened and the design features of the heaters themselves.

2. The regulation of the structural-phase state and thickness of the modified layer by varying the heating time and temperature makes it possible to implement optimal technological modes for obtaining various options for the physic-mechanical properties of steel.

3. An installation for thermal cyclic electrolyte-plasma hardening of materials was developed in order to carry out the thermal cyclic electrolytic plasma hardening of steels in an automated mode, which allows processing samples and steel products in an automated mode. The developed installation allows varying the electric-physical parameters within a wide range: to set the voltage, the duration of processing, the time of switching on and off the voltage. The unit is equipped with software for controlling the operation of the power supply using a personal computer.

*This paper was performed within the grant financing of scientific research for 2020-2022 of Committee of Science of the Ministry of Education and Science of the Republic of Kazakhstan. Grant AP08857733.*

## References

1 Рахадилов Б.К. Плазменные и пучковые технологии модифицирования поверхности материалов и нанесения покрытий: моногр. / Б.К. Рахадилов, М.К. Кылышканов, Ж.Б. Сагдолдина. — Усть-Каменогорск: Изд-во «Берел», 2018. — 202 с.

2 Перевертов В.П. Технологии обработки материалов концентрированным потоком энергии / В.П. Перевертов, И.К. Андрончев, М.М. Абулкасимов // Надежность и качество сложных систем. — 2015. — № 3 (11). — С. 69–79.

3 Ismail M.I.S. Experimental design and performance analysis in plasma arc surface hardening / M.I.S. Ismail, Z. Taha // World Academy of Science, Engineering and Technology. — 2011. — Vol. 56. — P. 1052–1058.

4 Leonhardt D. Fundamentals and applications of a plasma-processing system based on electron-beam ionization / D. Leonhardt, S.G. Walton, R.F. Fernsler // Physics of Plasmas. — 2007. — Vol. 14(5). — P. 057103.

5 Nie X. Sliding wear behaviour of electrolytic plasma nitrided cast iron and steel / X. Nie, L. Wang, Z.C. Yao, L. Zhang, F. Cheng // Surface Coatin Technology. — 2005. — Vol. 200(5–6). — P 1745–1750.

6 Балановский А.Е. Плазменное поверхностное упрочнение металлов / А.Е. Балановский. — Иркутск: Изд-во Иркут. гос. техн. ун-та, 2006. — 180 с.

7 Skakov M.K. Microstructure and Tribological Properties of Electrolyte Plasma Nitrided High Speed Steel / M.K. Skakov B.K. Rakhadilov, M. Scheffler // Materials testing. — 2015. — Vol. 4(57). — P. 360–365.

8 Zhurerova L.G. Effect of the PEN/C surface layer modification on the microstructure, mechanical and tribological properties of the 30CrMnSiA mild-carbon steel / L.G.Zhurerova, B.K. Rakhadilov, N.A. Popova, M.K.Kylyshkanov, V.V.Buraniche, A.D.Pogrebnjak // Journal of Materials Research and Technology. — 2020. — № 9. — P. 291–300.

9 Rakhadilov B.K. The cathodic electrolytic plasma hardening of the 20Cr2Ni4A chromium-nickel steel / B.K. Rakhadilov, V.V. Buranich, Z.A. Satbayeva, Zh.B. Sagdoldina, R.S. Kozhanova, A.D. Pogrebnjak // Journal of Materials Research and Technology. — 2020. — № 9. — P. 6969–6976.

10 Rahadilov B.K. Electrolyte-plasma surface hardening of 65G and 20GL low-alloy steels / B.K. Rahadilov, L.G. Zhurerova, A.V. Pavlov, W. Wieleba // Bulletin of the University of Karaganda-Physics. 2016. — № 4(84). — P. 8–14.

11 Belkin P.N. Plasma Electrolytic Hardening of Steels: Review / P.N. Belkin, S.A. Kusmanov // Surface Engineering and Applied Electrochemistry. — 2016. — Vol. 52. — No. 6. — P. 531–546.

12 Баранова Л.В. Металлографическое травление металлов и сплавов: справоч. / Л.В. Баранова, Э.Л. Демина. — М.: Металлургия, 1986. — 256 с.

13 Приборы и методы физического металловедения / под ред. Ф.Вейнберга; пер. с англ. — Вып. 1. — М.: Мир, 1973. — 427 с.

14 Григоревич В.К. Твердость и микротвердость металлов: учеб. пос. / В.К. Григоревич. — М.: Наука, 1976. — 230 с.

15 Ясногородский Я.З. Автоматический нагрев в электролите / Я.З. Ясногородский. — М.: Изд-во и типогр. Оборонгиза, 1947. — 24 с.

16 Yerokhin A.L. Plasma electrolysis for surface engineering / A.L. Yerokhin, X. Nie, A. Leyland, A. Matthews, S.J. Dowey // Surface and Coatings Technology. — 1999. — Vol. 122 (2–3). — P. 73–93.

17 Никитин В.Н. Исследование прикатодной зоны нестационарного режима электролитной обработки / В.Н. Никитин, К.И. Еретнов, А.В. Артемьев // Электролитная обработка материалов. — 1983. — № 2. — С. 35–37.

18 Словецкий Д.И. Механизм плазменно-электролитного нагрева металлов / Д.И. Словецкий, В.Г. Плеханов, С.Д. Терентьев // Теплофизика высоких температур. — 1986. — Т. 24. — № 2. — С. 353–363.

19 Черненко В.И. Теория и технология анодных процессов при высоких напряжениях / В.И. Черненко, Л.А. Снежко, И.И. Папанова, О.И. Литовченко. — Киев: Наук. думка, 1995. — 197 с.

20 Райзер Ю.П. Физика газового разряда / Ю.П. Райзер. — М.: Наука, 1992. — 536 с.

Б.К. Рахадилов, Р.С. Кожанова, Ю.Н. Тюрин, Л.Г. Журерова, Ж.Б. Сагдолдина

## Болаттарды термоциклдік электролитті плазмалық беріктендіру технологиясы

Мақалада термоциклдік электролитті плазмалық беріктендіру технология, сонымен қатар электролитті плазмалық қыздырғыштың құрылма ерекшеліктері сипатталған. Термоциклдік электролитті плазмалық әдіспен түрлі режимдерде беріктенген орташа көміртекті болаттың қаттылығын зерттеу нәтижелері келтірілген. Болаттарды термоциклдік электролитті плазмалық беріктендіру үдерісін автоматтандырылған режимде жүзеге асыру мақсатында материалдарды термоциклдік электролитті плазмалық беріктендірудің өнеркәсіптік қондырғысы жетілдірілді. Үлгілердің бетінде шыныққан қабаттар алынды, олардың қалыңдығы орта есеппен 0,5-тен 10 мм-ге дейін, ал қаттылығының шамасы 750 HV. $U_1$ = 320 В және $U_2$ = 200 В кернеулерінде электрлік потенциалды алмастырып қосу бетті 10 мм тереңдікке дейін қыздыруға мүмкіндік беретіндігі

тәжірибе жүзінде анықталды. Сонымен қатар, беттік қабаттың қаттылығының ең үлкен мәні (750 HV) беріктенген қабаттың қалыңдығына байланысты емес. Заттың беріктенген қабатының қаттылығы ең үлкен шамадан (750 HV) бастапқы күйдегі шамаға (280-300 HV) бірқалыпты өзгеріске ие болады. Жетілдірілген қондырғы электрлік физикалық параметрлерді, яғни кернеулердің шамасын, өңдеу үдерісінің жалпы уақытын, кернеуді қосу мен өшіру уақытын кең ауқымда түрлендіруге мүмкіндік береді.

*Кілт сөздер:* плазма, электролит, технология, құрылым, қаттылық, термоциклдік шынықтыру.

Б.К. Рахадилов, Р.С. Кожанова, Ю.Н. Тюрин, Л.Г. Журерова, Ж.Б. Сагдолдина

## Технология термоциклического электролитно-плазменного упрочнения сталей

В статье описаны технология термоциклического электролитно-плазменного упрочнения и особенности конструкции электролитно-плазменного нагревателя. Приведены результаты исследования твердости среднеуглеродистой стали, обработанные термоциклическим электролитно-плазменным упрочнением при разных режимах. Для проведения термоциклического электролитно-плазменного упрочнения сталей в автоматизированном режиме была разработана промышленная установка. Были получены на поверхности образцов закаленные слои со средними значениями толщины от 0,5 до 10 мм и твердости до 750 HV. Экспериментально установлено, что чередование включения электрического потенциала при напряжении $U_1$ = 320 В и $U_2$ = 200 В обеспечивает прогрев поверхности изделия на глубине до 10 мм. При этом максимальная твердость поверхностного слоя (750 HV) практически не зависит от толщины упрочненного слоя. Твердость упрочненного слоя изделия плавно понижается от максимальной (750 HV) к твердости основы (280-300 HV). Разработанная установка позволяет в широких пределах варьировать электрофизические параметры: задавать напряжения, продолжительность обработки, время включения и отключения напряжения.

*Ключевые слова:* плазма, электролит, технология, структура, твердость, термоциклическая закалка.

## References

1 Rahadilov, B.K., Kylyshkanov, M.K., & Sagdoldina, Zh.B. (2018). *Plazmennye i puchkovye tekhnolohii modifitsirovaniia poverkhnosti materialov i naneseniia pokrytii [Plasma and beam technologies for surface modification of materials and coating]*. Ust-Kamenogorsk: Izdatrelstvo «Berel» [in Russian].

2 Perevertov, V.P., Andronchev, I.K., & Abulkasimov, M.M. (2015). Tekhnolohii obrabotki materialov kontsentrirovannym potokom enerhii [Concentrated energy processing technologies]. *Nadezhnost i kachestvo slozhnykh sistem — Reliability and quality of complex systems, 3, 11,* 69–79 [in Russian].

3 Ismail, M.I.S. & Taha, Z. (2011). Experimental design and performance analysis in plasma arc surface hardening. *World Academy of Science, Engineering and Technology, 56.* 1052–1058.

4 Leonhardt, D., Walton, S.G. & Fernsler, R.F. (2007). Fernsler Fundamentals and applications of a plasma-processing system based on electron-beam ionization. *Physics of Plasmas, 14(5),* 057103.

5 Nie, X. Wang, L., Yao, Z.C., Zhang, L. & Cheng, F. (2005). Sliding wear behaviour of electrolytic plasma nitrided cast iron and steel. *Surface Coatin Technology, 200(5–6),* 1745–1750.

6 Balanovskij, A.E. (2006). *Plazmennoe poverhnostnoe uprochnenie metallov [Plasma hardening metal surface]*. Irkutsk: Izdatelstvo Irkitskoho hosudarstvennoho tekhnicheskoho universiteta [in Russian].

7 Skakov, M.K., Rakhadilov, B.K. & Scheffler, M. (2015). Microstructure and Tribological Properties of Electrolyte Plasma Nitrided High Speed Steel. *Materials testing, 4(57),* 360–365.

8 Zhurerova, L.G., Rakhadilov, B.K., Popova, N.A., Kylyshkanov, M.K., Buraniche, V.V., & Pogrebnjak, A.D. (2020). Effect of the PEN/C surface layer modification on the microstructure, mechanical and tribological properties of the 30CrMnSiA mild-carbon steel. *Journal of Materials Research and Technology, 9,* 291–300.

9 Rakhadilov, B.K., Buranich, V.V., Satbayeva, Z.A., Sagdoldina Zh.B., Kozhanova, R.S., & Pogrebnjak, A.D. (2020). The cathodic electrolytic plasma hardening of the 20Cr2Ni4A chromium-nickel steel. *Journal of Materials Research and Technology, 9,* 6969–6976.

10 Rahadilov, B.K., Zhurerova, L.G., Pavlov, A.V., & Wieleba, W. (2016). Electrolyte-plasma surface hardening of 65G and 20GL low-alloy steels. *Bulletin of the University of Karaganda-Physics, 4(84),* 8–14.

11 Belkin, P.N. & Kusmanov, S.A. (2016). Plasma Electrolytic Hardening of Steels: Review. *Surface Engineering and Applied Electrochemistry, 52, 6,* 531–546.

12 Baranova, L.V. & Demina, E.L. (1986). *Metallohraficheskoe travlenie metallov i splavov [Metallographic etching of metals and alloys]*. Moscow: Metallurhiia [in Russian].

13 Vejnberg F. (Ed.). (1973). *Pribory i metody fizicheskoho metallovedeniia [Devices and methods of physical metallurgy]*. Moscow: Mir [in Russian].

14 Grigorevich, V.K. (1976). *Tverdost i mikrotverdost metallov [Hardness and microhardness of metals]*. Moscow: Nauka [in Russian].

15 Yasnogorodskij, Ya.Z. (1947). *Avtomaticheskii nahrev v elektrolite [Automatic heating electrolyte]*. Moscow: Izdatelstvo i tipohrafiia Oboronhiza [in Russian].

16 Yerokhin, A.L., Leyland, A., Matthews, A. & Dowey, S.J. (1999). Plasma electrolysis for surface engineering. *Surface and Coatings Technology, 122(2–3),* 73–93.

17 Nikitin, V.N., Eretnov, K.I. & Artemev, A.V. (1983). Issledovanie prikatodnoi zony nestatsionarnoho rezhima elektrolitnoi obrabotki [Study of the near-cathode zone of non-stationary electrolyte treatment]. *Elektrolitnaia obrabotka materialov — Electrolytic material processing, 2,* 35–37 [in Russian].

18 Sloveckij, D.I., Plekhanov, V.G. & Terentev, S.D. (1986). Mekhanizm plazmenno-elektrolitnoho nahreva metallov [Mechanism of plasma electrolyte heating of metals]. *Teplofizika vysokikh temperatur — Thermal physics of high temperatures, 24, 2,* 353–363 [in Russian].

19 Chernenko, V.I., Snezhko, L.A., Papanova, I.I. & Litovchenko, O.I. (1995). *Teoriia i tekhnolohiia anodnykh protsessov pri vysokikh napriazheniiakh [Theory and technology of anodic processes at high voltage]*. Kiev: Naukova dumka [in Russian].

20 Rajzer, Yu.P. (1992). *Fizika hazovoho razriada [Gas discharge physics]*. Moscow: Nauka [in Russian].

DOI 10.31489/2021Ph1/35-45
UDC 625.7+338.5

V. A. Bogomolov[1], V. I. Klimenko[1], D. N. Leontiev[1], S. V. Ponikarovska[1],
A.A. Kashkanov[2*], V.Yu. Kucheruk[2]

[1]*Kharkiv National Automobile and Highway University, Ukraine;*
[2]*Vinnytsia National Technical University, Ukraine*
*(*E-mail: a.kashkanov@gmail.com)*

# Plotting the adhesion utilization curves for multi-axle vehicles

The paper presents a method for calculating normal reactions of the road bearing surface along the axles of a multi-axle wheeled vehicle, upon which it is possible to construct the adhesion utilization curves for all vehicle axles, considering that both independent axles and axles combined in balancing trolleys are present in the vehicle suspension. The main idea of this method is developing a universal mathematical model for determining the horizontal coordinate of the center of elasticity (center of rotation) of a multi-axle vehicle body with reference to which the normal reactions along the axles of the vehicle during its braking are determined. In addition, with a known distribution of braking forces, the adhesion utilization curves are plotted. In the overview part, an analysis is given that showed that there is no single methodology or recommendations today regarding determination of normal road reactions on the axles of a multi-axle wheeled vehicle. The developed methodology can be applied in engineering calculations when checking multi-axle wheeled vehicles for compliance with international requirements for brake systems (Appendix 10 to UN / ECE Regulation No. 13). The universality of the proposed methodology allows recommendation for its implementation in the given Rules No. 13. The calculations of the adhesion utilization curves made on the example of a 4-axle vehicle showed that consideration of the design features of a multi-axle wheeled vehicle suspension significantly affects the nature of the geometry of the adhesion utilization curves within the permissible limits specified by UN / ECE Regulation No. 13 (Appendix 10).

*Keywords:* multi-axle vehicle, distribution of braking forces, braking force, braking performance, adhesion utilization curves, off-road vehicle, multi-axle.

## *Introduction*

From the theory of car, we know that during the designing process and serial tuning all wheeled vehicles (WV) must be provided with the necessary braking performance in various conditions of their operation. To control the assessment of this performance, the standards and regulations have been developed in international practice [1, 2]. They provide for checking the geometry of the adhesion utilization curves of the WV axles [3–10] in predetermined so-called «corridors», that ensure road safety due to the rational choice of the brake system characteristics and implementation of the proper process of vehicle braking [11–17].

In regulatory documents [1, 2] evaluating the braking performance of a WV, the adhesion utilization curve of the *i*-th axle $(f_i)$ of the wheeled vehicle can be determined based on the equation:

$$f_i = \frac{T_i}{N_i}, \tag{1}$$

where $T_i$ is the braking force on the corresponding *i*-th axle of a WV, N; $N_i$ is the road reaction to the *i*-th axle of the WV, N.

The exact solution for (1) in the regulatory documents [1, 2] is proposed only for two-axle vehicles:

$$f_i = \frac{T_i}{P_i \pm z\frac{h}{L}G}, \tag{2}$$

where $P_i$ is the normal road reaction to the corresponding *i*-th axle of the WV in static conditions, N; $h$ is the height of the WV center of gravity, m; $L$ is the distance between the axles of the WV, m; $z$ is the braking coefficient of the WV; $G$ is the WV weight, N.

An expression similar to formula (2) can also be obtained for a three-axle WV in which the rear two axles are combined by the suspension in one so-called «balancing trolley» [18–20].

For multi-axle WVs [21], with three or more independent axles, it is necessary to develop original methods for each individual case of layout of their axles when determining the reaction of the road.

This approach is not always convenient when plotting adhesion utilization curves and determining the braking performance of a vehicle, consequently the aim of this work is creating a methodology for calculating the reaction of road on the *i*-th axle of a multi-axle WV when constructing its adhesion utilization curves.

The object of this study is the process of determining the reaction of road on the i-th axle of a multi-axle WV. The relevance lies in the rational determination of the nature of the distribution of the adhesion utilization curves of the multi-axle vehicles in order to ensure road safety and increase the braking efficiency of such vehicles.

*Methodology for determining the road reaction on the i-th axle of a multi-axle WV*

Work [22] offers to determine the reactions of road $N_i$ in the following form:

$$N_i = P_i + \Delta N_i, \tag{3}$$

where $\Delta N_i$ is a dynamic component of the normal reaction of the road to the corresponding *i*-th axle of the WV, caused by the appearance of the total braking force, which is equal to the inertia of the car, N;

The main advantage of this representation of quantity $N_i$ is the possibility of applying the so-called principle of superposition of forces acting on the WV. Therewith, value $P_i$ in equation (3) is a reference and depends on the distribution of the car weight relative to its center of gravity. Thus, when determining $\Delta N_i$, the mathematical and physical model of the WV is greatly simplified due to the lack of $P_i$ and $G$ quantities.

Structurally, such a physical model of a multi-axle vehicle can be represented in the form of a circuit depicted in Fig. 1.

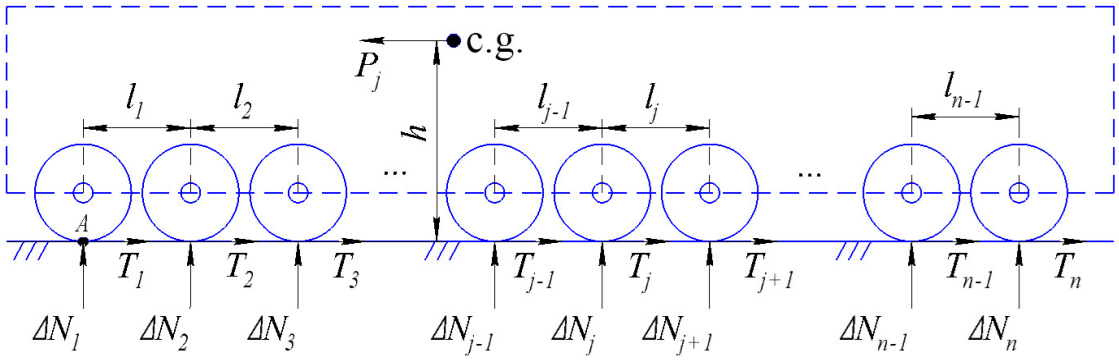


($T_1$, $T_2$, $T_3$, $T_{j-1}$, $T_j$, $T_{j+1}$, $T_{n-1}$, $T_n$ are braking forces on the corresponding axles of the n-axle WV;

$l_1$, $l_2$, $l_{j-1}$, $l_j$, $l_{n-1}$ are the distances between the corresponding axles of the n-axle WV; h is the height of the center of gravity (c.g.) of the WV; $P_j$ is the inertia force of the braking n-axle WV).

Figure 1. Diagram of the structural physical model of the n-axle braking WV

Based on the studies [18], it is obviously possible to accept:

$$P_j = j \cdot \frac{G}{g} = z \cdot G = \sum_{i=1}^{n} T_i. \tag{4}$$

It is well known from mathematics and theoretical mechanics that in order to find *n* of unknown quantities (3), it is necessary to obtain a system of *n* equations.

Since the weight of a WV does not change during braking, we can write the first equation in the following form:

$$\sum_{i=1}^{n} \Delta N_i = 0. \tag{5}$$

From the sum of the moments relative to point *A* (Fig. 1), we obtain the second equation in the form:

$$\sum_{k=2}^{n} \left( \Delta N_k \cdot \sum_{m=1}^{k-1} l_m \right) = -z \cdot G \cdot h. \tag{6}$$

From the scientific and technical literature [2, 18] we know that if, for example, some two axles *j* and *j* + 1 are combined into a balancing trolley, then we can assume the equality for them:

$$\Delta N_j - \Delta N_{j+1} = 0\,. \tag{7}$$

Equation (7) may also have a different form, depending on the design of the balancer suspension. There are as many such equations in the system as there are balancing trolleys in the design of the WV.

The practice of calculations [2, 18] shows that under the accepted assumption (7) the axles combined into the balancing trolley can often be conditionally replaced by a reduced axle with loads:

$$\begin{aligned} N_{j,(j+1)} &= N_j + N_{j+1};\\ P_{j,(j+1)} &= P_j + P_{j+1};\\ \Delta N_{j,(j+1)} &= \Delta N_j + \Delta N_{j+1};\\ T_{j,(j+1)} &= T_j + T_{j+1}, \end{aligned} \tag{8}$$

which is located at distance $0{,}5 \cdot l_j$ from the corresponding axle (Fig. 1).

In this case, the displacement (rotation) of the WV body during braking can be schematically represented in the form of a diagram, which is shown in Fig. 2.

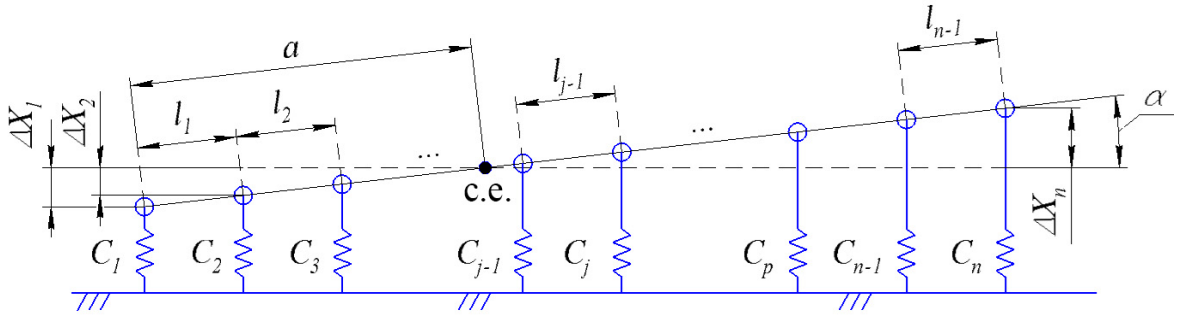


a is the distance from the center of elasticity (c.e.) to the first axle; $C_1$... $C_n$ are stiffness of the suspensions of the corresponding WV axles; $\Delta X_1$ ... $\Delta X_n$ are deformation of the suspensions of the corresponding axles; $\alpha$ is the angle of the body inclination relative to its initial position before the WV starts braking

Figure 2. Diagram of the rotation of the WV body during braking

From the diagram in Fig. 2 it is obvious that expression (5) can be rewritten in the form

$$\sum_{i=1}^{n}\left(\Delta X_i \cdot C_i\right) = 0\,. \tag{9}$$

From Fig. 2 it is also obvious that:

$$\Delta X_i = \left(a - \sum_{k=1}^{i} l_{k-1}\right) \cdot \sin\alpha\,, \tag{10}$$

where if $i = 1$, the distance is $l_0 = 0$.

After substituting expression (10) in (9) and performing simple algebraic transformations, we obtain:

$$a \cdot \sum_{i=1}^{n} C_i = \sum_{i=1}^{n}\left(C_i \cdot \sum_{k=1}^{i} l_{k-1}\right). \tag{11}$$

Dividing the numerator and denominator of expression (11) by the stiffness of the front axle suspension and considering that at $i = 1$ the distance is $l_0 = 0$, we obtain:

$$a \cdot = \frac{\sum_{i=2}^{n}\left(\frac{C_i}{C_1} \cdot \sum_{k=1}^{i} l_{k-1}\right)}{1 + \sum_{i=2}^{n}\frac{C_i}{C_1}}. \tag{12}$$

Assuming that during the transition of a vehicle from a running order to a loaded state its body moves parallel to itself [23], we can assume that there is an equality:

$$\Delta X_i^{\mathrm{n}} = const\,, \tag{13}$$

where $\Delta X_i^{\text{n}}$ is deformation in the *i*-th suspension when moving the body from the running order to the loaded state of the WV.

In that case, it is fair to accept:

$$\frac{C_i}{\Delta P_i} = const\,, \tag{14}$$

where $\Delta P_i$ is the difference between the loads on the *i*-th axle in the loaded state and running order of the WV.

Thus, we can assume that:

$$\frac{C_i}{C_1} = \frac{\Delta P_i}{\Delta P_1}\,, \tag{15}$$

after substituting expression (15) into (12), we finally obtain:

$$a = \frac{\sum\limits_{i=2}^{n}\left(\frac{\Delta P_i}{\Delta P_1}\cdot\sum\limits_{k=1}^{i} l_{k-1}\right)}{1+\sum\limits_{i=2}^{n}\frac{\Delta P_i}{\Delta P_1}}\,. \tag{16}$$

In equation (16), all components are the well-known reference data [24], which fact subsequently simplifies the calculation of the distance from the center of elasticity to the first axle by dependence (16).

In this regard, the missing equations for the target system of equations can be determined by the following procedure:

– after finding the distance from the center of elasticity to the first axle by dependence (16), we determine the position of the center of elasticity relative to the axles of the WV with index *j* and *n.* Moreover, from Fig. 1 and Fig. 2 we know that if:

$$a = \sum_{i=1}^{j-1} l_i\,, \text{ then for it } \Delta N_j = 0\,; \tag{17}$$

– for the axles to the left of the center of elasticity, from geometric relations and equation (10) for any *m*-th axle the following relation is right:

$$a\cdot\Delta X_m = \left(a - \sum_{i=1}^{m-1} l_i\right)\cdot\Delta X_1\,, \text{ где } m>1\,. \tag{18}$$

Considering expressions (5) and (9), after the corresponding transformations for the *m*-th axle, we obtain the equation:

$$\left(1-\frac{\sum\limits_{i=1}^{m-1} l_i}{a}\right)\cdot\frac{\Delta P_m}{\Delta P_1}\cdot\Delta N_1 - \Delta N_m = 0\,; \tag{19}$$

– for the axles located to the right of the center of elasticity, from geometric relationships for any *p*-th axle the following is valid:

$$\Delta X_p\left(\sum_{i=1}^{n-1} l_i - a\right) = \Delta X_n\left(\sum_{i=1}^{p-1} l_i - a\right). \tag{20}$$

After the transformations, which are similar to the transformations made earlier for expression (18), we obtain the equation:

$$\Delta N_p - \frac{\Delta P_p}{\Delta P_n}\cdot\left(\frac{\sum\limits_{i=1}^{p-1} l_i - a}{\sum\limits_{i=1}^{n-1} l_i - a}\right)\cdot\Delta N_n = 0\,. \tag{21}$$

Thus, from expressions (19), (21) we can obtain their missing number for the target system of equations.

*Plotting the adhesion utilization curves for multi-axle WV*

After solving the statically indeterminable system by the method described above and determining the increments of vertical loads on each WV axle during its braking, we find all values of vertical loads $N_i$ from expression (3), and using expression (1) we plot the adhesion utilization curves.

As an example, we address the plotting of adhesion utilization curves for a four-axle truck, schematically shown in Fig. 3, with the parameters [22]:

– the distances between the axles are $l_1 = 2,03$ m, $l_2 = 2,62$ m, $l_3 = 1,4$ m;

– two rear axles are combined by a balancing trolley;

– axle loads in running order $P_{n1} = 25000$ N, $P_{n2} = 25000$ N, $P_{n3} = 49000$ N, $P_{n4} = 49000$ N (axle loads in loaded state $P_{g1} = 73500$ N, $P_{g2} = 73500$ N, $P_{g3} = 131320$ N, $P_{g4} = 131320$ N);

– position of the coordinate of the center of gravity from the road surface when WV is in loaded state $h_n = 1,05$ m (position of the center of gravity coordinate from the road surface when WV is in loaded state $h_g = 1,55$ м);

Thus: $\Delta P_1 = P_{g1} - P_{n1} = 23500$ N, $\Delta P_2 = P_{g2} - P_{n2} = 23500$ N, $\Delta P_3 = \Delta P_4 = 51320$ N.

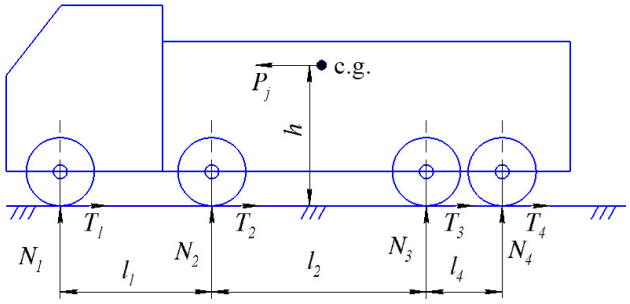


Figure 3. The scheme of the forces acting on the four-axle truck when braking

We assume that the braking forces are realized the same on all axles, i. e.: $T_1 = T_2 = T_3 = T_4 = 0,25 \cdot \sum_{i=1}^{4} T_i$. In this case, the system of equations, for example, for the WV in running order, will have the following form:

$$\begin{cases} \sum_{i=1}^{4} \Delta N_i = 0; \\ \sum_{j=2}^{4} \left( \Delta N_j \cdot \sum_{i=1}^{j-1} l_i \right) = -z \cdot h_n \cdot \sum_{i=1}^{4} P_{ni}; \\ \Delta N_3 - \Delta N_4 = 0; \\ \left(1 - \frac{l_1}{a}\right) \cdot \frac{\Delta P_{n2}}{\Delta P_{n1}} \cdot \Delta N_1 - \Delta N_2 = 0. \end{cases} \quad (22)$$

The results of calculations of the utilized adhesion made on the basis of the system of equations (22) using equations (1) and (3) are presented in Fig. 4 (a).

If we consider the same multi-axle vehicle, but without a balancing trolley, then the system of equations (22) will take the form (23). The results of calculations of the utilized adhesion performed according to the system of equations (23) using equations (1) and (3) are presented in Fig. 4 (b).

A comparative analysis of the results of calculations performed according to the systems of equations (22) and (23) shows their significant discrepancy. This allows us to conclude that neglecting the type of suspension when calculating the adhesion of a multi-axle vehicle is unacceptable, since this leads to significant errors in calculating distribution of braking forces between the axles of such WVs.

The calculations of the utilized adhesion for a loaded vehicle according to equations (22) and (23) using equations (1) and (3) also showed a significant discrepancy between the results. For convenience of analysis, the results of calculations of a loaded WV utilized adhesion are depicted in the form of graphs in Fig. 5.

$$\begin{cases} \sum\limits_{i=1}^{4}\Delta N_i = 0; \\ \sum\limits_{j=2}^{4}\left(\Delta N_j \cdot \sum\limits_{i=1}^{j-1} l_i\right) = -z \cdot h_{\text{n}} \cdot \sum\limits_{i=1}^{4} P_{ni}; \\ \Delta N_3 - \dfrac{\Delta P_{\text{n3}}}{\Delta P_{\text{n4}}} \cdot \left(\dfrac{\sum\limits_{i=1}^{2} l_i - a}{\sum\limits_{i=1}^{3} l_i - a}\right) \cdot \Delta N_4 = 0; \\ \left(1 - \dfrac{l_1}{a}\right) \cdot \dfrac{\Delta P_{\text{n2}}}{\Delta P_{\text{n1}}} \cdot \Delta N_1 - \Delta N_2 = 0. \end{cases} \tag{23}$$

As the analysis of the curves of the utilized adhesion of an *n*-axle WV showed, its distribution of braking forces depends significantly on the chosen calculation method.

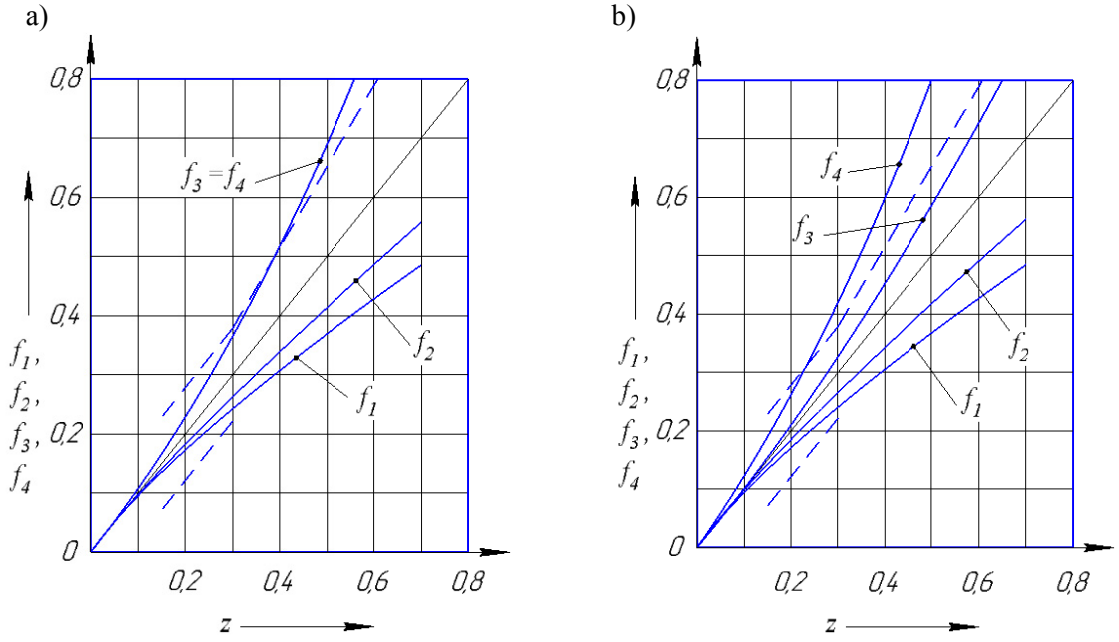


a) two rear axles are combined into a balancing trolley; b) two rear axles are not combined into a balancing trolley

Figure 4. The curves of the utilized adhesion of a four-axle WV in running order

The design of the axle suspensions of the *n*-axle WVs also affects the nature of the change in its utilized adhesion; therefore, the methodology for calculating the curves of the utilized adhesion of a multi-axle WVs must consider this when fulfilling the requirements of the UN / ECE Rules [1].

The analysis of the deviation in the average value of the utilized adhesion on the front axles for a four-axle vehicle with a balancing trolley and with independent axles is determined from the expression:

$$\Delta = \frac{\max\left(f_{\text{a}}^{\text{u}}; f_{\text{cp}}^{b}\right) - \min\left(f_{a}^{\text{u}}; f_{\text{a}}^{b}\right)}{\max\left(f_{a}^{\text{u}}; f_{\text{a}}^{\text{b}}\right)} \cdot 100\%, \tag{24}$$

where $f_a^{\text{u}}$ is an average adhesion utilized on the front or rear axles of a multi-axle wheeled vehicle with independent axles; $f_{\text{a}}^{\text{b}}$ is the average value of the adhesion utilized on the front or rear axles of a multi-axle wheeled vehicle with a balancing trolley in its design.

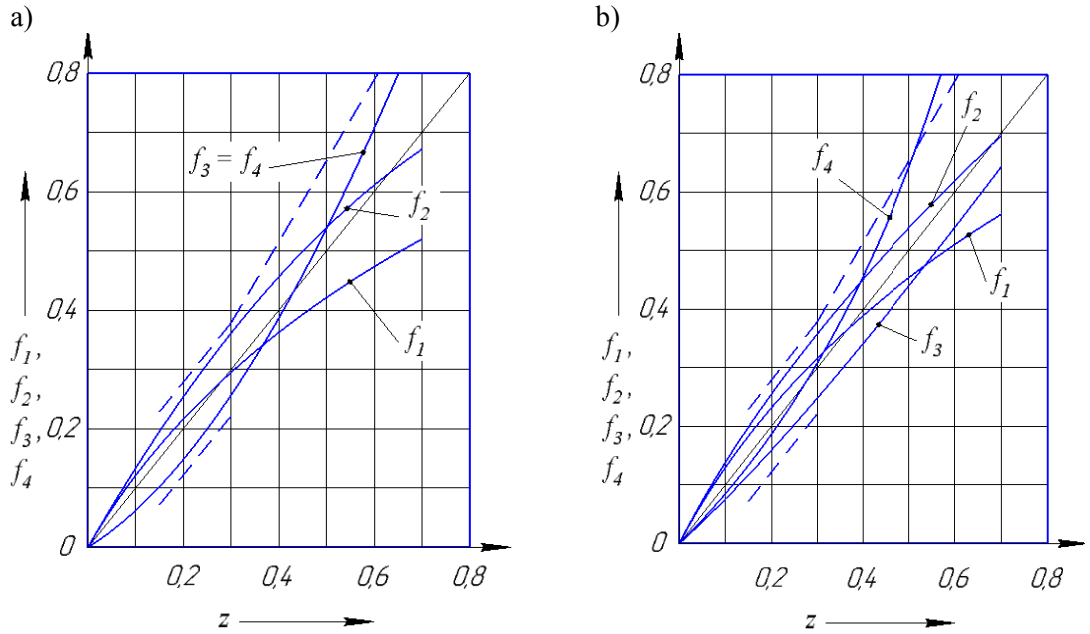


a) two rear axles are combined into a balancing trolley; b) two rear axles are not combined into a balancing trolley

Figure 5. The curves of the utilized adhesion of a loaded four-axle WV

The results of the calculated deviation in the average value of the utilized adhesion on the front axles and rear axles of a four-axle WV, when $z$ equals 0.5, are summarized for convenience in Table 1.

Table 1

**The average deviation of the utilized adhesion of a four-axle WV**

| Parameter | $f_a^b$ | $f_a^u$ | $\Delta$, % | $f_a^b$ | $f_a^u$ | $\Delta$, % |
|---|---|---|---|---|---|---|
| Mode | WV in running order | | | WV in loaded state | | |
| Front | 0,39 | 0,395 | 1,27 | 0,48 | 0,495 | 3,03 |
| Rear | 0,7 | 0,69 | 1,43 | 0,53 | 0,54 | 1,85 |

The table shows that, with an average deviation in the calculation results not exceeding 1.5 %, the curves of utilized adhesion shown in Fig. 4 significantly differ from each other by the nature of their geometry within the established limits [1].

A similar trend is also observed for a loaded multi-axle wheeled vehicle (Fig. 5). Moreover, the percentage deviation of the average utilized adhesion is almost doubled in comparison with the average value of the utilized adhesion of the WV in running order.

Table 2

**Deviation of the WV utilized adhesion from its average value**

| Parameter | $f_a^b$ | $f_a^u$ | $\Delta_b$, % | $\Delta_u$, % | $f_a^b$ | $f_a^u$ | $\Delta_b$, % | $\Delta_u$, % |
|---|---|---|---|---|---|---|---|---|
| Mode | WV in running order | | | | WV in loaded state | | | |
| $f_1$ | 0,36 | 0,37 | 7,69 | 6,33 | 0,42 | 0,45 | 12,5 | 9,09 |
| $f_2$ | 0,42 | 0,42 | 7,14 | 5,95 | 0,54 | 0,54 | 11,11 | 8,33 |
| $f_3$ | 0,7 | 0,58 | 0 | 15,94 | 0,53 | 0,43 | 0 | 20,37 |
| $f_4$ | | 0,8 | | 13,75 | | 0,64 | | 15,63 |

The deviation of the utilized adhesion from its average value (Table 2) showed that in calculation of the utilized adhesion for the WV with a balancing trolley in suspension the error $\Delta_b$ will be bigger when calculat-

ing the utilized adhesion of the front axles; and without such a trolley in the suspension the deviation $\Delta_u$ will be bigger when calculating the utilized rear axle adhesion.

It should be noted that the error in determining the utilized adhesion above 15 % is not permissible for engineering calculations, since under actual operating conditions of a multi-axle wheeled vehicle this can lead to a violation of road safety and, as a result, to injury of the road users.

*Conclusions*

The proposed method for calculating the distribution of normal reactions between the axles of an *n*-axle wheeled vehicle allows taking into account the design features of the car suspension when determining the adhesion utilization curves on its respective axles.

The universality of the proposed methodology for calculating the distribution of normal reactions between axles of an n-axle wheeled vehicle makes it possible to optimize the process of assessing the distribution of brake forces of a vehicle, both with a balancing trolley and with vehicle axles independent of each other.

The developed methodology for calculating the distribution of normal reactions between the axles of an *n*-axle wheeled vehicle can be used in engineering calculations when testing multi-axle vehicles for compliance with the international requirements of brake systems, Appendix 10 to Regulation No. 13 UN / ECE.

The performed calculations of the adhesion utilization curves, using the example of a 4-axle WV, showed that consideration of the design features of the multi-axle wheeled vehicle suspension significantly affects the nature of the geometry of the adhesion utilization curves within the permissible limits established by UN / ECE Regulation No. 13 (Appendix 10).

Analysis of the average deviation in the results of calculating the adhesion utilization curves with an error not exceeding 1.5 % for the WV in running order and 3 % for the WV in loaded state showed that the nature of the geometry of the adhesion utilization curves within the zone established by international rules UN / ECE No. 13 depends significantly on the type of a multi-axle wheeled vehicle suspensions.

## References

1 Regulation No 13 of the Economic Commission for Europe of the Combined Nations (UN/ECE) Uniform provisions concerning the approval of vehicles of categories M, N and O with regard to braking: on condition 18.02.2016 // Official Journal of the European Union. UN/ECE, 2016. — 262 p.

2 ГОСТ Р 41.13–2007. Единообразные предписания, касающиеся транспортных средств категорий *M*, *N* и *O* в отношении торможения. — М.: Стандартинформ, 2009. — 170 с.

3 Zalohin M.Y. Study of Proportional Pressure Modulator on the Basis of Electromagnetic-Type Linear Motor / M.Y. Zalohin, B.A. Liubarskyi, S.N. Schuklinov, M.G. Mychalevych, D.V. Leontiev // Science & Technique. — 2018. — 17(5). — P. 440–446.

4 Leontiev D. N. About Application the Tyre-Road Adhesion Determination of a Vehicle Equipped with an Automated System of Brake Proportioning / D. N. Leontiev, L. A. Ryzhyh, S. I. Lomaka, I. N. Nikitchenko, O. I. Voronkov, I. V. Hritsuk, S.V. Pylshchyk, O. V. Kuripka // Science & Technique. — 2019. — 18(5). — P. 401–408.

5 Bogomolov V. Impruving the brake control effectiveness of vehicles equipped with a pneumatic brake actuator / V. Bogomolov, V. Klimenko, D. Leontiev, L. Ryzhyh, O. Smyrnov, M. Kholodov // Science & Technique. — 2020. — 19(1). — P. 55–62.

6 Shaoyi B. Adhesion state estimation based on improved tire brush model / B. Shaoyi, L. Bo, Z. Yanyan // Advances in Mechanical Engineering. — 2018. — 10(1). — P. 1–9. doi: 10.1177/1687814017747706

7 Meljnikov D. Use of Simpack at the DaimlerChrysler Commercial Vehicles Division. Truck Product Creation (4P) / D. Meljnikov // Daimler Chrysler. — 2006. — 16 p.

8 Jazar R.N. Tire Dynamics / R.N. Jazar // Vehicle Dynamics: Theory and Aplicacion, Berlin, Springer. — 2008. — P. 95–163.

9 Braun O. M. On the Dependency of Friction on Load: Theory and Experiment / O. M. Braun, B. N. Persson, B. Steenwyk, A. Warhadpande // EPL (Europhysics Letters). — 2016. — 113 (5). https:// doi.org/10.1209/0295–5075/113/56002.

10 The tyre. Grip / Michelin Technology Society. — France: Clermont-Ferrand. — 2001. — 96 p.

11 Li Shengbo Predictive lateral control to stabilise highly automated vehicles at tire-road friction limits / Li Shengbo, Chen Hailiang, Li Renjie, Liu Zhengyu, Wang Zhitao, Xin Zhe // Vehicle System Dynamics. — 2020. — 58:5. — P.768–786. 58, DOI: 10.1080/00423114.2020.1717553.

12 Bode O. Possibilities and Limits of a Simple Tire-road Adhesion Determination — Represented at the Example of Brake Testing in Accordance with ECE-R 13 / O. Bode // Hannover Conference on Tires, Chassis, Roads. — 2001. — P. 69–86.

13 Miao YuTire-Pavement Friction Characteristics with Elastic Properties of Asphalt Pavements / Miao Yu, Guoxiong Wu, Lingyun Kong, Yu Tang // Applied Sciences. — 2017. — 7(11).

14 Artyomov N. Analyzing the dynamics of a single car wheel / N. Artyomov, M. Podrigalo, A. Abdulgazis // MATEC Web of Conferences 224, 02102, 2018. https://doi.org/ 10.1051/matecconf/201822402102

15 Kashkanov A. A. Inertial evaluation of the tyre-road interaction during emergency braking / A. A. Kashkanov, V.M. Diorditsa, V. Yu. Kucheruk, D. Zh. Karabekova, A. K. Khassenov, A. M. Sharzadin // Bulletin of the university of Karaganda-Physics. — 2019. — 2(94). — P. 82–91. DOI: 10.31489/2019Ph2/82–91.

16 Kashkanov A. A. Tyre-Road friction Coefficient: Estimation Adaptive System / A. A. Kashkanov, A. P. Rotshtein, V.Yu. Kucheruk, V. A. Kashkanov // Bulletin of the university of Karaganda-Physics — 2020. — 2(98). — P. 50–59. DOI: 10.31489/2020Ph2/50–59.

17 Saraiev O. Mathematical Model of the Braking Dynamics of a Car / O. Saraiev, Y. A. Gorb // SAE Technical Paper 2018–01–1893. — 2018. https://doi.org/10.4271/2018–01–1893

18 Туренко А.М. Функціональний розрахунок гальмівної системи автомобіля з барабанними гальмами та регулятором гальмівних сил / А.М. Туренко, В.О. Богомолов, В.І. Клименко, С.Я. Ходирєв, В.І. Кирчатий, М.Г. Михалевич // — Харків: ХНАДУ, 2003. — 120 с.

19 Leontiev D. Simulation of Working Process of the Electronic Brake System of the Heavy Vehiclet / D. Leontiev, V. Klimenko, M. Mykhalevych, Y. Don, A. Frolov // Advances in Intelligent Systems and Computing. — 2020. — Vol.1019. — P. 50–61. Springer, Cham. DOI: 10.1007/978–3-030–25741–5_6

20 Методичні рекомендації з визначення осьових навантажень транспортних засобів з урахуванням сил, що діють у плямі контакту шини з поверхнею дорожнього одягу. МР В.2.3–37641918–887:2017. — Київ: Укравтодор, 2017. — 31 с.

21 Аксенов П.В. Многоосные автомобили / П.В. Аксенов. — 2-е изд. перераб. и доп. — М.: Машиностроение, 1989. — 280 с.

22 Провести дослідження та розробити методичні рекомендації з визначення осьових навантажень багатовісних транспортних засобів з урахуванням сил тертя в площі контакту шини з дорожнім покриттям. Звіт про науково-дослідну роботу за договором № 5/35–79–16. Науковий керівник д.т.н., проф. Жданюк В.К. — № держреєстрації 0116U005525. — ХНАДУ. — 2017. — 159 с.

23 Ротенберг Р.В. Подвеска автомобиля и его колебания: учеб. // Р.В. Ротенберг. — М.: Машгиз, 1960. — 356 с.

24 Понизовкин А.Н. Краткий автомобильный справочник // А.Н. Понизовкин, Ю.М. Власко, М.Б. Ляликов и др. — М.: АО «Трансконсалтинг»; НИИАТ, 1994. — 779 с.

В.А. Богомолов, В.И. Клименко, Д.Н. Леонтьев,
С.В. Поникаровская, А.А. Кашканов, В.Ю. Кучерук

## Көпосьті көлік құралдары үшін ілінісуді жүзеге асыратын қисықтарды құру туралы

Жұмыста көпосьті доңғалақты көлік құралының осьтері бойымен жолдың тірек бетінің қалыпты реакцияларын есептеу әдісі ұсынылды, оның негізінде автомобильдің суспензиясында тәуелсіз осьтердің де, тепе-теңдік арбаларына біріктірілген осьтердің де болуын ескере отырып, көлік құралының барлық осьтері бойынша ілінісу қисықтарын құруға болады. Бұл әдістің негізгі идеясы көпосьті автомобиль корпусының серпімділік орталығының (айналу орталығының) көлденең координатасын анықтаудың әмбебап математикалық моделін жасау болып табылады, соның негізінде көлік құралының осьтері бойымен қалыпты реакциялар оның тежелу процесінде анықталады, ал тежегіш күштердің белгілі таралуымен жүзеге асырылатын ілінісу қисықтары да тұрғызылады. Шолу бөлімінде бүгінгі күні көп білікті доңғалақты көлік құралының осьтеріндегі жолдың қалыпты реакцияларын анықтауға қатысты бірыңғай әдістеме немесе ұсыныстар жоқ екенін көрсететін талдау келтірілген. Әзірленген әдістеме көп білікті доңғалақты көлік құралдарының тежегіш жүйелерге қойылатын халықаралық талаптарға сәйкестігін тексеру кезінде инженерлік есептеулерде қолданылуы мүмкін (UN/ECE № 13 Ережесінің 10-шы қосымшасы). Ұсынылған әдістеменің әмбебаптығы жоғарыда аталған Ережелерді енгізуде ұсыныс жасауға мүмкіндік береді. Төрт осьті көлік құралының мысалында жүзеге асырылатын ілінісу қисықтарының орындалған есептеулері көпосьті дөңгелекті көлік құралының аспа құрылымының ерекшеліктерін есепке алу UN/ECE № 13 Ережелерінде (10 Қосымша) белгіленген рұқсат етілген шектеулер шегінде жүзеге асырылатын ілінісу қисықтарының орналасу сипатына айтарлықтай әсер ететінін көрсетті.

*Кілт сөздер:* көпосьті көлік құралы, тежегіш күштердің таралуы, тежегіш күші, тежеу тиімділігі, ілінісу қисықтары, жоғары жылдамдықты автомобиль, көпосьті.

В.А. Богомолов, В.И. Клименко, Д.Н. Леонтьев,
С.В. Поникаровская, А.А. Кашканов, В.Ю. Кучерук

## О построении кривых реализуемого сцепления для многоосных транспортных средств

Предложен метод расчета нормальных реакций опорной поверхности дороги по осям многоосного колесного транспортного средства, на основе которого можно построить кривые реализуемого сцепле-

ния по всем осям транспортного средства с учетом наличия в подвеске автомобиля как независимых осей, так и осей, объединенных в балансирные тележки. Основная идея этого метода заключается в разработке универсальной математической модели определения горизонтальной координаты центра упругости (центра поворота) кузова многоосного автомобиля, на основе чего и определяются нормальные реакции по осям транспортного средства в процессе его торможения, а при известном распределении тормозных сил строятся и кривые реализуемого сцепления. В обзорной части приведены данные анализа, который показал, что на сегодняшний день отсутствуют единая методика или рекомендации в отношении определения нормальных реакций дороги на осях многоосного колесного транспортного средства. Разработанная методика может быть применена в инженерных расчетах при проверке многоосных колесных транспортных средств на соответствие международным требованиям к тормозным системам (Приложение 10 к Правилам № 13 UN/ECE). Универсальность предложенной методики позволяет рекомендовать ее к внедрению в указанных выше Правилах. Расчеты кривых реализуемого сцепления на примере четырехосного транспортного средства показали, что учет особенностей конструкции подвески многоосного колесного транспортного средства существенно влияет на характер расположения кривых реализуемого сцепления в пределах допустимых ограничений, установленных Правилами № 13 UN/ECE.

*Ключевые слова:* многоосное транспортное средство, распределение тормозных сил, тормозная сила, эффективность торможения, кривые реализуемого сцепления, автомобиль повышенной проходимости, многоосник.

## References

1 UN/ECE. (2016). Regulation № 13 of the Economic Commission for Europe of the United Nations (UN/ECE) — Uniform provisions concerning the approval of vehicles of categories M, N and O with regard to braking: on condition 18.02.2016 — Official Journal of the European Union.

2 HOST R 41.13–2007. (2009). *Edinoobraznye predpisaniia, kasaiuschiesia transportnykh sredstv katehorii M, N i O v otnoshenii tormozheniia [Uniform regulations concerning M, N and O vehicles for braking]*. Moscow: Standartinform [in Russian].

3 Zalohin, M.Y., Liubarskyi, B.A., Schuklinov, S.N., Mychalevych, M.G., & Leontiev, D.V. (2018). Study of Proportional Pressure Modulator on the Basis of Electromagnetic-Type Linear Motor. Science & Technique, 17(5), 440–446.

4 Leontiev, D.N., Ryzhyh, L.A., Lomaka, S.I., Nikitchenko, I.N., Voronkov, O.I., Hritsuk, I.V., et al. (2019). About Application the Tyre-Road Adhesion Determination of a Vehicle Equipped with an Automated System of Brake Proportioning. Science & Technique, 18(5), 401–408.

5 Bogomolov, V., Klimenko, V., Leontiev, D., Ryzhyh, L. Smyrnov, O., & Kholodov M. (2020). Improving the brake control effectiveness of vehicles equipped with a pneumatic brake actuator. Science & Technique, 19(1), 55–62.

6 Shaoyi, B., Bo, L., & Yanyan, Z. (2018). Adhesion state estimation based on improved tire brush model. Advances in Mechanical Engineering, 01. doi:10.1177/1687814017747706

7 Meljnikov, D. (2006). Use of Simpack at the DaimlerChrysler Commercial Vehicles Division. Truck Product Creation (4P). DaimlerChrysler.

8 Jazar, R.N. (2008). Tire Dynamics. Vehicle Dynamics: Theory and Aplicacion, Berlin, Springer, 95–163.

9 Braun, O. M., Persson, B. N., Steenwyk, B., & Warhadpande, A. (2016). On the Dependency of Friction on Load: Theory and Experiment. EPL (Europhysics Letters), 113 (5), https:// doi.org/10.1209/0295–5075/113/56002.

10 The tyre. Grip. (2001). Michelin Technology Society, France, Clermont-Ferrand.

11 Li, Shengbo, Chen, Hailiang, Li, Renjie, Liu, Zhengyu, Wang, Zhitao, & Xin, Zhe. (2020). Predictive lateral control to stabilise highly automated vehicles at tire-road friction limits. Vehicle System Dynamics. 58, 768–786. DOI: 10.1080/00423114.2020.1717553

12 Bode, O. (2001). Possibilities and Limits of a Simple Tire-road Adhesion Determination — Represented at the Example of Brake Testing in Accordance with ECE-R 13. Hannover Conference on Tires, Chassis, Roads, Hannover, Germany, 69–86.

13 Miao, Yu, Guoxiong, Wu, Lingyun, Kong, & Yu, Tang (2017). Tire-Pavement Friction Characteristics with Elastic Properties of Asphalt Pavements. Applied Sciences, 7(11).

14 Artyomov, N., Podrigalo, M., & Abdulgazis, A. (2018) Analyzing the dynamics of a single car wheel. MATEC Web of Conferences 224, 02102, https://doi.org/ 10.1051/matecconf/201822402102.

15 Kashkanov, A. A., Diorditsa. V. M., Kucheruk, V. Yu., Karabekova, D. Zh., Khassenov, A. K., & Sharzadin, A. M. (2019). Inertial evaluation of the tyre-road interaction during emergency braking, Bulletin of the university of Karaganda-Physics. 2(94), 82–91. https://doi.org/10.31489/2019Ph2/82–91.

16 Kashkanov, A. A., Rotshtein, A. P., Kucheruk, V. Yu., & Kashkanov, V. A. (2020). Tyre-Road friction Coefficient: Estimation Adaptive System. Bulletin of the university of Karaganda-Physics. 2(98). P. 50–59. DOI: 10.31489/2020Ph2/50–59.

17 Saraiev, O., & Gorb, Y. (2018). A Mathematical Model of the Braking Dynamics of a Car. SAE Technical Paper 2018–01–1893. https://doi.org/10.4271/2018–01–1893.

18 Funktsionalnyi rozrakhunok halmivnoi systemy avtomobilia z barabannymy halmamy ta reguliatorom halmivnykh syl [Functional calculation of the car brake system with drum brakes and regulator of braking forces]. (2003). / [A.M. Turenko, V.O. Bohomolov, V.I. Klymenko ta insh.] — Kharkiv: KhNADU [in Ukrainian].

19 Leontiev, D., Klimenko, V., Mykhalevych, M., Don, Y., & Frolov, A. (2020) Simulation of Working Process of the Electronic Brake System of the Heavy Vehicle. Advances in Intelligent Systems and Computing, 1019, P. 50–61. Springer, Cham. DOI: 10.1007/978–3-030–25741–5_6

20 Metodychni rekomendatsii z vyznachennia osovykh navantazhen transportnykh zasobiv z urakhuvanniam syl, shcho diiut u pliami kontaktu yoho shyn z poverkhneiu dorozhnoho odiahu [Methodological recommendations for determining the axial loads of vehicles taking into account the forces acting in the spot of contact of its tires with the road surface]. (2017). MR V.2.3–37641918–887:2017. Kyiv: Ukravtodor [in Ukrainian].

21 Aksenov, P.V. (1989). *Mnohoosnye avtomobili [Multi-axle vehicles]*. (2d Ed.). Moscow: Mashinostroenie [in Russian].

22 Zhdaniuk, V.K. (2017). Provesty doslidzhennia ta rozrobyty metodychni rekomendatsii z vyznachennia osovykh navantazhen bahatovisnykh transportnykh zasobiv z urakhuvanniam syl tertia v ploshchi kontaktu shyny z dorozhnim pokryttiam [Carry out research and develop methodological recommendations for determining axial loads of multi-axle vehicles, taking into account the friction forces in the contact area of the tire with the road surface]. *Zakliuchnyi zvit pro naukovo-doslidnu robotu za temoiu № 5/35–79–16 / Kharkivskyi natsionalnyi avtomobilno-dorozhnii universytet. № DR 0116U005525* [in Ukrainian].

23 Rotenberg, R.V. (1960). *Podveska avtomobilia i eho kolebaniia [Suspension of the car and its oscillations]*. Moscow: Mashhiz [in Russian].

24 Ponizovkin, A.N., Vlasko, Yu. M., & Lyalikov, M.B. et al. (1994). *Kratkii avtomobilnyi spravochnik [A brief car directory]*. Moscow: AO «Transkonsaltinh»; NIIAT [in Russian].

DOI 10.31489/2021Ph1/46-56
UDC 004.89+528–187.4

I.Y. Cherepanska[1*], A.Y. Sazonov[2], N.I. Krushynska[3], V.A. Priadko[1], M.V. Lukiniuk[2]

[1*] *Polissya National University, Zhytomyr, Ukraine;*
[2] *National Technical University of Ukraine «Igor Sikorsky Kyiv Polytechnic Institute», Kyiv, Ukraine;*
[3] *Zhytomyr Polytechnic State University, Zhytomyr, Ukraine*
*(*E-mail: cherepanskairina@gmail.com)*

# Quaternion Method of Calculating Angles while Measuring via Goniometric Precision Instrument System

The article is devoted to the topical problem: increasing accuracy and performance of angle measurements necessary in various branches of science and technology. One of the ways of increasing accuracy and performance of angle measurements is using modern algorithmic methods and mathematic devices for processing measurement information. Thus, in order to increase accuracy and speed of angle measurements on the example of the well-known goniometric precision instrument system (GPIS), it was offered quaternion calculation of angle values while performing goniometric measurements in the work. The efficiency of quaternion calculation is unquestioned as quaternions unlike other traditional methods (in particular matrix with the use of Euler angles, direction cosines) are presented only with four parameters describing angle positions of the objects and have only one connection equation unlike six equations for matrix methods, in particular for direction cosines. The suggested quaternion calculation is used in GPDS as general theoretic and information basis of contactless precision goniometric measurements in preliminary setting navigation sensitive elements (NSE), plane angles, pyramid prisms etc. The usage of the developed quaternion calculation enabled to increase accuracy by 0,25″ (in 3 times) and measurement performance in 9 times (up to 6.5 sec.) in comparison with the famous ones. Applying quaternion calculation of angle values implies using a smaller RAM capacity of PC that increases performance of system work. Besides, a smaller amount of mathematic operations performed in quaternion way of calculating angles, except increasing performance, enables to decrease a rounding error in calculation results that is accumulated in multiple measurements and may reach great values. Thus, accuracy and performance of measurements increase.

*Keywords:* quaternion, goniometric system, accuracy, performance, measuring angles, precision.

## *Introduction*

*Setting the general problem.* Precision angle (goniometric) measurements serve as an important metrological task aimed to provide quality of production. Precision angle measurements are conducted in various branches of machine-building and instrumentation (for example, in producing such precision joints and parts as direction ones like «dovetail» joint, conical seats of precision axes, optical prisms etc.), in preliminary setting navigation sensitive elements (NSE) [1] (accelerometers and gravity meters used in modern systems of orientation and navigation in directing the motion of different moving objects — cars, aircraft systems of various purposes, systems of artillery shells guiding), verification of dividing heads [2], determining straightness tolerance of positioning work benches angles, rounding error of measuring automated-measuring systems [3] etc. At the same time the branches of applying angle measuring means are constantly being expanded and their quality is also dramatically increasing, in particular, their quality; besides, their functional abilities are expanded, the automation of measuring and processing measurement information is provided.

One of the topical ways to increase accuracy and performance of goniometric systems, for example, a famous goniometric precision instrument system (GPIS) [5] is using modern algorithmic methods and mathematical apparatus for processing measurement information, in particular, mathematical apparatus of quaternions.

*Famous research and publications analysis.* [1–9] showed that mathematical apparatus of quaternions may be successfully applied in tasks of spatial measurement of angles and enables to increase performance and accuracy. It relates to the fact that unlike other classic methods (in particular, matrix ones), quaternions are introduced by four parameters only describing angle positions and have only one constraint equation unlike six equations for classic matrix methods, in particular, for direction cosines.

Thus, in works [1, 2] it was introduced the research results of two algorithms of auto-collimation measurements of object's spatial turn based on the matrix and quaternion models. It was shown the advantage of a quaternion algorithm according to the criterion of reducing measurement rounding error. However, the issue of applying quaternion calculation in angle measurements via modern goniometric systems are fragmentary shown. It was introduced a new quaternion filter for gyroscopes and accelerometers in spatial measurement of angles in the work [3]. So called projected quaternion is calculated by the authors on the basis of angle speed of a gyroscope. It was shown by the authors that application of quaternions increases efficiency of calculations and measurement accuracy. However, unfortunately, the practical aspects of work are only partially shown.

The authors developed quaternion algorithm of determining angular rotation with high calculating efficiency in any positions of measurement objects in the article [4]. It was proved by the authors the opportunity of increasing accuracy and rate of angle measurements. However, the issues of applying quaternions in modern goniometric measurement systems while measuring plane angles of polygonal prisms, pyramidality of prisms and other production objects are not considered.

In the work [5] it was introduced the results of calculations concerning measured angles in spatial turns of the objects. The issues of measuring plane angles of polygonal prisms, pyramidality of prisms and other production objects are not considered by the authors. In the work [6] it was given the results of quaternions application in the formalized description of objects angle motion; it was proved their advantage over other mathematical methods. The issue of applying quaternions in goniometric measurements is not considered by the authors. In the work [7] it was stated that quaternions application is of a special importance in cases when quaternion is used not only for setting object's orientation in three-dimensional space, but also for determining some additional scalar value. Practical aspects of applying quaternions in goniometric measuring plane angles of polygonal prisms, prisms pyramidality and other production objects, except NSE, are not highlighted.

In the work [8] it was introduced the results of modelling a quaternion algorithm of determining spatial angles via accelerometer and gyroscope that demonstrate its advantage. However, the possibility of using quaternions in other goniometric systems is not considered.

In the work [9] it was considered the application of quaternions in auto-collimation measurements of the preliminary setting NSE and it was determined its efficiency compared to the matrix method. The given results of computer modelling prove the efficiency of quaternion models for increasing accuracy of angle measurements.

Thus, the perspective of applying quaternions in precision goniometric measurements regarding to the experience obtained, is unquestionable. At the same time the issue of applying quaternions in precision goniometric systems, for example, a famous goniometric precision instrumental system (GPIS) [10], have not been considered yet.

*Highlighting the unsolved part of the problem set.* Thus, it is possible to claim that despite essential scientific and practical achievements the problem of measuring values of plane angles with high precision and performance has not been solved completely. Rounding errors of the vast majority of modern goniometric systems are unacceptably large and comprise from 1″ till 0,12″. Impossibility of applying such goniometric systems is caused by the fact that according to the international standards of quality, modern production always sets tougher and tougher requirements concerning accuracy and performance of measurements. One of the most effective ways of increasing accuracy and performance of angle measurements is developing new and improving well-known devices and measurement apparatus for processing measurement information including mathematical apparatus of quaternions.

*The purpose of the article* implies offering quaternion calculation of angle values to provide increasing accuracy and performance in goniometric contactless measurements via famous IPAMS, with preliminary setting NSE, plane angles, prisms pyramidality etc.

*Description of the suggested quaternion calculation of angles*

Goniometric precision instrumental system (GPIS) [10] (Figure 1) developed on the basis of precision angle-measurement system GS1L [12] (ARSENAL SDP SE (Kyiv, Ukraine)). GPIS may be applied for contactless precision goniometric measurements with preliminary setting NSE, plane angles, prisms pyramidality and other production objects, optical glass index deflection.

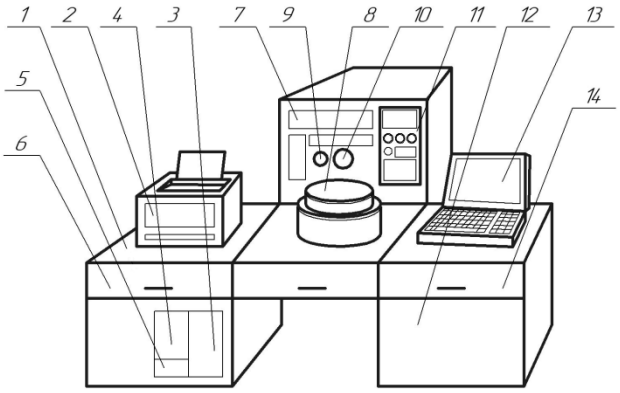


Figure 1. GPIS Scheme: 1 — side bar; 2 — printer; 3 — rectifier; 4 — power supply unit; 5 — voltage stabilizer; 6, 14 — box for implements; 7 — measuring bar; 8 — rotating device with angle converter and subject board; 9 — autocollimator; 10 — spectral (laser) emitter; 11 — panel of switches and control lever; 12 — side bar with the unit of initial processing and managing information; 13 — personal computer (PC)

In order to increase accuracy and performance of GPIS it is offered to apply the previously developed methodology of calculating necessary amount of measurement in multiple observations [13], algorithmic correction of measurement results [14] and the suggested quaternion measurement of angles in goniometric measurements based on the theorems and axioms of quaternions Algebra in a complex and serves as a general theoretic and information basis of defining various angles in preliminary setting NSE, plane angles, prisms pyramidality and other production objects. Applying the stated methodology of calculating the necessary amount of measurements and algorithmic correction of measurement results [13, 14] as for processing measurement results in complex with the suggested quaternion measurement of angles in goniometric measurements will enable to conduct measurements of IPAMS with the increased accuracy and performance. Description of methodology for calculating the necessary amount of measurements in multiple observation and algorithmic correction of measurement results is introduced in sources [13, 14].

In general, quaternion $q$ itself is a structured four of real numbers $s, a, b, c$, connected in between via four basic elements $1, i, j, k$ (Figure 2), and have the following properties: $i^2 = j^2 = k^2 = -1$; $i \cdot j = k$; $j \cdot k = i$; $k \cdot i = j$; $j \cdot i = -k$; $k \cdot j = -i$; $i \cdot k = -j$.

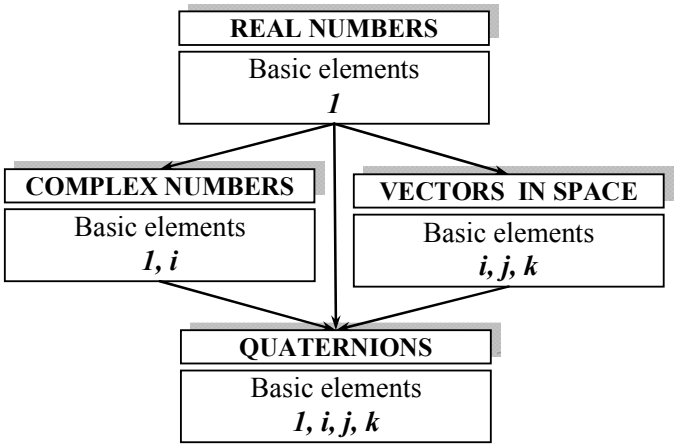


Figure 2. Numeral systems and basic elements of quaternions

Quaternion $q$ is introduced in different ways:

– as a sum of two quaternions: scalar ($s$) i vector ($a \cdot i + b \cdot j + c \cdot k$), that is $q = s(q) + v(q) = [scalar; (vector)]$;

– as a number and 3D-vector, that is as a hyper-complex number with three imaginative units $i, j, k$, that is $q = [s, a, b, c] = [scalar, (vektor)] = [s, (a, b, c)] = s \cdot 1 + a \cdot i + b \cdot j + c \cdot k = s + v$;

– as a vector — a quaternion looks like a vector in case its scalar part is equal to zero: $q(vector) = a \cdot i + b \cdot j + c \cdot k$; $scalar = 0$;

– as a sum $\cos\frac{\omega}{2}$ and $\sin\frac{\omega}{2}$ in solving goniometric tasks, that is $q(v,\omega) = \cos\frac{\omega}{2} + v \cdot \sin\frac{\omega}{2}$, where $v$ — a unit vector, co-directed with pivot axis; ω — angular rotation.

An important peculiarity of quaternions lies in the fact that their subset comprises real numbers (*s*, *0*, *0*, *0*); complex numbers (*s*, *a*, *0*, *0*); vectors in three-dimensional space (*0*, *a*, *b*, *c*), and the law of commutativity is not obeyed in performing multiplication while multiplying quaternions, that is $q_1 \cdot q_2 \neq q_2 \cdot q_1$.

Besides, three imaginative basic units *i, j, k* of quaternions may be interpreted as basic vectors of Cartesian coordinates system *XYZ* in three-dimensional space (Figure 3).

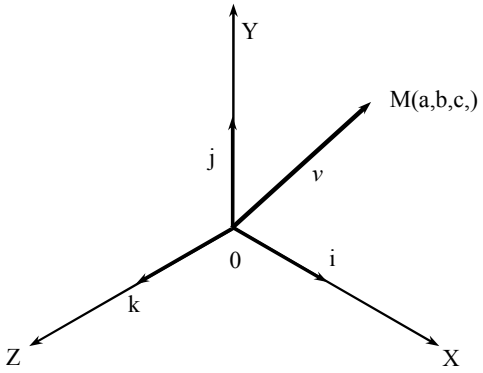


Figure 3.

While conducting GPIS goniometric measurements in three-dimensional space, for example, in preliminary setting NSE angles, at the last stage it is necessary to fix the reflecting element, for instance, a mirror, sensitive to its movements. NSE setting is conducted before navigation system functioning via the method of angle coordination, enabling to reach higher accuracy and comprises comparison of angle position of coordinate system of the local coordinate system *xyz* NSE regarding axes of absolute, in advance adopted Cartesian coordinate system (Figure 1, a). In this case, NSE turns will be defined as altering position of coordinate system *xyz* of reflecting element regarding Cartesian coordinate system XYZ, connected with GPIS autocollimator (Figure 4, b).

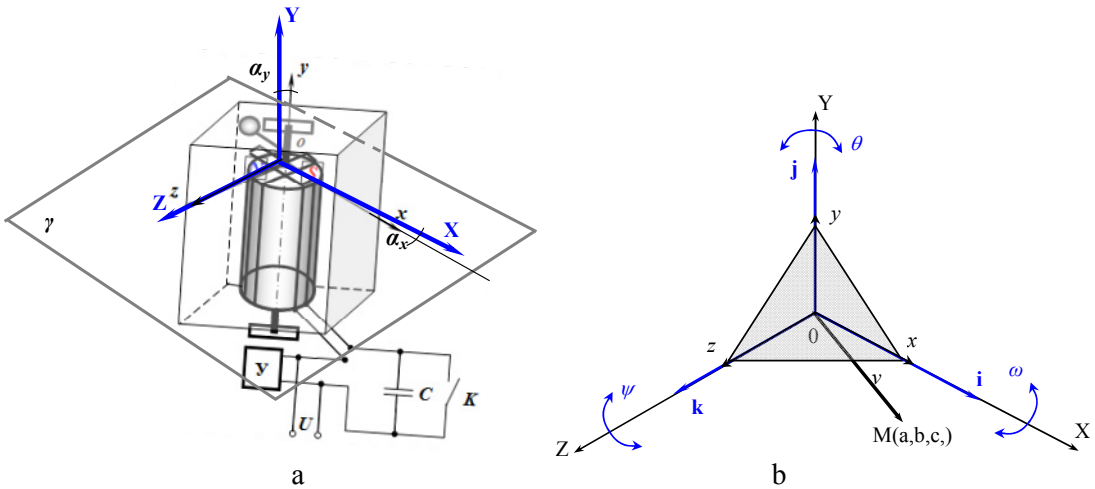


Figure. 4. Example of setting NSE (pendulum accelerometer): a — rounding error of setting, b — position of light-reflecting element coordinate system *xyz* regarding Cartesian coordinate system *XYZ*

The position of NSE is described by turns of axes *XYZ* in coordinate system of autocollimator into angles $\omega, \theta, \psi$, accordingly. The result of some sequence in NSE movements while its setting is a turn in coordinate system *XYZ* to a certain angle *XYZ* regarding the axis, collinear to the unit vector (Fig.4, b). Correcting movements as for setting initial NSE coordinates and its levelling may be introduced via quaternion $q_k(v;\varphi) = (\cos\frac{\varphi_k}{2} + v\sin\frac{\varphi_k}{2})$, and sequence of movements — via corresponding turn parameters — product of proper quaternions, introduced via expression (1):

$$q_1(v;\omega) = (\cos\frac{\omega_k}{2} + i\sin\frac{\omega_k}{2}),$$
$$q_2(v;\theta) = (\cos\frac{\theta_k}{2} + j\sin\frac{\theta_k}{2}), \quad (1)$$
$$q_3(v;\psi) = (\cos\frac{\psi_k}{2} + k\sin\frac{\psi_k}{2}).$$

Product $Q$ of quaternions $q_1(v;\omega)$, $q_2(v;\theta)$, $q_3(v;\psi)$, is calculated by formulae (2) performing multiplication operations according to the rules of quaternions multiplication:

$$Q(v;\varphi) = (\cos\frac{\omega_k}{2} + i\sin\frac{\omega_k}{2})\cdot(\cos\frac{\theta_k}{2} + j\sin\frac{\omega_k}{2})\cdot(\cos\frac{\psi_k}{2} + k\sin\frac{\psi_k}{2}) = S + iA + jB + kC, \quad (2)$$

where $S = \cos\frac{\omega_k}{2}\cos\frac{\theta_k}{2}\cos\frac{\psi_k}{2} - \sin\frac{\omega_k}{2}\sin\frac{\theta_k}{2}\sin\frac{\psi_k}{2}$;

$A = \sin\frac{\omega_k}{2}\cos\frac{\theta_k}{2}\cos\frac{\psi_k}{2} + \cos\frac{\omega_k}{2}\sin\frac{\theta_k}{2}\sin\frac{\psi_k}{2}$;

$B = \cos\frac{\omega_k}{2}\sin\frac{\theta_k}{2}\cos\frac{\psi_k}{2} - \sin\frac{\omega_k}{2}\cos\frac{\theta_k}{2}\sin\frac{\psi_k}{2}$;

$C = \sin\frac{\omega_k}{2}\sin\frac{\theta_k}{2}\cos\frac{\psi_k}{2} + \cos\frac{\omega_k}{2}\cos\frac{\theta_k}{2}\sin\frac{\psi_k}{2}$.

For example, while setting NSE it was performed turns $\omega = 10°$ $\theta = 27°$ $\psi = 40°$. Hence the beam of a circular laser IPAMS will be reflected from the reflecting element, fixed on NSE to CMOS-matrix of IPAMS autocollimator at an angle of 50°52′ with coordinates (0.158, 0.189, 0.350) calculated in the following way:

$$q_1(v;10)\cdot q_2(v;27)\cdot q_3(v;40) =$$
$$= (\cos\frac{10}{2} + i\sin\frac{10}{2})\cdot(\cos\frac{27}{2} + j\sin\frac{27}{2})\cdot(\cos\frac{40}{2} + k\sin\frac{40}{2}) =$$
$$= \cos 24.43 + (i0.158 + j0.189 + k0.350)\sin 25.43 =$$
$$= 50.86 + (i0.158 + j0.189 + k0.350) \Rightarrow q(v;50^\circ 52').$$

While conducting goniometric measurement of plane angle values, for example, polygonal prisms with $n$-number of facets, the lengths of which comprise $l_0, l_1, \ldots, l_n$ and proper angles $\varphi_k$, where $k \in (0, 1, \ldots, n)$; if each vertex is connected with right Cartesian coordinates system with unit basis $i, j, k$ (Figure 5), it is possible to use the normalized quaternion as:

$$q_k(v;\varphi) = (\cos\frac{\varphi_k}{2} + v\sin\frac{\varphi_k}{2}), \quad (3)$$

where: $v$ — unit vector, regarding which the value of angle $\varphi$, $v \in (i, j, k)$ is figured out

$\varphi$ — flat angle value;

$k$ — ordinary number of angle (facet), $k \in (0, 1, \ldots, n)$.

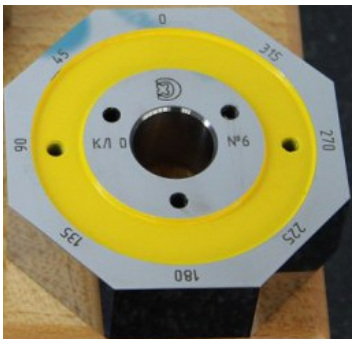

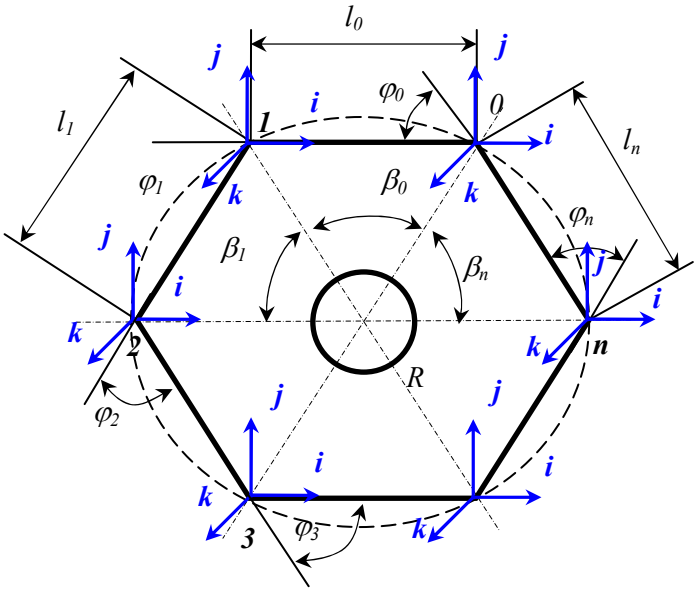


Figure 5.

Each *n*-vertex of polygonal prism is connected with Cartesian coordinates system with unit basis $i, j, k$ (Fig. 5). Resulting this, $n$ of coordinates system is formed, each system is supplied quaternion in accordance (3). Then, for each vertex (and angle accordingly $\varphi_k \mid k \in (0, 1, \ldots, n)$) of polygonal prism, it is possible to form a proper quaternion $q_1(v; \varphi_1), q_2(v; \varphi_2), \ldots, q_n(v; \varphi_n)$.

Quaternions of plane angles in polygonal prism $\varphi_k$ in three-dimensional space of coordinates system with basis $i, j, k$ is convenient to introduce in the form of a vector in the following way:

$$q_k(v; \varphi) = (\cos \frac{\varphi_k}{2}; i \sin \frac{\varphi_k}{2}; j \sin \frac{\varphi_k}{2}; k \sin \frac{\varphi_k}{2}). \quad (4)$$

At the same time, if proper quaternion (4) constituents equate zero, angle $\varphi_k$ will be defined regarding one or two coordinates axes of right Cartesian coordinates system with unit basis $i, j, k$. Thus, for example, if angle $\varphi_k$ is defined regarding axis $X$, then quaternion (4) will have the following simple expression:

$$q_k(v; \varphi) = (\cos \frac{\varphi_k}{2}; i \sin \frac{\varphi_k}{2}; 0; 0).$$

Quaternions of so-called exponential angles $\beta$ (Fig. 5) in three-dimensional space of coordinates system with basis $i, j, k$ are convenient to introduce in vector form in the following way:

$$q_k(v; \beta) = (\cos \frac{\beta_k}{2}; i \sin \frac{\beta_k}{2}; j \sin \frac{\beta_k}{2}; k \sin \frac{\beta_k}{2}), \quad (5)$$

where $\beta_k = \arccos(1 + \frac{l_k^2}{2R})$, figured out via cosines theorem, where $R$ — radius;

$k$ — ordinary angle number, $k \in (0, 1, \ldots, n)$.

In a similar way, if angle $\beta$ is defined regarding certain coordinates axis of right Cartesian coordinates system, collinear to one of the vectors of basic elements $i, j, k$, then corresponding constituents of quaternion (5), connected with other basic elements, will equate zero. In this case quaternion (5) will have a simple form.

For example, presenting quaternion (5) in the form $q_2(v; \beta) = (\cos \frac{45}{2}; 0; j \sin \frac{45}{2}; 0)$, means that exponential angle $\beta_2$ between 2nd and 3rd vertices of polygonal prisms (Fig.5) equals 45° and it was determined regarding axis $Y$ of right Cartesian coordinates system, collinear to unit vector $j$ and basis $i, j, k$.

Taking into account properties of quaternions, their application for calculating angles in goniometric measurements of GPIS in preliminary setting NSE, plane angles, prisms pyramidality etc., enables to figure out directly angle values, and also axis of rotation and coordinates of laser radiation reflection onto CMOS-matrix of GPIS auto-collimator.

Random examples of quaternion introduction of angles in absolute right Cartesian coordinates system with basis *i, j, k,* are introduced in Table 1.

Table 1

**Random examples of quaternion introduction of angle values in absolute right Cartesian coordinates system with basis, *i, j, k***

| Values of turning angles OB regarding absolute coordinates system *X, Y, Z* | | | Results of turns | | | |
|---|---|---|---|---|---|---|
| | | | Position of vector v regarding basis of absolute coordinates system *X, Y, Z* | | | |
| ***ω°*** | ***θ°*** | ***ψ°*** | ***φ*** | ***i*** | ***j*** | ***k*** |
| 5 | 5 | 5 | 9 | 0.45 | 0.45 | 0.42 |
| 7 | 7 | 7 | $12^0 47'$ | 0.64 | 0.64 | 0.57 |
| 10 | 27 | 40 | $50^0 52'$ | 0.158 | 0.189 | 0.350 |
| 60 | 25 | 70 | $82^0 5'$ | 0.5070 | - 0.1269 | 0.3967 |
| 60 | 25 | 70 | $101^0 52'$ | 0.5070 | -0.1269 | 0.5736 |
| 60 | 25 | 70 | $101^0 52'$ | 0.2923 | 0.4333 | 0.5736 |
| 60 | 25 | 70 | $82^0 5'$ | 0.2923 | -0.1269 | 0.5736 |
| 60 | 25 | 70 | $101^0 52'$ | 0.5070 | 0.4333 | 0.3967 |
| 90 | 90 | – | 120 | 0.5 | 0.5 | 0.5 |
| – | 90 | 90 | 120 | -0.5 | 0.5 | 0.5 |
| 50 | 40 | – | $63^0 17'$ | 0.397 | 0.31 | 0.145 |
| – | 50 | 30 | $57^0 52'$ | 0.11 | 0.409 | 0.236 |
| 53 | 53 | – | 74 | 0.399 | 0.399 | 0.199 |

In general, the algorithm of quaternion angle calculation in IPAMS may be introduced in the following sequence of steps:

1. Angle description via product of proper quaternions in expressions (1), (2);
2. Resulting quaternion calculation in accordance with quaternions characteristics:

– commutativity and associativity in addition: $q_1 + q_2 = q_2 + q_1$, $(q_1 + q_2) + q_3 = q_2 + (q_1 + q_3)$,

– non-commutativity in multiplication: $q_1 \cdot q_2 \neq q_2 \cdot q_1$,

– associativity in multiplication: $(q_1 \cdot q_2) \cdot q_3 = q_1 \cdot (q_2 \cdot q_3)$,

– distributivity: $q_1 \cdot (q_2 + q_3) = q_1 \cdot q_2 + q_1 \cdot q_3$;

3. Definition of angle, direction and coordinates of light beam reflection to CMOS-matrix of IPAMS.

Application of the quaternion method of calculating angles in goniometric measurements IPAMS implies performing 29 mathematic operations, in particular 16 multiplication operations, 12 addition operations and 1 operation to figure out angle arccosine. While applying classic matrix method engaging Euler's angles, described in sources [15], it is necessary to fulfil 45 mathematic operations, in particular 30 multiplication operations, 15 addition operations and 3 operations to define arccosines of angles in the similar case.

It is obvious that applying quaternion calculation method enables to decrease the number of mathematic operations in 1.55 times compared with classic matrix methods of angle calculation. At the same time, taking into account the fact that multiple observations are applied in measurement, the number of results *N* may be quite large, so it obviously leads to decreasing the time spent and RAM capacity of computer system of IPAMS. Measurement performance increases due to this fact. In general, a complex approach to applying quaternion methods of calculating angles and other methods and means of automated processing of measurement information in GPIS, described in sources [6, 10, 13, 14] enabled to increase performance of goniometric measurements in 9 times (up to 6.5 sec) in comparison with well-known goniometric means [12, 16].

The developed algorithm of GPIS functioning and software allowing application of a quaternion method and measuring GPIS angles in the automatic mode with the increased accuracy and performance (Figure 6).

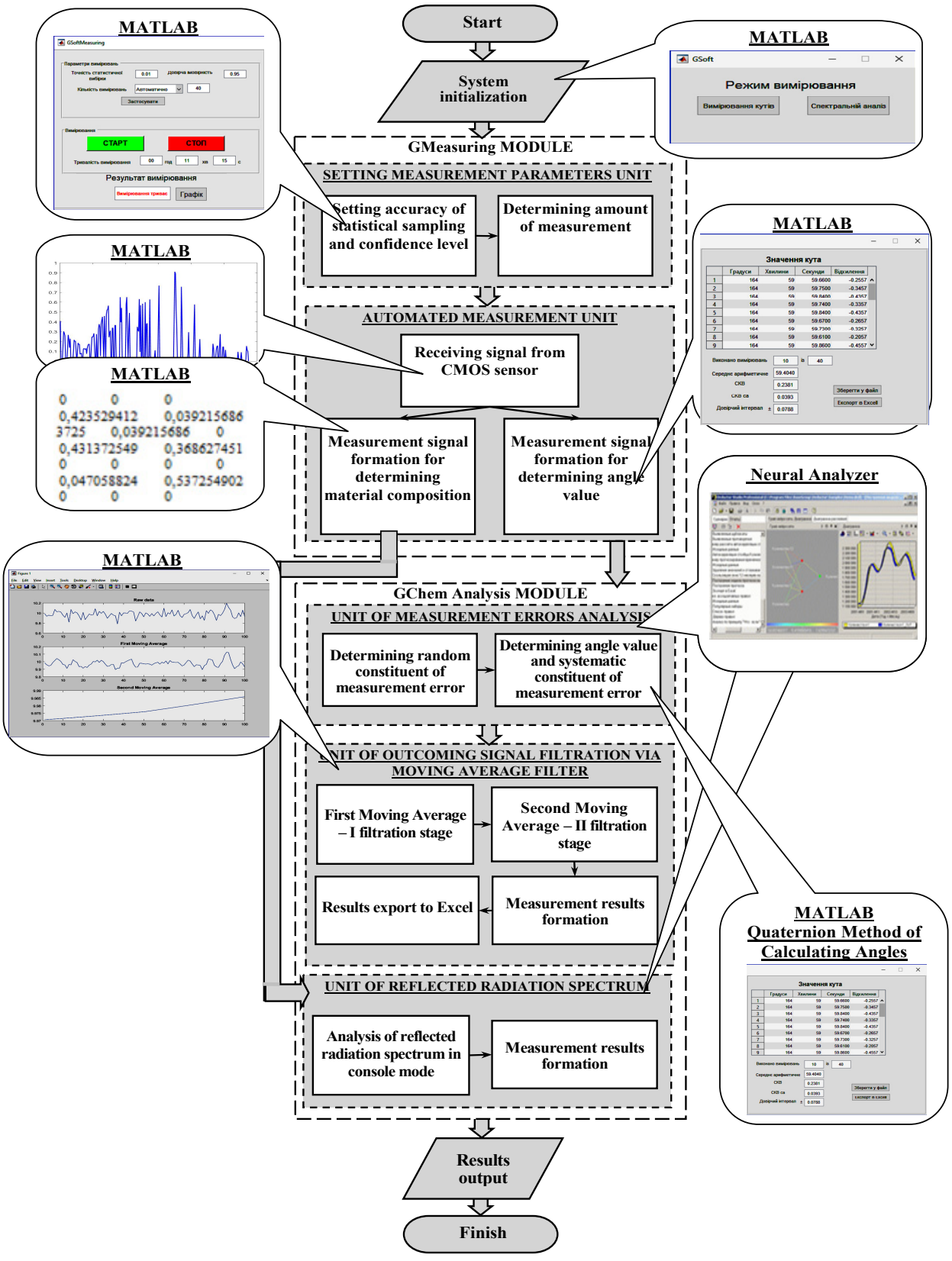


Figure. 6. Structure scheme of GPIS software functioning

Increasing accuracy of goniometric measurements GPIS in applying the suggested quaternion method of angles calculation is reached due to a smaller number of mathematical operations. It allows reducing rounding errors for both end and intermediate results of calculation that are accumulated in multiple measurements and may reach rather large values. In general, application of a quaternion method of calculating angles in IPAMS in complex with other methods and means of automated processing measurement information, described in sources [5, 10, 13, 14], enabled to increase accuracy in 3 times (by 0.2″), compared to famous goniometric means [12, 14].

*Conclusion*

1. It was introduced a quaternion method of calculation in goniometric measurements that serves as a basic theoretical and information ground for contactless precision goniometric measurements GPIS, with preliminary setting NSE, plane angles prisms pyramidality etc.

2. Application of a quaternion method of calculation in GPIS enables to expand its functional abilities, providing measurements of angle values in three-dimensional space with preliminary setting NSE, and also plane angles of polygonal prisms, and may be used in determining prisms pyramidality and other production objects, index of optical glass deflection.

3. It was defined that quaternion models enable calculation of angle values with preliminary setting NSE, plane angles of polygonal prisms and may be applied in determining prisms pyramidality and other production objects, index of optical glass deflection. Applying quaternion models of calculating angle values requires a smaller RAM capacity of PC and increases measurement performance.

4. A comparatively smaller amount of mathematical operations performed via quaternion method of angles calculation enables to reduce rounding errors in calculation results accumulated in multiple measurements and may reach larger values. Thus, measurement accuracy increases.

5. Application of quaternion method of angles calculation in GPIS enabled to increase accuracy by 0.2″ (3 times) and measurement performance from 6.5 s (9 times) compared to the well-known goniometric means.

References

1 Коняхин И.А. Экспериментальные исследования трехкоординатной автоколлимационной системы / И.А. Коняхин, Х.В. Фонг, Х.А. Фыонг // Изв. высш. учеб. зав. Приборостроение. — 2018. — Т. 61, № 9. — С. 751–755.

2 Хоанг В.Ф. Анализ погрешности измерения параметров поворота объекта методом автоколлимации с помощью компьютерных моделей на основе кватернионов / В.Ф. Хоанг, И.А. Коняхин // Изв. высш. учеб. зав. Приборостроение. — 2017. — Т. 60, № 12. — С. 1157–1160.

3 Valenti R.G. Keeping a Good Attitude: A Quaternion-Based Orientation Filter for IMUs and MARGs / R.G. Valenti, I. Dryanovski, J. Xiao // Journal List Sensors (Basel). — 2015. — Vol.15(8). — P. 19302–19330.

4 Xu X. A Robust Incremental-Quaternion-Based Angle and Axis Estimation Algorithm of a Single-Axis Rotation Using MARG Sensors. / X. Xu, X. Tian, L. Zhou. // *IEEE Access*. — 2018. — Vol. 6. — P. 42605–42615.

5 Кирилович В.А. Теорія кватерніонів як теоретична основа формалізованого опису орієнтуючих рухів об’єктів автоматизованих виробництв / В.А. Кирилович, І.Ю. Черепанська // Якість-2006: Всеукраїнська наук.-техн. конф. (22–25 лютого 2006 р.). — Харків: Стандартизація, сертифікація, якість, 2006. — С. 88–91.

6 Черепанська І.Ю. Теорія і принципи побудови автоматизованої системи для лінійних і кутових переміщень об'єктів виробництва з використанням математичного апарату кватерніонів і елементів штучного інтелекту: моногр. / І.Ю. Черепанська, В.А. Кирилович, А.Ю Сазонов. — Житомир: ЖДТУ, 2016. — 326 с.

7 Гордеев В.Н. Кватернионы и бикватернионы с приложениями в геометрии и механике / В.Н. Гордеев. — Киев: Изд-во «Сталь», 2016. — 316 с.

8 Fei L. An improved quaternion Gauss–Newton algorithm for attitude determination using magnetometer and accelerometer. / L. Fei, L. Jie, W. Haifu // Chinese Journal of Aeronautics. — 2014. — Vol. 27, Issue 4. — P. 986–993.

9 Коняхин И.А. Применение кватернионов для расчета параметров отражателя автоколлимационной углоизмерительной системы / И.А. Коняхин, В.Ф. Хоанг // Науч.-техн. вестн. информ. техн., механики и оптики. — 2016. — Т. 16, № 5. — С. 773–779.

10 Черепанська І.Ю.Інтелектуальна система вимірювання кутів / І.Ю. Черепанська, О.М. Безвесільна, А.Ю. Сазонов // Патент України на корисну модель 127373, МПК: G 01 B 21/22 (2006.01), 25.07.2018

11 Лазерная измерительная система XL-80. [Электронный ресурс]. — Режим доступа: https://www.renishaw.ru/media/pdf/ru/97a84b986e1642a09035d3d9f24e72e5.pdf

12 Гониометр. КП СПС «Арсенал» [Электронный ресурс]. — Режим доступа: http://zavodarsenal.kiev.ua/goniometr-spektrometr-gs2/

13 Cherepanska I. The procedure for determining the number of measurements in the normalization of random error of an information–measuring system with elements of artificial intelligence / I. Cherepanska, E. Bezvesilna, A. Sazonov. // Eastern–European journal of enterprise technologies. — 2017. — № 5/9 (89). — P. 58–67.

14 Черепанська І.Ю. Алгоритмічна корекція результатів вимірювання прецизійної приладової гоніометричної системи / Черепанська І.Ю., Безвесільна О.М., Сазонов А.Ю. // Вчені зап. Таврій. нац. ун-ту ім. В.І. Вернадського. Сер. Технічні науки. — № 2, Т. 30 (69). — Київ, 2019. — С. 6–11

15 Кураш А. Г. Курс высшей алгебры / А. Г. Кураш. — М.: Наука, 1975. — 302 с.

16 Безвесільна О. М. Автоматизований прецизійний пристрій для вимірювання кутів: моногр. / О.М. Безвесільна. — Житомир: ЖДТУ, 2010. — 258 с.

И.Ю. Черепанская, А.Ю. Сазонов, Н.И. Крушинская, В.А. Прядко, Н.В. Лукинюк

## Гониометриялық дәл аспаптық жүйемен өлшеу кезінде бұрыштарды есептеудің кватерниялық әдісі

Мақала ғылым мен техниканың әр түрлі салаларында қажетті бұрыштық өлшеулердің дәлдігі мен жылдамдығын арттырудың өзекті мәселесіне арналған. Бұрыштық өлшеулердің дәлдігі мен жылдамдығын арттырудың жолы — өлшеу ақпаратын өңдеу үшін соңғы алгоритмдік әдістер мен математикалық құрылғыларды қолдану. Сондықтан, бұрыштық өлшеулердің дәлдігі мен әсер етуін арттыру мақсатында жұмыста белгілі гониометриялық дәл аспаптық жүйенің (ГДАЖ) мысалында гониометриялық өлшеулердегі бұрыштардың шамаларын сандық есептеу ұсынылды. Кватерниондық есептеудің тиімділігі күмән тудырмайды, өйткені басқа дәстүрлі әдістерден айырмашылығы, кватерниондар (атап айтқанда Эйлер бұрыштарын қолданатын матрицалар, косинус бағыттаушылары) объектілердің бұрыштық позицияларын сипаттайтын төрт параметрмен ғана ұсынылған және алтыдан айырмашылығы бір ғана байланыс теңдеуі бар, матрицалық әдістер үшін, атап айтқанда, косинус бағыттаушыларына арналған. Ұсынылған кватерниондық есептеу ГДАЖ бағыттағыш сезімтал элементтердің (БСЭ), жазық бұрыштардың, призмалардың пирамидалығының және т.б. алдын ала көрсету үшін жанаспайтын дәл гониометриялық өлшемдердің жалпы теориялық-ақпараттық негізі ретінде пайдаланылды. Әзірленген кватерниондық есептеуді қолдану белгілі есептермен салыстырғанда дәлдікті 0,25 (3 есе) және өлшеу жылдамдығын 9 есе (6,5 С дейін) арттыруға мүмкіндік береді. Бұрыштардың шамаларын кватерниондық есептеуді қолдану дербес компьютердің жедел жадының аз көлемін пайдалануды көздейді, бұл жүйенің жұмысын жақсартады. Сонымен қатар, бұрыштарды есептеудің квадрат әдісін қолдана отырып орындалатын математикалық операциялардың аз саны, өнімділікті арттырумен қатар, бірнеше өлшеулерде жиналатын және үлкен мәндерге жететін есептеу нәтижелерінің жуықтау қатесін азайтуға мүмкіндік береді. Осылайша өлшеулердің дәлдігі мен жылдамдығы артады.

*Кілт сөздер:* кватернион, гониометриялық жүйе, дәлдік, жылдамдық, бұрыштарды өлшеу, дәл жүйе.

И.Ю. Черепанская, А.Ю. Сазонов, Н.И. Крушинская, В.А. Прядко, Н.В. Лукинюк

## Кватернионный метод расчета углов при измерениях гониометрической прецизионной приборной системой

Статья посвящена актуальной проблеме — повышению точности и быстродействия угловых измерений, необходимых в различных областях науки и техники. Одним из путей повышения точности и быстродействия угловых измерений является применение новейших алгоритмических методов и математических аппаратов для обработки измерительной информации. Поэтому в работе с целью повышения точности и быстройдействия угловых измерений на примере известной гониометрической прецизионной приборной системы (ГППС) предложен кватернионный расчет величин углов при гониометрических измерениях. Эффективность кватернионного расчета не вызывает сомнения, поскольку, в отличие от других традиционных методов (в частности, матричных с применением углов Эйлера, направляющих косинусов), представляется только четырьмя параметрами, описывающими угловые положения объектов, и имеет лишь одно уравнение связи, в отличие от шести, для матричных методов, в частности, для направляющих косинусов. Предложенный кватернионный расчет используется в ГППС как общая теоретико-информационная основа бесконтактных прецизионных гониометрических измерений при предварительной выставке навигационных чувствительных элементов, плоских углов, пирамидальности призм и т.п. Применение разработанного кватернионнного расчета позволило повысить точность на 0,25″ (в 3 раза) и быстродействие измерения в 9 раз (до 6,5 с) по сравнению с известными. Применение кватернионного расчета величин углов предусматривает использование меньшего объема оперативной памяти персонального компьютера, что повышает быстродействие работы системы. Кроме того, меньшее количество математических операций, выполняемых с использованием кватернионного способа расчетов углов, кроме повышения быстродействия, позволяет уменьшить по-

грешность округления результатов вычислений, которая накапливается при многократных измерениях и может достигать больших значений. Таким образом, повышаются точность и быстродействие измерений.

*Ключевые слова:* кватернион, гониометрическая система, точность, быстродействие, измерение углов, прецизионная система.

## References

1 Koniakhin, I.A., Hoang, V.Ph., & Hoang, A.Ph. (2018). Eksperimentalnye issledovaniia trekhkoordinatnoi avtokollimatsionnoi sistemy [Experimental Study Of Threecoordinate Autocollimation System]. *Izvestiia vysshikh uchebnykh zavedenii. Priborostroenie — Scientific and Technical Journal «Priborostroenie», 61, 9,* 751–755 [in Russian].

2 Hoang, V.Ph., & Koniakhin, I.A. (2017). Analiz pohreshnosti izmereniia parametrov povorota obekta metodom avtokollimatsii s pomoshchiu kompiuternykh modelei na osnove kvaternionov [Error Analysis of Object Rotation Parameters Measurement with Autocollimation Method Using Computer Models on the Base of Quaternions]. *Izvestiia vysshikh uchebnykh zavedenii. Priborostroenie — Scientific and Technical Journal Priborostroenie, 60, 12,* 1157–1160 [in Russian].

3 Valenti, R.G., Dryanovski, I., & Xiao, J. (2015). Keeping a Good Attitude: A Quaternion-Based Orientation Filter for IMUs and MARGs. *Journal List Sensors (Basel), 15(8),* 19302–19330.

4 Xu, X., Tian, X., & Zhou, L. (2018). A Robust Incremental-Quaternion-Based Angle and Axis Estimation Algorithm of a Single-Axis Rotation Using MARG Sensors, *IEEE Access, 6,* 42605–42615.

5 Kyrylovych, V.A., & Cherepanska, I.Yu. (2006). Teoriia kvaternioniv iak teoretichna osnova formalizovanoho opisu orientuiuchikh rukhiv obektiv avtomatizovanikh virobnitstv [Quaternions Theory as Theoretical Basis of Formalized Description of Production Objects Orientation Movements in Automated Productions]. Proceedings from the all-Ukrainian Scientific and Technical Conference Quality ’06: *Yakist’-2006. Vseukrainska naukovo-tekhnichna konferentsiia (22–25 liutoho 2006 r.).* (pp 88–91). Kharkiv: Standartyzatsiia, sertyfikatsiya, yakist [in Ukrainian].

6 Cherepanska, I.Yu., Kyrylovych, V.A., & Sazonov, A.Yu. (2016). *Teoriia i printsipi pobudovi avtomatizovanoi sistemi dlia liniinikh i kutovikh peremishchen obektiv virobnitstva z vikoristanniam matematichnogo aparatu kvaternioniv i elementiv shtuchnoho intelektu [Theory and Principles of Design of Automation Systems for Linear and Angular Movements with Use of Quaternions and Artificial Intelligence]*. Zhytomyr: ZhDTU [in Ukrainian].

7 Gordeiev, V.N. (2016). *Kvaterniony i bikvaterniony s prilozheniiami v heometrii i mekhanike [Quaternions and Biquaternions with Applications for Geometry and Mechanics]*. Kiev: Izdatelstvo «Stal» [in Russian].

8 Fei, L., Jie, L., & Haifu, W. (2014). An improved quaternion Gauss-Newton algorithm for attitude determination using magnetometer and accelerometer. *Chinese Journal oy Aeronautics*, *27, 4,* 986–993.

9 Koniakhin, I.A. & Hoang, V.Ph. (2016). Primenenie kvaternionov dlia rascheta parametrov otrazhatelia avtokollimatsionnoi uhloizmeritelnoi sistemy [Application of Quaternions for Reflector Parameter Determination of the Autocollimation Angle Measuring System]. *Nauchno-tekhnicheskii vestnik informatsionnykh tekhnolohii, mekhaniki i optiki — Scientific and technical Bulletin of information technologies, mechanics and optics*, *16, 5,*773–779 [in Russian].

10 Cherepanska, I.Yu., Bevesilna, O.M. & Sazonov, A.Yu. (2018). Intelektualna systema vymiryuvannya kutiv [Intelligent System for Angles Measurement]. *Patent Ukraïni na korisnu model — Patent of Ukraine for an invention*, 127373, MPK: G 01 B 21/22 (2006.01) [in Ukrainian].

11 Lazernaia izmeritelnaia sistema XL-80 [Laser Measuring System XL-80]. *renishaw.ru.* Retrieved from https://www.renishaw.ru/media/pdf/ru/97a84b986e1642a09035d3d9f24e72e5.pdf [in Russian].

12 Honiometer. KP SPS «Arsenal» [Goniometer, KP SPS Arsenal]. *zavodarsenal.kiev.ua.* Retrieved from http://zavodarsenal.kiev.ua/goniometr-spektrometr-gs2/ [in Ukrainian].

13 Cherepanska, I., Bezvesilna, E., & Sazonov, A. (2017). The procedure for determining the number of measurements in the normalization of random error of an information-measuring system with elements of artificial intelligence. *Eastern-European journal of enterprise technologies*, *5/9, (89),* 58–67.

14 Cherepanska, I.Yu., Bezvesilna, O.M. & Sazonov, A.Yu. (2019). Alhoritmichna korektsiia rezultativ vimiriuvannia pretsiziinoi priladovoi honiometrichnoi sistemi [Algorithmic Correction of Measuring Results of the Precise Instrument Goniometric System]. *Vcheni zapiski Tavriiskoho natsionalnoho universitetu imeni V.I. Vernadskoho Seriia: Tekhnichni nauki — Scientific notes of Taurida National V.I. Vernadsky University». Series: Technical Sciences, 2, 30(69),* 6–11 [in Ukrainian].

15 Kurash, A.G. (1975). *Kurs vysshei alhebry [Higher algebra course]*. Moscow: Nauka [in Russian].

16 Bezvesilna, O.M. (2010). *Avtomatizovanii pretsiziinii pristrii dlia vimiriuvannia kutiv [Automated precise instrument for angles measurement]*. Zhytomyr: ZhDTU [in Ukrainian].

DOI 10.31489/2021Ph1/57-62
UDC 621.374: 537.524

A.K. Khassenov[1*], M. Stoev[2], D.Zh. Karabekova[1], G.A. Bulkairova[1], D.A. Nurbalayeva[1]

[1]*Karaganda University of the name of academician E.A. Buketov, Kazakhstan*
[2]*Neofit Rilski South-West University, Blagoevgrad, Bulgaria*
(**E-mail: ayanbergen@mail.ru)*

# Electro-pulse method for obtaining raw materials for subsequent flotation enrichment of ore

The main method of enrichment of polymetallic ores is flotation. The peculiarity of solid mineral processing is the preliminary preparation of raw materials. The essence of this stage is the grinding and sorting of raw materials in order to fully reveal the useful substance from the waste rock. The article is devoted to the study of the effect of electric pulse discharges on the grinding of ore containing non-ferrous metals. This article proposes an electro-pulse method for obtaining raw materials for subsequent flotation enrichment of ore in order to extract valuable components. This method of grinding ores is based on the use of the energy of a pulsed shock wave that occurs as a result of a spark electric discharge in a liquid. An experimental electric pulse unit with a crushing unit is described. When electrohydraulic action on solid particles in an aqueous solution increases the intensity of the grinding process under the influence of additional pressure associated with cavitation. The object of the study was the natural ore of the Akbastau mine. Ore grinding operations were performed at various parameters of the electric pulse plant. The dependences of ore grinding on the electrical and geometric parameters of the electric pulse installation, the value of the interelectrode gap on the switching device, the pulse repetition frequency and discharge energies are determined. It is found that with increasing discharge energies introduced into the discharge channel, the fraction of the crushed fraction increases.

*Keywords:* ore, flotation, electric pulse installation, working electrode, degree of grinding, crushing, discharge energy.

## *Introduction*

The flotation method is used for the enrichment of most non-ferrous metal ores, in combination with other methods for the enrichment of ferrous metal ores. The wide prevalence of flotation is explained by the universality of the process for the mining industry, associated with the possibility of separating almost any minerals, enriching poor ores with a very thin impregnation of useful minerals.

Flotation in the most general form can be defined as a method of separating relatively small particles of different solid phases suspended in a liquid from each other (or separating solid particles from a liquid) by their ability to adhere to gas bubbles introduced into the suspension, followed by their floating to the surface of the liquid and the formation of foam [1, 2].

To extract valuable components from the waste rock by flotation, the ore is first crushed to the required size. In most cases, the final size of the crushed ore is 0.074 mm. The main purpose of the grinding process is to ensure the release of individual minerals contained in the pieces of the host rock.

Grinding of minerals is carried out in mills, metal rods, balls, and large pieces of the ore itself are used as grinding bodies. In processing plants, cylindrical drum ball or rod mills are mainly used. When using drum mills with steel crushing bodies, the cost of covering the wear of balls, rods and liners is one of the main costs of grinding and reaches energy costs, and sometimes exceeds them. For example, when enriching Kryvyi Rih magnetite quartzites, the cost of rods and balls is 30-35% of the total cost of crushing. During dry grinding, the balls wear out mainly as a result of abrasive action. When wet grinding in aggressive (chemically active) aqueous media, abrasive wear is accompanied by corrosion, in which the metal is destroyed as a result of chemical or electrochemical interaction with the environment. Thus, wear of the balls is a very complex process due to many conditions: the properties of the metal (alloy) made of balls, their size, the abrasive properties of the ground material, its size and the size of the product and the method of grinding (dry or water), aggressive environment (acidic, alkaline), its temperature, the presence of surfactants, high-speed mode of the mill (cascade waterfall), grinding circuit (open or closed cycle), etc. Corrosion wear during wet grinding is the main component of the overall wear, so the loss coefficients are higher than during dry grinding [3, 4].

A radical solution to the problems of complex use of mineral raw materials, increasing the completeness of obtaining minerals with a deterioration in their initial quality in conditions of increasing production and processing volumes can be achieved on the basis of new methods of crushing and grinding, characterized by a high degree of destruction, high selectivity of mineral detection. One of the best methods for grinding solid materials is the electric pulse method. Since the working tool for electric pulse destruction is a spark, there are no problems with contamination of the grinding product with metal, the material of grinding bodies, which is typical for mechanical methods of grinding materials. Therefore, electropulse crushing of highly abrasive materials, especially pure materials, is preferable to mechanical crushing [5-7].

*Problem statement and method description*

Based on the above problems, the influence of electric pulse discharges on the grinding of ore containing non-ferrous metals is studied in the scientific work. As the conducted experiments show, this method of grinding is economical, environmentally friendly, and easily integrated into any technological chain. The essence and distinctive feature of the proposed technology is that the processing of ore and man-made raw materials using pressure energy released during electrohydraulic action allows you to obtain a product of a given dispersion that is quickly crushed and easily cleaned of undesirable impurities, which can then be used directly for subsequent enrichment [8].

Electropulse crushing is an effective method of grinding various materials, which allows you to obtain a product with a given degree of grinding with a certain granulometric composition and has a high selectivity of crushing. The technological process of electric pulse grinding is easily automated. Maintenance of electric pulse installations does not require a large number of highly qualified workers. In electric pulse crushers, almost any solid material can be crushed and crushed [9]. When working, these devices do not form dust, occupy relatively small production areas and allow them to combine the processes of crushing, mixing and flotation of materials [8].

An electric pulse unit with a crushing unit was developed and assembled to study ore grinding [10]. The electric pulse unit is made in the form of functional blocks (Figure 1), which consist of a control panel, a generator with a spark gap, a protection unit with a capacitor.

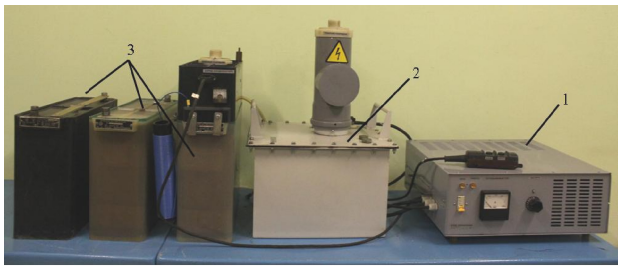


Figure 1. Electric pulse installation. 1-control panel, 2-generator with a spark gap (switching device), 3-protection unit with a capacitor.

In the crushing unit there is a cylindrical chamber in which a linear system of electrodes is installed. The positive electrode is located vertically, and the negative electrode is the bottom of the metal chamber of a hemispherical shape. When a powerful pulse passes through a liquid medium, which is a moistened mass, an electric breakdown is created, accompanied by a hydraulic shock of great destructive force.

The water medium in which the high-voltage electric discharge occurs is a transformer of the energy released in the discharge channel, and due to its low compressibility, it leads to a sharp increase in pressure. Under the influence of electrohydroimpulse action, hydrodynamic fluid flows and an acoustic wave occur in the treated medium, and cavitation occurs as a result of a local decrease in pressure in the liquid. In this case, the cavitation bubble, moving with the flow of liquid to the area with a more significant pressure, closes and emits a shock wave. After the collapse of the bubbles, micro-shocks of cumulative jets will form. The mixture, having received acceleration from the discharge channel expanding at high speed, moves away from it in all directions. At the beginning of the process, the discharge channel increases with the maximum speed, at the end of the current flow, the cavity of the discharge channel continues to expand due to the inertia of the medium, reaches the largest size and then begins to contract. The temperature and pressure in it fall during the expansion of the cavity, and increase during compression, i.e., there are damped pulsations of the cavity.

When electrohydraulic action on solids in an aqueous solution increases the intensity of the grinding process as a result of the additional pressure associated with cavitation. Indeed, a cavitation micro-cavity appears on each solid particle, which, collapsing, increases the mechanical effect [7, 11, 12].

The versatility of electric pulse destruction is due to the possibility of large-scale regulation of the nature of the dynamic impact of discharge factors on the material. The peculiarity of electro-pulse grinding is that the area of impact on the material through the discharge channel is localized in a limited volume of the interelectrode interval. This allows you to multi-dimensionally organize the process of destruction and removal of the product in the chamber and, consequently, control the granulometric composition of the crushed product. It is much easier to implement a multi-stage grinding process with electric pulse destruction, including in a single device. In the multi-electronic design of the working chamber, it is possible to influence the granulometric composition of the grinding product by an appropriate ratio of the pulse frequency to the classification ability of the device [13, 14].

*Analysis of experimental results*

The object of the study was the natural ore of the Akbastau mine with initial diameters ($d_0$) from 10 mm to 25 mm. Since the energy efficiency of crushing the material depends on the size of the ore particles and the parameters of pulsed discharges, the work on crushing the ore was performed at different values of the discharge energy. The discharge energy W varied depending on the capacity of the energy storage capacitor and the discharge voltage. In addition, the efficiency of the electro-pulse method of grinding the material is characterized by the corresponding frequency of pulse discharges.

Ore grinding operations were performed at various parameters of the electric pulse plant:

– interelectrode gap on the switching device, mm – 8; 10; 12; 14; 16 (Figure 2);
– frequency of pulse repetition, Hz – 1,5; 2; 2,5; 3; 3,5; 4 (Figure 3);
– capacity of the storage capacitor, μF – 0,25; 0,4; 0,8;
– discharge voltage (breakdown voltage of the interelectrode gap on the switching device), kV– 22; 26; 30; 34; 38.

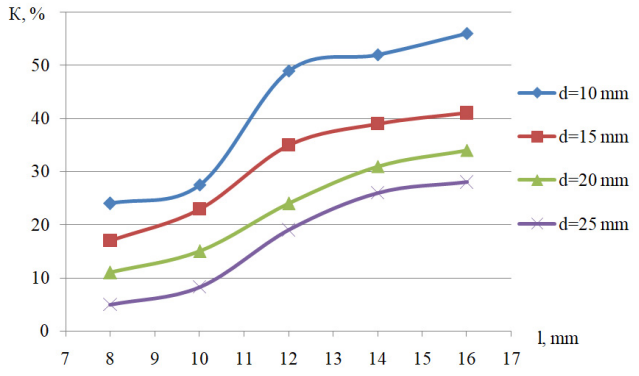


Figure 2. Dependence of the degree of ore grinding on the value of the interelectrode gap on the switching device

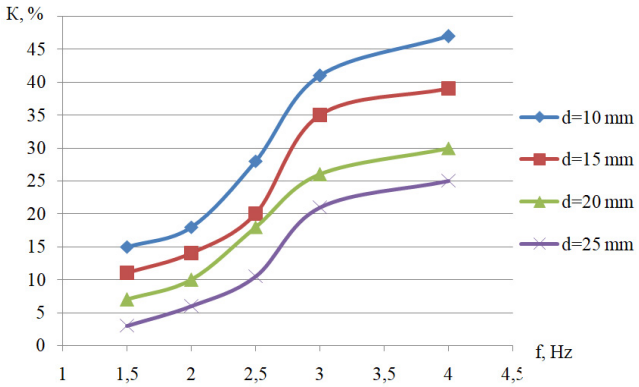


Figure 3. Graph of the dependence of ore grinding on the pulse repetition frequency

The influence of the interelectrode gap on the switching device was carried out with the constancy of other parameters of the installation, which allows you to choose the optimal value necessary for reproducing experiments. According to the results obtained, the optimal interelectrode gap l=12 mm, at which the output was the highest (Figure 2). A further increase in the interelectrode gap stabilizes the output of finished products, but the pulse repetition rate changes. With an increase in the pulse repetition frequency, a uniform grinding is established (Figure 3, the results are obtained at *l*=12 mm). With an increase in the discharge energy ($W=CU^2/2$) introduced into the discharge channel, the fraction of the crushed fraction increases (Figure 4).

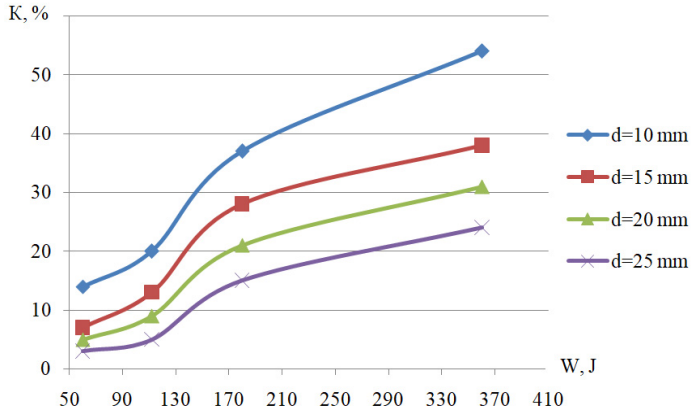


Figure 4. Dependence of the degree of ore grinding on the discharge energy

Given the obtained optimal values of the adjustable parameters (l=12 mm, C=0,4 μF, W=180 J) and duration of treatment 5 minutes to obtained the desired product fraction ≤0.07 mm in the amount of about 37%, 28%, 21%, and 15% for ore initial fraction of 10 mm, 15 mm, 20 mm and 25 mm, respectively. During the experiment, the most optimal value of the interelectrode gap on the switching device is 12 mm, and the diameter of the fractions subjected to the most intense destruction is 10 mm. The degree of grinding increases with an increase in the specific energy introduced into the discharge channel, which is explained by the fact that a network of microcracks is first formed in the structure of the substance on the path of the shock wave, which creates a continuous stress state.

## *Conclusion*

According to experimental data, the prerequisites for regulating the granulometric composition of the processed material during electric pulse grinding are shown. This is due to the possibility of creating favorable conditions for obtaining the necessary product by changing the electrical and geometric parameters of the pulse installation in different ranges. Using the electro-pulse method, raw materials for flotation enrichment were obtained, intended for further extraction of valuable components from ore.

## References

1 Лыкасов А.А. Обогащение руд цветных металлов / А.А. Лыкасов, Г.М. Рысс, М.С. Павловская. — Челябинск: Южно-Урал. гос. ун-т, 2010. — 85 с.

2 Абрамов А.А. Переработка, обогащение и комплексное использование твердых полезных ископаемых / А.А. Абрамов. — М.: Моск. гос. гор. ун-т, 2004. — 509 с.

3 Пузыревская И.А. Обогащение полезных ископаемых / И.А. Пузыревская. — Благовещенск: Амур. гос. ун-т, 2014. — 96 с.

4 Борщёв В.Я. Оборудование для измельчения материалов: дробилки и мельницы / В.Я. Борщёв. — Тамбов: Тамбов. гос. тех. ун-т, 2004. — 75 с.

5 Усов А.Ф. Опыт разработки техники и технологии электроимпульсного разрушения материалов / А.Ф. Усов // Ученые записки Петрозавод. гос. ун-т. — 2011. — № 6 (119). — С. 115–120.

6 Усов А.Ф. Полувековой юбилей электроимпульсного способа разрушения материалов / А.Ф. Усов // Вестн. Кольск. науч. центра РАН. — 2012. — № 4 (11). — С. 166–193.

7 Юткин Л.А. Электрогидравлический эффект и его применение в промышленности / Л.А. Юткин. — Л.: Машиностроение, 1986. — 253 с.

8 Нусупбеков Б.Р. К вопросу о совершенствовании технологии комплексного извлечения редких и рассеянных металлов электроимпульсным методом / Б.Р. Нусупбеков, К. Кусаиынов, С.Е. Сакипова, А.К. Хасенов, А.Ж. Бейсенбек // Металлофизика и новейшие технологии. — 2014. — Т. 36. — № 2. — С. 275–286.

9 Кривицкий Е.В. Динамика электровзрыва в жидкости / Е.В. Кривицкий. — Киев: Наук. думка, 1986. — 120 с.

10 Kurytnik I.P. Disintegration of copper ores by electric pulses / I.P. Kurytnik, B.R. Nussupbekov, A.K. Khassennov, D.Zh. Karabekova // Archives of metallurgy and materials. — 2015. — № 60(4). — P. 2549–2551.

11 Нусупбеков Б.Р. Разрушение металлургического кремния электрогидравлическими импульсными разрядами / Б.Р. Нусупбеков, А.К. Хасенов, А.Б. Нусупбеков // Деформация и разрушение материалов. — 2012. — № 9. — С. 37–39.

12 Nussupbekov B.R. Coal pulverization by electric pulse method for water-coal fuel / B.R. Nussupbekov, A.K. Khassenov, D.Zh. Karabekova, U.B. Nussupbekov, M. Stoev, M.M. Bolatbekova // Bulletin of the University of Karaganda-Physics. — 2019. — № 4(96). — P. 80–84.

13 Курец В.И. Электроимпульсная дезинтеграция материалов / В.И. Курец, А.Ф. Усов, В.А. Цукерман. — Апатиты: КНЦ РАН, 2002. — 324 с.

14 Курец В.И. Особенности гранулометрии электроимпульсной дезинтеграции руд и материалов / В.И. Курец, В.А. Цукерман, А.Ф. Усов // Горн. информ.-аналит. бюл. — 2005. — № 9. — С. 96–101.

А.К. Хасенов, М. Стоев, Д.Ж. Карабекова, Г.А. Булкаирова, Д.А. Нурбалаева

## Кенді флотациялық байытуға қажетті шикізатты алудың электримульсті әдісі

Полиметалл кендерін байытудың негізгі әдісі флотация болып табылады. Қатты пайдалы қазбаларды байытудың ерекшелігі — шикізатты алдын-ала дайындау. Бұл кезең бос жыныстағы пайдалы затты неғұрлым толық ашу үшін шикізатты ұнтақтау және сұрыптауға арналған. Мақала құрамында түсті металдар бар кеннің ұнтақталуына электроимпульсті разрядтардың әсерін зерттеуге арналған. Авторлар құнды компоненттерді алу үшін кенді флотациялық байытуға қажетті шикізатты алудың электроимульсті әдісін ұсынған. Кендерді ұсақтаудың әдісі сұйықтықтағы ұшқынды электр разряды нәтижесінде пайда болатын импульстік соққы толқынының энергиясын пайдалануға негізделген. Ұсақтағыш түйіні бар эксперименттік электроимпульсті қондырғы сипатталды. Су ерітіндісіндегі қатты заттарға электрогидравликалық әсер ету кезінде кавитациямен байланысты қосымша қысым әсерінен ұнтақтау процесінің қарқындылығы артады. Зерттеу нысаны ретінде Ақбастау кенішінің табиғи кені алынды. Кенді ұнтақтау жұмыстары электроимпульсті қондырғының әр түрлі параметрлерінде жүргізілді. Кенді ұсақтаудың электроимпульсті қондырғысының электрлік және геометриялық параметрлеріне, коммутациялық құрылғыдағы электрод аралығының шамасына, импульстар жиілігіне және разряд энергиясына тәуелділігі анықталды. Арнаға енгізілетін разрядтың энергиясының жоғарылауымен ұсақталған фракцияның үлесі артатыны дәлелденді.

*Кілт сөздер:* кен, флотация, электроимпульсті қондырғы, жұмыс электроды, ұсақтау дәрежесі, бөлшектеу, разряд энергиясы.

А.К. Хасенов, М. Стоев, Д.Ж. Карабекова, Г.А. Булкаирова, Д.А. Нурбалаева

## Электроимпульсный метод получения сырья для последующего флотационного обогащения руды

Основным методом обогащения полиметаллических руд является флотация. Особенность обогащения твердых полезных ископаемых состоит в предварительной подготовке сырья. Сущностью этой стадии являются измельчение и сортировка сырья с целью наиболее полного раскрытия полезного вещества из пустой породы. Статья посвящена исследованию влияния электроимпульсных разрядов на измельчение руды, содержащей цветные металлы. Авторами предложен электроимульсный метод получения сырья для последующего флотационного обогащения руды с целью извлечения ценных компонентов. Данный способ измельчения руд основан на использовании энергии импульсной ударной волны, возникающей в результате искрового электрического разряда в жидкости. Описана экспериментальная электроимпульсная установка с дробильным узлом. При электрогидравлическом воздействии на твердые частицы в водном растворе интенсивность процесса измельчения возрастает под действием дополнительного давления, связанного с кавитацией. Объектом исследования являлась природная руда Акбастауского рудника. Работы по измельчению руды выполнялись при различных параметрах электроимпульсной установки. Определены зависимости измельчения руды от электрических и геометрических параметров электроимпульсной установки, величины межэлектродного промежутка на коммутационном устройстве, частоты следования импульсов и энергий разряда. Установлено, что с увеличением энергии разряда, вводимой в канал разряда, доля измельченной фракции возрастает.

*Ключевые слова:* руда, флотация, электроимпульсная установка, рабочий электрод, степень измельчения, дробление, энергия разряда.

## References

1 Lykasov, A.A., Ryss, G.M., & Pavlovskaia, M.S. (2010). *Obohashchenie rud tsvetnykh metallov [Enrichment of non-ferrous metal ores]*. Chelyabinsk: South Ural State University [in Russian].

2 Abramov, A.A. (2004). *Pererabotka, obohashchenie i kompleksnoe ispolzovanie tverdykh poleznykh iskopaemykh [Processing, enrichment and integrated use of solid minerals]*. Moscow: Moscow State Mining University [in Russian].

3 Puzyrevskaia, I.A. (2014). *Obohashchenie poleznykh iskopaemykh [Mineral processing]*. Blagoveshchensk: Amur State University [in Russian].

4 Borshchev, V.Ya. (2004). *Oborudovanie dlia izmelcheniia materialov: drobilki i melnitsy [Equipment for grinding materials: crushers and mills]*. Tambov: Tambov State Technical University [in Russian].

5 Usov, A.F. (2011). Opyt razrabotki tekhniki i tekhnolohii elektroimpulsnoho razrusheniia materialov [Experience in the development of techniques and technologies of electro-pulse destruction of materials]. *Uchenye zapiski Petrozavodskoho hosudarstvennoho universiteta — Scientific notes of Petrozavodsk State University, 6(119),* 115-120 [in Russian].

6 Usov, A.F. (2012). Poluvekovoi yubilei elektroimpulsnoho sposoba razrusheniia materialov [Half-century anniversary of the electric pulse method of destruction of materials]. *Vestnik Kolskoho nauchnoho tsentra Rossiiskoi akademii nauk — Bulletin of the Kola Scientific Center of the Russian Academy of Sciences, 4(11),* 166-193 [in Russian].

7 Iutkin, A.A. (1986). *Elektrohidravlicheskii effekt i eho primenenie v promyshlennosti [Electrohydraulic effect and its application in industry]*. Leningrad: Mechanical Engineering [in Russian].

8 Nussupbekov, B.R., Kussaiynov, K., Sakipova, S.E., Khassenov, A.K., & Beisenbek, A.Zh. (2014). K voprosu o sovershenstvovanii tekhnolohii kompleksnoho izvlecheniia redkikh i rasseiannykh metallov elektroimpulsnym metodom [On improvement of technology of complex extraction of rare and trace metals by electropulse method]. *Metallofizika i noveishie tekhnolohii — Metallophysics and the latest technologies, 36, 2,* 275-286 [in Russian].

9 Krivitskii, E.V. (1986). *Dinamika elektrovzryva v zhidkosti [Dynamics of electric explosion in a liquid]*. Kiev: Naukova dumka [in Russian].

10 Kurytnik, I.P., Nussupbekov, B.R., Khassennov, A.K., & Karabekova, D.Zh. (2015). Disintegration of copper ores by electric pulses. *Archives of metallurgy and materials, 60 (4),* 2549-2551.

11 Nussupbekov, B.R., Khassenov, A.K., & Nusupbekov, A.B. (2012). Razrushenie metallurhicheskoho kremniia elektrohidravlicheskimi impulsnymi razriadami [Destruction of metallurgical silicon by electrohydraulic pulsed discharges]. *Deformatsiia i razrushenie materialov — Deformation and destruction of materials, 9,* 37-39 [in Russian].

12 Nussupbekov, B.R., Khassenov, A.K., Karabekova, D.Zh., Nussupbekov, U.B., Stoev, M., & Bolatbekova, M.M. (2019). Coal pulverization by electric pulse method for water-coal fuel. *Bulletin of the University of Karaganda-Physics, 4,* 96, 80-84.

13 Kurets, V.I., Usov, A.F., & Tsukerman, V.A. (2002). *Elektroimpulsnaia dezintehratsiia materialov [Electro-pulse disintegration of materials]*. Apatity: Kol Scientific Center of the Russian Academy of Sciences [in Russian].

14 Kurets, V.I., Tsukerman, V.A., & Usov, A.F. (2005). Osobennosti hranulometrii elektroimpulsnoi dezintehratsii rud i materialov [Features of granulometry of electro-pulse disintegration of ores and materials]. *Hornyi informatsionno-analiticheskii biulleten — Mining information and Analytical Bulletin, 9,* 96-101 [in Russian].

# ФИЗИКАНЫ ОҚЫТУ ӘДІСТЕМЕСІ
# МЕТОДИКА ПРЕПОДАВАНИЯ ФИЗИКИ
# METHODS OF TEACHING PHYSICS

DOI 10.31489/2021Ph1/63-70
UDC 378.147.88

S.K. Damekova[1], N.N. Shuyushbayeva[1*], N.K. Tanasheva[2], G.S. Altayeva[1], A.K. Kaliyeva[1]

## Additional education of schoolchildren in physics at the Children's University

*[1]Sh. Ualikhanov Kokshetau University, Kazakhstan;*
*[2]E.A. Buketov Karaganda University, Kazakhstan*
*(E-mail: [*]nn_shuish@mail.ru)*

The article describes physics projects created by students as future physics teachers to organize classes on the educational platform of the Children's University. The study was aimed at examining the performance of physics students through physics projects. The advantages of the Labster 3D virtual reality learning environment for motivating students to study physics are also considered. Generally, the results of the study showed an increase in interest among primary school students in STEM education and science. The study involved children from 10 to 12 years old in the amount of 250 schoolchildren in the city of Kokshetau (Kazakhstan). The article used methods such as mixed methods, questionnaires, and semi-structured interviews for children. The Likert scale questions allowed the analysis using descriptive statistics. Open-ended questions and data from the interviews were classified using content analysis and analytically interpreted through the theory of the development of cognitive interest in children. Children were provided by links to short 10-minute educational videos posted on Youtube video hosting called FIZMAT KSU While they were working remotely. During distance learning, children used different forms of virtual laboratory work. The results and conclusions of the study revealed the followings: visiting the Children's University increases children's interest in STEM - education and science, as well as the participation of future physics teachers in the activities of the Children's University forms the skills of organizing informal forms of work with children.

*Keywords:* future physics teachers, additional education, children, Children's University, experiments, virtual 3D Labster laboratory, project, STEM.

### *Introduction*

*Relevance*

The purpose of creating a Children's University at the university is to identify and study indicators of extracurricular activities in STEM education, as well as to demonstrate the successful activities of university students and school students through the use of entertaining forms of education that are developed by future teachers and teachers of the university. Discussion of learning outcomes is conducted under the guidance of teachers based on the theory of the development of cognitive interests of younger students [1].

The basis for conducting STEM education at the Children's University was the creation of an informal learning environment that stimulates interest in science, research on the activities of the Children's University was carried out in the work of Susanne Walan, Niklas Gericke, 2019 [2]. There are many ways to stimulate interest in the exact sciences, in our study we offer several: first, voluntary participation in these activities (Potvin and Hasni) [3]; second, non-evaluative activities; third, interactivity of classes (Shabi, Assaraf) [4]; fourth, the use of 3D gaming virtual laboratory work.

The format of the Children's University in the pedagogical environment is not new, so the European Children's Universities Network has been created in Europe [5]. The activities of teachers and students involved in the Children's University of Sh. Ualikhanov Kokshetau University is focused on creating new learning platforms, expanding the educational space, and implementing joint pedagogical and didactic research. The format of the Children's University captures not only the creativity of using teaching approaches but also the active involvement of students - future teachers in the education of students, when the boundaries of communication are blurred and there is interest in serious academic subjects, both on the part of students and on the part of students. Such meetings became possible thanks to the Children's University, which became the main one in the strategy of cooperation of university teachers, parents, students, and teachers of the Akmola region [6].

*Materials and methods*

When forming a cognitive interest in the system of non-formal education, it is necessary to take into account the psychological factors of its formation by L. S. Vygotsky [7-9].

It is generally accepted that not all academic subjects are of interest, and when the content of research affects the daily life of a person, students are interested. So in our study, we conducted 4 classes and then asked students to choose the most interesting topics.

The system of additional education, which has been conceptually introduced in Kazakhstan since 2019 [10], is considered the most important component of the educational space, and it is not just an element of the existing system of general education, but an independent source of education that contributes to the achievement of key competencies in various areas of the child's life self-determination. In the Republic of Kazakhstan, the system of additional education of students requires the availability of qualified teachers who have basic training in the field of additional education and can implement interesting and modern educational programs.

Ualikhanov Children's University makes a significant contribution to the system of additional education in Kazakhstan. The purpose of the children's university is to stimulate the scientific interest of children aged 8 years-12 to STEM. Since 2016, the Children's University has been working to expand the horizons of students, deepen scientific knowledge in several natural sciences, as well as form an active life position for children.

Students of the city's schools are offered eight classes, which are held every month during the academic year at the university. Students of the 3rd year of pedagogical specialties of the Faculty of Natural Sciences under the guidance of methodologists conduct practical classes and laboratory experiments in physics, chemistry, biology, mathematics, computer science, geography and talk about their applied features of the application in human life.

By the time, classes last about 2 hours, usually in the morning, for example, from 10.00 to 12.00 with 10-minute psychological training or musical warm-up activities every 20 minutes. In the context of the pandemic in 2020, classes of the Children's University were held in a remote format.

Training under the program of the Children's University developed and successfully implemented by the teaching staff of the departments of the Faculty of Natural Sciences and aimed at deepening knowledge in biology, chemistry, physics, mathematics, computer science, geography. The summer camp of DU allowed uniting children who show interest in research work, in order to organize their interaction with peers, with university teachers in the conditions of joint creative, research activities.

The main strategy of the Children's University is for children to meet with researchers, visit the university's laboratories, and be able to conduct simple physical experiments on their own. To date, about 250 children have visited the Children's University, not counting those students who signed up for our classes again.

In the study, the following tasks were set (Q1): does attending a Children's University increase children's interest in STEM? (Q2) How did physics students evaluate the experience of participating in the organization and conduct of a Children's University? The use of a mixed-method, including both questionnaires and semi-structured interviews, was developed specifically for the Children's University in order to determine the growth of interest in STEM, their general interest in science. Closed elements of the Likert scale [11] were used in the questionnaire to check whether students report an increase in interest due to participation in extracurricular activities of the Children's University (Q1). The ratings were: 1 = not interesting at all, 2 =not very interesting, 3 = no opinion, 4 = interesting and 5 = very interesting.

During the summer vacation period of 2019 and 2020, semi-structured interviews with 60 children were conducted in the classes of the Children's University. The children volunteered to participate in the interviews, and the parents ' consent was obtained. Interviews were conducted in focus groups of four to six students to encourage discussion and allow children to be more talkative. These interviews were conducted after the Children's University classes when the season was closed and was conducted in parallel by all researchers (the authors of the article). Each of the interviews was recorded audio and lasted about 8-10 minutes.

The Likert style questions in the questionnaire were analyzed based on descriptive statistics to highlight the characteristics of the change in interest (Q1). The open points of the questionnaire were analyzed using content analysis. Audio recordings from the interview were transcribed verbatim and also analyzed using content analysis, transcripts (from open questionnaire items and interview transcripts) were read repeatedly.

Children who participated in the study were encoded as I = interview, Q= questionnaire, B or G for a boy or girl, the number of the respondent, for example, IG4 means an interview with a girl who was identified as the fourth among all respondents.

*Results of the research*

In the second half of the 2016-2017 academic year at the Children's University, all children who attended classes in the second semester were offered a questionnaire. 100 percent of the children answered (40 responses in total). The questionnaire was submitted on paper after classes, the adults who accompanied the children were informed about the questionnaire and we asked them to help the children if there were any questions that they did not understand. Most of the children who answered the questionnaire were students from the same class.

The question «How does attending a Children's University affect children's interest in STEM?» was answered as follows (Figure 1).

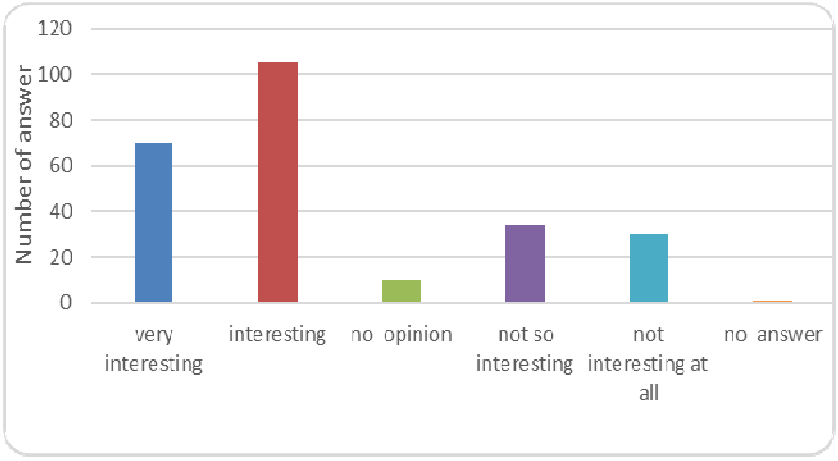


Figure 1. Children's interest in science before attending a Children's university

About 42 percent (105 children) rated science as interesting, and 28 percent (70 children) rated science as very interesting before attending a Children's University. In this question, the answers can be ranked from not at all interesting to very interesting; therefore, the answers can be considered as ranked on the points of the Likert scale, with as the most positive answer. The average was 3.6 out of 5.0 for the total number of responses.

Regarding the question of whether interest changed after attending a Children's University, children found science as interesting as before attending (120 children, 48 %), or even more interesting (110 children, 44%) (Figure 2). This can be thought of as a three-point Likert scale, giving an average of 2.4 out of 3.0.

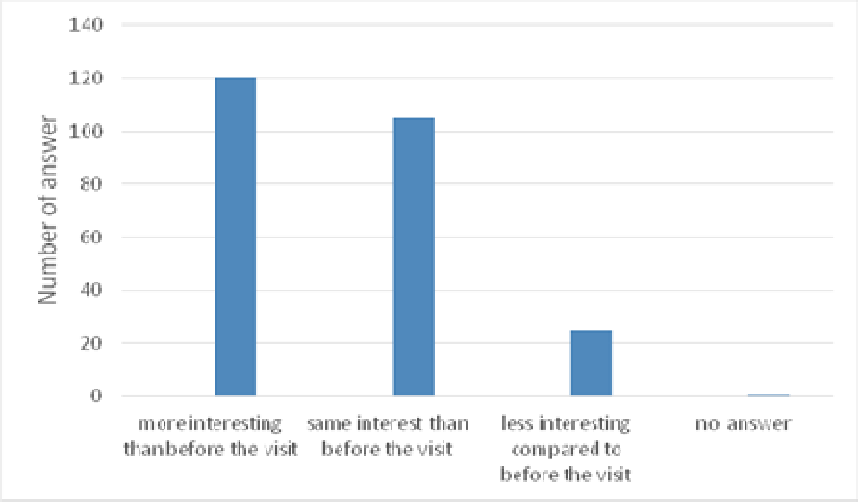


Figure 2. Children's interest after attending a children's university

We compared how the children rated the topics of the Children's University most of the children from the interview attended all classes.

In setting the topic, we sought to ensure that the activities of children at the Children's University were a continuation and deepening of the school's physics curriculum. The emphasis in working with children is not so much on improving their general education performance, preparing for exams, etc., as on educating future researchers, inventors, and creative personalities.

Participants of the Children's University summer camp in June 2020 had the opportunity to work in Labster virtual laboratories on the following topics: Newton's Law of Motion, Electrical Resistance, Fundamentals of Electricity, Electromagnetic Spectrum, Wave Model of light.

Activities in the 3D Labster laboratory are scientific and educational with a practical focus, during which the student must learn new things and learn to act, feel, and make decisions. It is carried out by including extra-curricular issues and problems of science in classes, as well as at the expense of a higher scientific level and depth of disclosure of program material.

Labster.com - this is a web service built on the principle of cloud technologies, with the help of which virtual laboratory work is performed and research activities are modeled.

In the educational sphere, this service is almost unknown even in neighboring Russia, a unique opportunity is provided by Sh. Ualikhanov KU. Performing 3D virtual laboratory work contributes to the development of cognitive interest due to the dynamic, well-animated plot of laboratory work, as well as develops visual-figurative and abstract-logical thinking through additional and virtual reality in a playful way.

Labster stimulates the imagination of the student, promotes the development of a creative approach, the development of their creative abilities in the organization of scientific and technical work. As previous experience shows, it is very interesting and comfortable for children to work with this service, as well as an aesthetic function, the process gives students more pleasure and scope of creative thought, makes it possible to go beyond the standard and limited vision.

Labster is an English-language service and the default language of the program interface is English. You can use the online photo translator program. This contributes to the adaptation of children to a foreign language and is an additional language practice for both teachers and students. This laboratory considers areas of natural sciences such as biology, physics, and chemistry. The virtual 3D lab includes more than 159 simulations. Of these, 39 in biology, 18 in physics, and 98 in chemistry are simulations.

The short 10-minute training videos posted on the Youtube channel of FIZMAT KSU [13], which the children used while performing virtual laboratory work, helped the children a lot in remote work.

In the responses of children, it was noted that working in a learning environment with physical devices stimulated their interest. This is the device of the nuclear magnetic resonance laboratory, which they saw at the university, and the virtual research environment Labster [14].

In the course of classes, the basic knowledge about the subject of activity is assimilated and the techniques of working with real objects and devices of educational laboratories of physics departments are developed. The classes not only covered science, but also included aspects from the entire STEM spectrum.

Any lesson is interesting because there is a mandatory feedback, such as we see, this is the active participation of students, future teachers, who came up with various reflexive and relaxation techniques for students, so that children do not get tired.

Students of physics of the 3rd year of the Faculty of Natural Sciences at the Children's University conducted: mass holidays with elements of intellectual activity, intellectual games and projects, practical classes with elements of research activities, an excursion to the NMR laboratory, individual work with children to perform research works of different levels.

A vivid example is the celebration of the New Year for children (photos and videos on the university's website). During the holiday, a special information table was organized, where children received information about the work of the Children's University, colorful advertisements, balloons were distributed, and enrollment in study groups was conducted.

Survey of 3rd year physics students after completion of professional practice. The majority of physics students rated their experience of participating in the organization of a Children's University as very interesting (52%) or interesting (32%) (Figure 3). Using the same thing on the Likert score scale as in the previous question, the average was 4.0 out of 5.0 for the total number of responses.

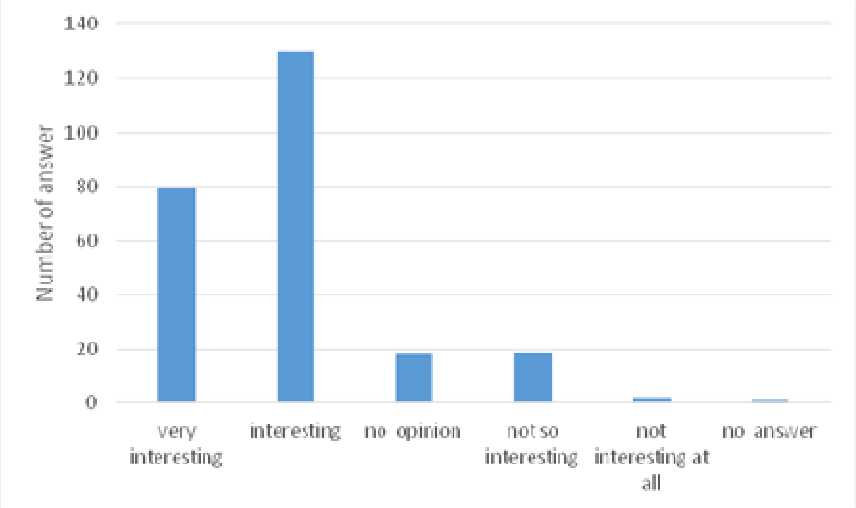


Figure 3. Results of a survey of 3rd year physics students after completing their professional practice

In addition to students and teachers, adults, teachers, and parents also took part in the work of the Children's University. Children attended these events with their teachers or relatives until 2020. The high degree of interaction between children and adults at the Children's University can be explained by the fact that children realize the importance of their families during the Covid-19 pandemic. The work is carried out in close contact with parents who acted as consultants during the first virtual laboratory work and strongly supported the children. Children, answering questions of the questionnaire, noted high activity and emotionality of adults. Parents ' reviews are posted on the website of the Children's University of KU.

*Discussion of the results*

Many researchers Baram-Tsabari and Yarden [15] Jones, Howe, and Rua [16], Holbrook [17] Newton [18] argue that the relevance of the topic is important to motivate students and interest them in physics. Since most of the children in our study rated the proposed topics as interesting, it can be concluded that choosing different topics at a children's university stimulates interest in STEM. Previous researchers Agranovich, S., and B. B. Z. Assaraf have indicated an interest in the experiments [19]. The results of our study suggest that topics should be seriously considered when planning future extracurricular activities.

Early research by Susanne Walan, Niklas Gericke notes the importance of impressive, spectacular activities in extracurricular activities. We used virtual laboratory works of the company Labster in the remote work of the children's University, which aroused great interest of children and parents, including those whose experience was not previously investigated. It is important to note here that the complexity of mastering a new software interface is evident in the first lesson with virtual laboratories. But the 3D effect, anima-

tion, and game form of presentation of scientific material motivate children to quickly get acquainted with the Labster program.

In our study, children talked about the Labster STEM learning environment. The Labster online laboratory allows you to engage in science, opens access to complex experiments and scientific discoveries from anywhere in the world. At the same time, students in Labster do not study haphazardly, but according to pre-prepared lessons playfully. This means that in the laboratory they do not just experiment and have fun, but learn to work with laboratory equipment and learn real physical, chemical, and biological laws. The kids found Labster jobs impressive and most interesting, often calling them cool.

Creative physics students with high academic and research achievements were allowed to prepare and conduct classes. The children talked a lot about the student researchers who conducted the classes. When the children were asked questions about the researchers presented at the Children's University, they had positive comments.

The children noted that there were a lot of students at the Children's University and unlike one teacher for the whole class, this is very good. Participation of students in the activities of the Children's University allows you to individualize the learning process, this is not enough for children at school. Parents spoke about the need to accompany the research and creative activities of children, which can also be implemented with the help of students. The activity of the Children's University belongs to the field of non-formal education, related to the individual development of the child in culture, which he chooses himself by his desires and needs. This is a key area for future research, as well as an area where there are opportunities to improve the training of future teachers at the university.

We were interested in what happened after the visits, in the cultures where children spend time (at home and school). The children were asked if they later discussed the lectures with their classmates, teachers, and relatives. All the students claimed that there were discussions in their classrooms after the visit. Children told their parents about their visit to the Children's University and we received feedback from parents via messenger. Therefore, it is also an important area for improvement that the children's university should develop, that is, cooperation with schools, teachers, with relatives to improve training and integration into school activities, to create a common culture of science education.

## *Conclusions and suggestions*

Extracurricular activities are an important factor in helping students make future choices when it comes to studying and pursuing a career in STEM. However, along with other activities and hopefully good school teaching, attending extracurricular STEM events such as a Children's University can serve as a trigger for developing interests.

3D Labster laboratory, integrating different areas of knowledge and providing flexibility, multilingualism the variable nature of additional education allows you to introduce new 3D technologies of additional and virtual reality in the system of additional education of schools in Kokshetau.

Students of physics of Sh. Ualikhanov KU during the period of professional practice mastered the skills of working in the 3D Labster laboratory and developed video sessions for remote work in virtual STEM laboratories.

As shown in this study in the organization of extracurricular activities, students must experience some of their regular exercises. First of all, the place is important, that is, the learning environment, the extracurricular environment.

Topics should be chosen with the potential to surprise children, entertainment should be created, and ultimately, the program should be aimed at a cognitive level of activity, as children expect to learn something.

The results of our study highlight indicators that may also be of interest to various STEM activities to generate interest in the study of physics. Having the opportunity to learn something new in a learning-friendly environment, under the guidance of energetic student lecturers, in an eco-friendly environment, or a virtual 3D lab is essential for children.

## References

1 Щукина Г.И. Педагогические проблемы формирования познавательного интереса студентов / Г.И. Щукина. — М.: Просвещение, 2005. — 288 с.

2 Susanne Walan. Factors from informal learning contributing to the children's interest in STEM — experiences from the out-of-school activity called Children's University / Susanne Walan, Niklas Gericke // Research in Science & Technological Education. —2019. — P. 1–21.

3 Potvin P. Interest, Motivation, and Attitude Towards Science and Technology at K-12 Levels: A Systematic Review of 12 Years of Educational Research / P.Potvin, A. Hasni // Studies in Science Education. — 2014. — № 50 (1). — P. 85–129.

4 Shaby N. The Particular Aspects of Science Museum Exhibits that Encourage Students' Engagement / N. Shaby, O.B. Z.Assaraf, T.J. Tal // Journal of Science Education and Technology. — 2017. — № 26–3. — P. 253–268.

5 European Children's Universities Network [Electronic resource]. — Access mode: https://eucu.net/

6 Website of the Children's University KU SH Ualikhanov [Electronic resource]. — Access mode: https://www.kgu.kz/detski_universitet

7 Выготский Л.С. Психология развития человека / Л.С. Выготский. — М.: Изд-во «Смысл»; Эксмо, 2005. — 1136 р.

8 Krishnamurthi, A. What Afterschool STEM Does Best: How Stakeholders Describe Youth Learning Outcomes / A. Krishnamurthi, B. Bevan, J. Rinehart, V.R. Coulon // Afterschool Matters 18. — 2013. — № 18. — P. 42–49.

9 Shuyushbayeva N.N. Formation of ICT competencies for future physics teachers / N.N. Shuyushbayeva, S.K. Damekova, N.K. Tanasheva, G.S. Altayeva // Bulletin of the university of Karaganda-Physics. — 2020. — № 4(100). — P. 95–104.

10 Концептуальные подходы к развитию дополнительного образования детей в Республике Казахстан [Электронный ресурс]. — Режим доступа: https://www.ziyatker.org/legislation

11 Volkova N.V. Likert and Rush scales: comparative analysis of the results / Modern methods of data mining in economic, humanitarian and natural science research: materials of the international scientific and practical conference (24 November, 2016 y.). — Pyatigorsk: Publishing house of the Russian University of Economics, 2016. — P. 438–447.

12 Cohen L. Research Methods in Education / L. Cohen, L. Manion, K. Morrison // New York, NY: Routledge. — 2012. — № 38(3). — P. 507–509.

13 YouTube channel of the Department of Physics and Mathematics of KU Sh Ualikhanov [Electronic resource]. — Access mode: https://www.youtube.com/channel/UCBc-ICBg0cUGLBXzqAgUQGA

14 Official website of Labster company [Electronic resource]. — Access mode: https://www.labster.com/

15 Baram-Tsabari A., Characterizing Children's Spontaneous Interests in Science and Technology / A. Baram-Tsabari, A. Yarden // International Journal of Science Education. — 2005. — № 2 (7). — P. 803–826.

16 Jones M.G. Gender Differences in Students' Experiences, Interests, and Attitudes toward Science and Scientists / M.G. Jones, A. Howe, M.J. Rua // Science Education. — 2000. — № 84. — P. 180–192.

17 Holbrook J. Introduction to the Special Issue of Science Education International Devoted to PARSEL / J. Holbrook // Science Education International. — 2008. — № 19 (3). — P. 257–266.

18 Newton D.P. Making Science Education Relevant / D.P. Newton. — London, England: Kogan Page, 1988. — 105 p.

19 Agranovich, S. What Makes Children like Learning Science? An Examination of the Attitudes of Primary School Students Towards Science Lessons / S. Agranovich, B.Z. Assaraf // Journal of Education and Learning. — 2013. — № 2 (1). — P. 55–69.

С.К. Дамекова, Н.Н. Шуюшбаева, Н.К. Танашева, Г.С. Алтаева, А.К. Калиева

## Балалар университетінде физика пәні бойынша оқушыларға қосымша білім беру

Мақалада Балалар университетінің оқу платформасында сабақтарды ұйымдастыру үшін студенттердің, соның ішінде болашақ физика мұғалімдері жасаған физика жобалары сипатталған. Зерттеу жұмысы физика жобалары арқылы физика студенттері қызметінің тиімділігін зерттеуге бағытталған. Сондай-ақ оқушыларды физиканы оқуға ынталандыру үшін Labster 3D-виртуалды болмысының оқу ортасының артықшылықтары қарастырылған. Зерттеу нәтижелері негізгі мектеп оқушыларының STEM арқылы білім беру және жалпы ғылымға деген қызығушылығының артқанын көрсетті. Зерттеуге Көкшетау қаласының (Қазақстан) мектептерінен 250 оқушы, яғни 10-нан 12 жасқа дейінгі балалар қатысты. Авторлар аралас әдіс, сауалнама және балалардың жартылай құрылымдалған сұхбаттары сияқты әдістерді қолданған. Лайкерт шкаласының сұрақтары сипаттамалық статистиканы қолдана отырып талдау жүргізуге мүмкіндік берді. Сұхбаттағы ашық сұрақтар мен мәліметтер мазмұнды талдау арқылы жіктелді және балалардың танымдық қызығушылығының даму теориясы арқылы аналитикалық түрде түсіндірілді. Балалармен қашықтықтан жұмыс істеу кезінде КМУ ФИЗМАТ деп аталатын You Tube видеохостингінде орналастырылған қысқа 10 минуттық оқыту бейнелеріне сілтемелер берілді. Қашықтықтан оқыту кезінде балалар виртуалды зертханалық жұмыстарды орындаудың әр түрлі формаларын қолданды. Зерттеу нәтижелері мен қорытындылары мынадай болды: балалардың Балалар университетіне баруы, STEM арқылы білім алуы мен ғылымға деген қызығушылығын арттырады. Сонымен қатар болашақ физика мұғалімдерінің Балалар университетінің қызметіне қатысуы балалармен жұмыс жасаудың бейресми түрлерін ұйымдастыру дағдыларын қалыптастырады.

*Кілт сөздер:* болашақ физика мұғалімдері, қосымша білім беру, балалар, Балалар университеті, тәжірибелер, Labster виртуалды 3D зертханасы, жоба, STEM.

С.К. Дамекова, Н.Н. Шуюшбаева, Н.К. Танашева, Г.С. Алтаева, А.К. Калиева

# Дополнительное образование школьников по физике в Детском университете

В статье описаны проекты по физике, созданные студентами — будущими учителями физики, для организации занятий на учебной платформе Детского университета. Исследование было направлено на изучение эффективности деятельности студентов-физиков посредством проектов по физике. Рассмотрены преимущества учебной среды 3D-виртуальной реальности Labster для мотивации учащихся к изучению физики. Результаты исследования показали рост интереса у учащихся основной школы к STEM-образованию и, в целом, к науке. В эксперименте приняли участие 250 учащихся школ г. Кокшетау (Казахстан) в возрасте от 10 до 12 лет. Авторами были использованы следующие методы: смешанный метод, анкета и полуструктурированные интервью детей. Вопросы шкалы Лайкерта позволили провести анализ с использованием описательной статистики. Открытые вопросы и данные из интервью были классифицированы с помощью контент-анализа и аналитически интерпретированы через теорию развития познавательного интереса детей. При дистанционной работе с детьми были предоставлены ссылки на краткие 10-минутные обучающие видео, размещенные на видеохостинге YouTube под названием ФИЗМАТ КГУ. Во время дистанционного обучения дети использовали разные формы выполнения виртуальных лабораторных работ. Резюмируя, можно отметить, что посещение Детского университета повышает интерес детей к STEM-образованию и науке, а также участие будущих учителей физики в деятельности Детского университета формирует навыки организации неформальных форм работы с детьми.

*Ключевые слова:* будущие учителя физики, дополнительное образование, дети, Детский университет, эксперименты, виртуальная 3D-лаборатория Labster, проект, STEM.

## References

1 Shchukina, G.I. (2005). *Pedahohicheskie problemy formirovaniia poznavatelnoho interesa uchashchikhsia [Pedagogical problems of the formation of the cognitive interest of students]*. Moscow: Prosveshchenie [in Russian].

2 Susanne, Walan., & Niklas, Gericke. (2019). Factors from informal learning contributing to the children's interest in STEM — experiences from the out-of-school activity called Children's University. *Research in Science & Technological Education, 20,* 1–21.

3 Potvin, P. & Hasni, A. (2014). Interest, Motivation, and Attitude Towards Science and Technology at K-12 Levels: A Systematic Review of 12 Years of Educational Research. *Studies in Science Education, 50, 1,* 85–129.

4 Shaby, N. Assaraf, O.B.Z. & Tal T.J. (2017). The Particular Aspects of Science Museum Exhibits that Encourage Students' Engagement. *Journal of Science Education and Technology, 26,* 253–268.

5 European Children's Universities Network. *eucu.net.* Retrieved from https://eucu.net/

6 Website of the Children's University KU Sh. Ualikhanov. *kgu.kz.* Retrieved from https://www.kgu.kz/detski_universitet

7 Vygotsky, L.S. (2005). *Psikholohiia razvitiia cheloveka [Psychology of human development]*. Moscow: Izdatelstvo «Smysl»; Eksmo [in Russian].

8 Krishnamurthi, A., Bevan, B., Rinehart, J., & Coulon, V.R. (2013). What Afterschool STEM Does Best: How Stakeholders Describe Youth Learning Outcomes. *Afterschool Matters 18,* 42–49.

9 Shuyushbayeva, N.N., Damekova, S.K., Tanasheva, N.K., & Altayeva G.S. (2020) Formation of ICT competencies for future physics teachers. *Bulletin of the university of Karaganda-Physics, 4,100,* 95–104.

10 Kontseptualnye podkhody k razvitiiu dopolnitelnoho obrazovaniia detei v Respublike Kazakhstan [Conceptual approaches to the development of additional education for children in the Republic of Kazakhstan]. *ziyatker.org.* Retrieved from https://www.ziyatker.org/legislation [in Russian].

11 Volkova, N.V. (2016). Likert and Rush scales: comparative analysis of the results / Modern methods of data mining in economic, humanitarian and natural science research: materials of the international scientific and practical conference (24 November, 2016 y.). Pyatigorsk: Publishing house of the Russian University of Economics.

12 Cohen, L. Manion, L., & Morrison, K. (2012). *Research Methods in Education.* New York, NY: Routledge, 38, 3, 507–509.

13 YouTube channel of the Department of Physics and Mathematics of KU Sh Ualikhanov. *youtube.com.* Retrieved from https://www.youtube.com/channel/UCBc-ICBg0cUGLBXzqAgUQGA

14 Official website of Labster company. *labster.com.* Retrieved from https://www.labster.com/

15 Baram-Tsabari A., & Yarden, A. (2005). Characterizing Children's Spontaneous Interests in Science and Technology. *International Journal of Science Education, 2 (7),* 803–826.

16 Jones, M. G., Howe A., & Rua M. J. (2000). Gender Differences in Students' Experiences, Interests, and Attitudes toward Science and Scientists. *Science Education, 84,* 180–192.

17 Holbrook, J. (2008). Introduction to the Special Issue of Science Education International Devoted to PARSEL. *Science Education International, 19 (3),* 257–266.

18 Newton, D. P. (1988). *Making Science Education Relevant.* London, England: Kogan Page.

19 Agranovich, S. & Assaraf, B.Z. (2013). What Makes Children like Learning Science? An Examination of the Attitudes of Primary School Students Towards Science Lessons. *Journal of Education and Learning, 2 (1),* 55–69.

# АВТОРЛАР ТУРАЛЫ МӘЛІМЕТТЕР
# СВЕДЕНИЯ ОБ АВТОРАХ
# INFORMATION ABOUT AUTHORS


**Altayeva, G.S.** — Master of Natural Sciences, Senior Lecturer of the Department of Physics and Mathematics, Sh.Ualikhanov Kokshetau University, Kazakhstan, E-mail: vip.gusia@mail.ru

**Bogomolov, V.A.** — Professor, Doctor of science (Engineering), Professor of the Department of Automobiles named after A. B. Hredeskul, Prof., DSci (Engineering), Kharkiv National Automobile and Road University, Ukraine, E-mail: bv@khadi.kharkov.ua

**Bulkairova, G.A.** — senior lecturer, Karagandy University named after academician E.A. Buketov, Kazakhstan, E-mail: gulden2111@mail.ru

**Cherepanska, I.Y.** — D.Sc., Professor of the Department of Computer Technologies and Systems Modelling; Polissia National University, Zhytomyr, Ukraine, E-mail: cherepanskairina@gmail.com.

**Damekova, S.K.** — Candidate of Pedagogical Sciences, Head of the Department of Physics and Mathematics, Sh.Ualikhanov Kokshetau University, Kazakhstan, E-mail: damekova_s@mail.ru

**Dann, D.D.** — Ph.D, Researcher, Problem Research Laboratory of Electronics, Dielectrics and Semiconductors, Research School of High Energy Process Physics, Tomsk Polytechnic University, Russia, E-mail: dddann@tpu.ru

**Fedotov, P.I.** — Ph.D., Research, Problem Research Laboratory of Electronics, Dielectrics and Semiconductors, Research School of High Energy Process Physics, Tomsk Polytechnic University, Russia, E-mail: pif@tpu.ru

**Imanbaeva, S.B.** — PhD student of the Department of Geology and Exploration of Mineral Deposits, Karaganda Technical University, Kazakhstan, E-mail:svetakaz77@mail.ru

**Kaliyeva, A.K.** — Master of Natural Sciences, Senior Lecturer of the Department of Physics and Mathematics, Sh.Ualikhanov Kokshetau University, Kazakhstan, E-mail: aleka_8_7@mail.ru

**Karabekova, D.Zh.** — PhD, Docent, Karagandy University named after academician E.A. Buketov, Kazakhstan, E-mail: karabekova71@mail.ru

**Kashkanov, A.A.** — Associate Professor, Doctor of science (Engineering), Professor of the Department of Automobiles and Transport Management, Vinnytsia National Technical University, Ukraine, E-mail: a.kashkanov@gmail.com

**Khassenov, A.K.** — PhD, Docent, Karagandy University of the name of academician E.A. Buketov, Kazakhstan, E-mail: ayanbergen@mail.ru

**Klimenko, V.I.** — Professor, Doctor of science (Engineering), Head of the Department of Automobiles named after A.B. Hredeskul, Prof., DSci (Engineering), Kharkiv National Automobile and Road University, Ukraine, E-mail: valeriy.klimenko@gmail.com

**Kozhanova, R.S.** — PhD student of 6D072300 - «Thecnical physics», Shakarim University, Semey; Junior Researcher of the «PlasmaScience» LLP, Ust-Kamenogorsk, Kazakhstan, E-mail: kozhanovars@yandex.ru

**Krushynska, N.I.** — Lecturer, Zhytomyr Polytechnic State University, Zhytomyr, Ukraine.

**Kucheruk, V.Yu.** — Professor, Doctor of science (Engineering), Head of the Department of Metrology and Industrial Automation Vinnytsia National Technical University, Ukraine, E-mail: vladimir.kucheruk@gmail.com

**Leontiev, D.N.** — Associate Professor, Candidate of technical sciences, Associate Professor Head of the Department of Automobiles named after A.B. Hredeskul, Prof., DSci (Engineering), Kharkiv National Automobile and Road University, Ukraine, E-mail: dima.a3alij@gmail.com

**Lukiniuk, M.V.** — Senior Lecturer, Department of Hardware and Software of Automation, National Technical University of Ukraine «Igor Sikorsky Kyiv Polytechnic Institute», Ukraine.

**Mahajan, O.H.** — Associate Professor at M.J. College, affiliated to K.B.C. North Maharashtra University, Jalgaon, India.

**Mausymbaeva, A.D.** — PhD, Cand.of Tech. Sci. of the Department of Geology and Exploration of Mineral Deposits, Karaganda Technical University, Kazakhstan, E-mail: maussymbayevaaliya@gmail.com

**Nurbalayeva, D.A.** — Master student, Karagandy University of the name of academician E.A. Buketov, Kazakhstan, E-mail: didara_na@mail.ru

**Petrov, M.V.** — Junior Researcher, Problem Research Laboratory of Electronics, Dielectrics and Semiconductors, Research School of High Energy Process Physics, Tomsk Polytechnic University, Russia, E-mail: mvp17@tpu.ru

**Ponikarovska, S.V.** — Senior Lecturer, Deputy Head of the Department of Foreign Languages Kharkiv National Automobile and Road University, Ukraine, E-mail: ponikarovska@gmail.com

**Portnov, V.S.** — Doct.of Tech. Sci., of the Department of Geology and Exploration of Mineral Deposits, Karaganda Technical University, Kazakhstan, E-mail:vs_portnov@mail.ru,

**Priadko, V.A.** — Senior Lecturer, Polissia National University, Zhytomyr, Ukraine.

**Rakhadilov, B.K.** — PhD, Senior Researcher of the Research Center «Surface Engineering and Tribology», S. Amanzholov East Kazakhstan University, Ust-Kamenogorsk, Kazakhstan, E-mail: rakhadilovb@mail.ru

**Reva, N.V.** — Doct.of Tech. Sci., of the Department of Geophysics, Taras Shevchenko National University of Kyiv, Ukraine, E-mail: mvreva@mail.ru,

**Sagdoldina, Zh.B.** — PhD, Head of the Research Center «Surface Engineering and Tribology», S. Amanzholov East Kazakhstan University, Ust-Kamenogorsk, Kazakhstan, E-mail: sagdoldina@mail.ru

**Sarode, A.P.** — Associate Professor and Head of Physics Department at Dr. A.G.D. Bendale Girls College, affiliated to K. B. C. North Maharashtra University, Jalgaon, India, e-mail: abhijitsarode@yahoo.com

**Sazonov, A.Y.** — PhD; Assoc.Prof.; Associate Professor of the Department of Hardware and Software of Automation, National Technical University of Ukraine «Igor Sikorsky Kyiv Polytechnic Institute», Ukraine, E-mail: a.sazonov@kpi.ua.

**Sheveleva, E.A.** — Ph.D., Assistant Professor Department of «Control and Diagnostics» Tomsk Polytechnic University, Russia, E-mail: vasendina@tpu.ru

**Shuyushbayeva, N.N.** — PhD, Associate Professor of the Department of Physics and Mathematics, Sh.Ualikhanov Kokshetau University, Kazakhstan, E-mail: nn_shuish@mail.ru

**Stoev, Mitko** — Associate professor, PhD, Doctor engineering, Southwestern University «Neophyte Rilski», Blagoevgrad, Bulgaria, E-mail: stoev.mitko@gmail.com

**Sultan, A.D.** — 2nd year Master student of the Department of Geology and Exploration of Mineral Deposits, Karaganda Technical University, Kazakhstan, E-mail: sultanad@mail.ru

**Tanasheva, N.K.** — PhD, Senior Lecturer of the Department of Engineering Thermophysics Zh.S. Akylbaeva, Karaganda University named after E.A. Buketov, Kazakhstan, E-mail: nazgulya_tans@mail.ru

**Tyurin, Y.N.** — Doctor of engineering science; Head of laboratory of the E.O. Paton Electric Welding Institute, Kyiv, Ukraine, E-mail: ynturin9@gmail.com

**Yurov, V.M.** — Cand. of Tech. Sci. of the Ye.A. Buketov Karaganda University, Kazakhstan, E-mail:exciton@inbox.ru,

**Zhurerova, L.G.** — PhD, Senior Researcher of the Research Center «Surface Engineering and Tribology»; S. Amanzholov East Kazakhstan University, Ust-Kamenogorsk, Kazakhstan, E-mail: leila_uka@mail.ru